INSTITUTO SUPERIOR TÉCNICO

FACULDADE DE MEDICINA

DE LISBOA

ACQUISITION SYSTEM FOR AUTOMATIC SLEEP IDENTIFICATION
The Algorithm

João Branco Silva, n.º 51354

Dissertação para obtenção do Grau de Mestre em

Engenharia Biomédica

Júri

Presidente:	Professor Fernando Lopes da Silva (UVA)
Orientadores:	Professor Raúl Carneiro Martins (IST)
	Professora Teresa Paiva (FML)
Vogal:	Professor Fernando Janeiro (UE)

Novembro de 2007

Acknowledgments

First of all, to the supervisors of this thesis for the suggestion of the idea behind this work. To Professor Raúl Martins for the continuous support, helpful discussions and work guidance through the whole project. Without his support Digital Signal Processing would have been an extremely complicated task. To Professora Teresa Paiva for the supportive medical background and sleep analysis guidance as well as for the donated training set used to test the designed algorithm.

I would also like to thank to the lab colleagues Luís and Nuno for their help in crucial milestones of this work.

To "Instituto Superior Técnico", particularly to the "Instituto de Telecomunicações" for the excellent working conditions provided during the whole project.

To my workgroup colleagues Armando and Luís, for it was a unique experience working continuously with them.

To all my curious friends for their outmost opinions and helpful tips, and ultimately to my family for the support and all the conditions I have been given.

Abstract

The goal of this thesis consists in the development of a computational tool capable of automated Rapid Eye Movement (REM) sleep stage detection making use of data acquired from standard sleep analysis sources: electromyogram (EMG), electroencephalogram (EEG) and electro-oculogram (EOG).
Sleep identification and classification are major research areas in neurosciences not only due to common sleep disorders, such as difficulty in falling asleep or other sleep parameters that can reflect a broad range of pathologies, but also by the recognition and quantification of each sleep stage and the evaluation of its purpose, promoting a better understanding of each stage and its relation with the rejuvenative functions attributed to sleep, e.g. immune system recovery and growth hormone restoration.
Although different approaches have been developed lately, contemporary sleep classifications still find worldwide acceptance mainly by the visual classification of sleep stages according to Rechtschaffen & Kales rules (1968), which is an extremely difficult and time consuming task that must be performed by experienced human scorers. Since these criteria can be objectively defined they can be used as premises in a mathematical tool, stated as Boolean conditions.
In this sense the project here presented, an automatic REM sleep stage detector, is of great value in order to reduce time and costs of the analysis and increase the sensitivity of subsequent statistical analyses. For this purpose an acquisition system for biological signals has been developed. This device acquires EMG, EEG and EOG channels with adequate parameters, processing the data in near real-time according to several characteristic criteria of REM sleep stage in frequency and time domain, exporting the result of each evaluated 30 second epoch in a REM stage probability percentage.

Keywords: REM sleep stage, EEG, EMG, EOG, near real-time REM Automatic detection tool.

Contents

Acknowledgments i

Abstract ii

List of Figures vi

1 Introduction 1
- 1.1 Background . . . 1
- 1.2 Sleep . . . 4
- 1.3 Detected Biosignals . . . 6
  - 1.3.1 EEG . . . 6
  - 1.3.2 EMG . . . 13
  - 1.3.3 EOG . . . 14
- 1.4 Sleep Stages . . . 15

2 Acquisition System 20
- 2.1 Overview . . . 21
- 2.2 Acquisition System Design . . . 21
  - 2.2.1 Environmental Conditioning . . . 21
  - 2.2.2 Specifications . . . 22
- 2.3 Interface . . . 23
  - 2.3.1 Features and Objectives . . . 23

3 Digital Signal Processing 25
- 3.1 Literature Review . . . 25
- 3.2 Tools . . . 27
  - 3.2.1 FFT . . . 27
  - 3.2.2 Digital Filters . . . 33
  - 3.2.3 ICA . . . 38
- 3.3 Algorithm . . . 40
  - 3.3.1 EEG Algorithm . . . 40
  - 3.3.2 EMG Algorithm . . . 42
  - 3.3.3 EOG Algorithm . . . 45
- 3.4 Real Time Algorithm . . . 48

4 Results **49**
4.1 Training Data . . . 49
4.1.1 Subject 1 . . . 49
4.1.2 Subject 2 . . . 54
4.1.3 Subject 3 . . . 57
4.1.4 Subject 4 . . . 60
4.1.5 Subject 5 . . . 63
4.1.6 Subject 6 . . . 66
4.2 DAQ trial . . . 69
4.2.1 First evaluation . . . 69
4.2.2 Trial 1 . . . 76
4.2.3 Trial 2 . . . 79

5 Conclusions **86**
5.1 Discussion points and future work . . . 88

Bibliography **90**

A Sleep Disorders **94**

B Signal Processing **96**

C Data analysis **98**
C.1 EEG criteria analysis . . . 98
C.1.1 Subject 1 . . . 99
C.1.2 Subject 2 . . . 99
C.1.3 Subject 3 . . . 100
C.1.4 Subject 4 . . . 100
C.1.5 Subject 5 . . . 101
C.1.6 Subject 6 . . . 101
C.2 EMG criteria analysis . . . 102
C.2.1 Subject 1 . . . 102
C.2.2 Subject 2 . . . 102
C.2.3 Subject 3 . . . 103
C.2.4 Subject 4 . . . 103
C.2.5 Subject 5 . . . 104
C.2.6 Subject 6 . . . 104
C.3 EOG criteria analysis . . . 105
C.3.1 Subject 1 . . . 105
C.3.2 Subject 2 . . . 105
C.3.3 Subject 3 . . . 106
C.3.4 Subject 4 . . . 106
C.3.5 Subject 5 . . . 107
C.3.6 Subject 6 . . . 107

D European Data Format **108**

E Criteria analysis **109**
E.1 EEG indicators 110
E.1.1 Trial 1 110
E.1.2 Trial 2 110
E.2 EMG indicators 111
E.2.1 Trial 1 111
E.2.2 Trial 2 111
E.3 EOG indicators 112
E.3.1 Trial 1 112
E.3.2 Trial 2 112

List of Figures

1.1 10-20 system: Odd electrodes=left hemisphere, Even electrodes=right hemisphere; Fp=frontopolar, F=frontal, C=central, T=temporal, O=occipital, A=auricular. [6] 2
1.2 Neuronal interference: temporal and spatial summation. [31] 7
1.3 One second EEG signal. [30] 8
1.4 1second Δ signal profile. [30] 8
1.5 1 second θ signal profile. [30] 9
1.6 1 second α signal profile. [30] 9
1.7 1 second β signal profile. [30] 9
1.8 1 second γ signal profile. [30] 10
1.9 Representation of characteristic wave forms:sleep spindle and K-complex. [30] 10
1.10 Frequency analysis of a epileptic attack - high frequencies are highly expressed. [29] 12
1.11 EEG Electrode placement. [26] 12
1.12 Generic muscular contraction detection setup. [28] 13
1.13 EMG Electrode placement. [26] 13
1.14 electro-oculogram signal generated by horizontal movement of the eyes. [27] 14
1.15 EOG electrode placement. [26] 14
1.16 Awake subject demonstrating EMG activation and eye movements. [26] . . 15
1.17 Subject with eyes closed and drowsy. Alpha frequency dominates the EEG record. [26] 15
1.18 Stage 1 sleep. Alpha frequency EEG is no longer present. The EEG is now a lower frequency and amplitude than when awake. Slow rolling eye movements can be seen. [26] 16
1.19 Stage 2 sleep. K-complexes and spindles now appear on the EEG record (highlighted). [26] 17
1.20 Stage 3 sleep. Delta waves (1-2 Hz) now represent at least 50% of the EEG trace. Parallel EOG traces represent EEG artefact. [26] 17
1.21 Stage 4 sleep. Delta waves (1-2 Hz) now represent at least 75% of the EEG trace. Parallel EOG traces represent EEG artefact. [26] 18
1.22 Rapid Eye Movement (REM) sleep. Signals similar to Stage 1 with rapid eye movements on the EOG channel and low amplitude EMG signal with sporadic muscle twitches. [26] 18
1.23 Summarized sleep stages rules. [32] 19

2.1 Structure of the designed biosignal digital analysis system. The upper branch of the scheme represents analog preprocessing of the signals and the lower branch digital processing steps.DAQ system is highlighted in blue. [31] 22
2.2 Structure of the designed biosignal digital analysis system. The upper branch of the scheme represents analog preprocessing of the signals and the lower branch digital processing steps.Interface system is highlighted in green. [31] 23

3.1 Spectral coefficients of the example signal containing only sinusoids. 29
3.2 Periodicity of the DFT's time domain signal. In the upper figure the signal can be viewed as N samples, while the lower figure represents the signal as an infinitely long periodic signal. [46] 30
3.3 Spectral coefficients for two example signals. Blue signal consisting of two harmonic sinusoids; Green signal consisting of a harmonic and one non-harmonic sinusoid. 30
3.4 Comparison between the number of operations in a DFT and a FFT 32
3.5 FFT butterfly. A and B - complex numbers ; W_N^p - Twiddle factor with p an integer between 0 and $N-1$ 33
3.6 Detail of an 8-point FFT [47] 33
3.7 Example of a tolerance diagram for the amplitude characteristic of a low pass filter 34
3.8 Example of a tolerance diagram for the amplitude characteristic $H_d(\exp j\theta)$ of a low pass filter 35
3.9 Ideal filter time domain signal $h_d[n]$ 35
3.10 Truncated filter time domain signal $h_d[n]$ 36
3.11 Shifted filter time domain signal $h_d[n]$ 36
3.12 Time domain signal truncation. Left column: Time domain multiplication. Right column: Frequency domain convolution 37
3.13 Mixed signal 38
3.14 Independent components 38
3.15 Manipulation towards Independent Components 39
3.16 Structure of the designed biosignal digital analysis system. The upper branch of the scheme represents analog signal preprocessing and the lower branch digital processing steps.DSP system is highlighted in red. [31] . . . 40
3.17 Suggested EEG Algorithm. 40
3.18 Example of an EEG signal segmentation. 41
3.19 Example of signal analysis. The upper picture represents a 5 second EEG signal, while the lower picture represents the corresponding FFT transform. 42
3.20 Suggested EMG Algorithm. 43
3.21 thirty second NREM epoch EMG register. 43
3.22 Thirty second REM epoch EMG register. 44
3.23 One second EMG data with fast muscular contraction. 44
3.24 Suggested of EOG Algorithm. 45
3.25 Tolerance diagram of the implemented digital filter. 45

3.26 EOG data example. At 13037 seconds LOC and ROC registers are completely out of phase - Synchronous movement. At 13035 seconds data signals are in phase - Artefact or non-synchronous eye movement. 46
3.27 EOG data example. Instant of NIP maximum is focused and its vicinity evaluated 0.2 seconds before and after for REM detection 47
3.28 EOG data example. Two clear NIP patterns are recognized. Before reaching 12000 seconds several artefacts are detected inducing a NREM stage, from that point forward there is an artefact free interval. 47

4.1 Subject 1 EEG analysis. Upper plot - EEG data vector; Amplitude μV. Middle plot - REM identifier. Lower plot - Epoch energy minus mean energy 50
4.2 Total register time-step FFT. 50
4.3 Subject 1 EMG analysis. Upper plot - EMG data vector; Amplitude μV. Middle plot - REM identifier. Lower plot - Epoch energy minus mean energy 51
4.4 Subject 1 EOG analysis. Upper plot - EOG data vector; Amplitude μV. Middle plot - REM identifier. Lower plot - Epoch energy minus mean energy 52
4.5 Algorithm evaluation of the presented subject 53
4.6 Expert evaluation of the presented subject 53
4.7 Subject 2 EEG analysis. Upper plot - EEG data vector; Amplitude μV. Middle plot - REM identifier. Lower plot - Epoch energy minus mean energy 54
4.8 Total register time-step FFT. 54
4.9 Subject 2 EMG analysis. Upper plot - EMG data vector; Amplitude μV. Middle plot - REM identifier. Lower plot - Epoch energy minus mean energy 55
4.10 Subject 2 EOG analysis. Upper plot - EOG data vector; Amplitude μV. Middle plot - REM identifier. Lower plot - Epoch energy minus mean energy 55
4.11 Algorithm evaluation of the presented subject 56
4.12 Expert evaluation of the presented subject 56
4.13 Subject 3 EEG analysis. Upper plot - EEG data vector; Amplitude μV. Middle plot - REM identifier. Lower plot - Epoch energy minus mean energy 57
4.14 Total register time-step FFT. 57
4.15 Subject 3 EMG analysis. Upper plot - EMG data vector; Amplitude μV. Middle plot - REM identifier. Lower plot - Epoch energy minus mean energy 58
4.16 Subject 3 EOG analysis. Upper plot - EOG data vector; Amplitude μV. Middle plot - REM identifier. Lower plot - Epoch energy minus mean energy 58
4.17 Algorithm evaluation of the presented subject 59
4.18 Expert evaluation of the presented subject 59
4.19 Subject 4 EEG analysis. Upper plot - EEG data vector; Amplitude μV. Middle plot - REM identifier. Lower plot - Epoch energy minus mean energy 60
4.20 Total register time-step FFT. 60
4.21 Subject 4 EMG analysis. Upper plot - EMG data vector; Amplitude μV. Middle plot - REM identifier. Lower plot - Epoch energy minus mean energy 61
4.22 Subject 4 EOG analysis. Upper plot - EOG data vector; Amplitude μV. Middle plot - REM identifier. Lower plot - Epoch energy minus mean energy 61
4.23 Algorithm evaluation of the presented subject 62
4.24 Expert evaluation of the presented subject 62

4.25 Subject 5 EEG analysis. Upper plot - EEG data vector; Amplitude μV. Middle plot - REM identifier. Lower plot - Epoch energy minus mean energy 63
4.26 Total register time-step FFT. 63
4.27 Subject 5 EMG analysis. Upper plot - EMG data vector; Amplitude μV. Middle plot - REM identifier. Lower plot - Epoch energy minus mean energy 64
4.28 Subject 5 EOG analysis. Upper plot - EOG data vector; Amplitude μV. Middle plot - REM identifier. Lower plot - Epoch energy minus mean energy 64
4.29 Upper plot - Algorithm evaluation of the presented subject. Lower plot - Zoomed algorithm evaluation of the presented subject 65
4.30 Expert evaluation of the presented subject 65
4.31 Subject 6 EEG analysis. Upper plot - EEG data vector; Amplitude μV. Middle plot - REM identifier. Lower plot - Epoch energy minus mean energy 66
4.32 Total register time-step FFT. 66
4.33 Subject 6 EMG analysis. Upper plot - EMG data vector; Amplitude μV. Middle plot - REM identifier. Lower plot - Epoch energy minus mean energy 67
4.34 Subject 6 EOG analysis. Upper plot - EOG data vector; Amplitude μV. Middle plot - REM identifier. Lower plot - Epoch energy minus mean energy 67
4.35 Upper plot - Algorithm evaluation of the presented subject. Lower plot - Zoomed algorithm evaluation of the presented subject 68
4.36 Expert evaluation of the presented subject 68
4.37 Designed DAQ signals preliminary analysis. Upper plot - 5 second signal. Lower plot - Frequency analysis of the acquired signal. 69
4.38 EEG analysis. Upper plot - EEG data vector; Amplitude μV. Middle plot - REM identifier. Lower plot - Epoch energy minus mean energy 71
4.39 Total register time-step FFT. 71
4.40 EMG analysis. Upper plot - EMG data vector; Amplitude μV. Middle plot - REM identifier. Lower plot - Epoch energy minus mean energy . . . 72
4.41 EOG analysis. Upper plot - EOG data vector; Amplitude μV. Middle plot - REM identifier. Lower plot - Epoch energy minus mean energy 72
4.42 Algorithm evaluation of the presented trial 73
4.43 Raw signal vs. Desired signal quality. Left plots - Raw signal. Right plots - Desired signals. 73
4.44 EMG analysis. Upper plot - EMG raw data. Middle plot - EMG processed data. Lower plot - EMG new processed data 74
4.45 Somnologica software interface 75
4.46 Trial 1 EEG analysis. Upper plot - EEG data vector; Amplitude μV. Middle plot - REM identifier. Lower plot - Epoch energy minus mean energy 76
4.47 Total register time-step FFT. 76
4.48 Trial 1 EMG analysis. Upper plot - EMG data vector; Amplitude μV. Middle plot - REM identifier. Lower plot - Epoch energy minus mean energy 77
4.49 Trial 1 EOG analysis. Upper plot - EOG data vector; Amplitude μV. Middle plot - REM identifier. Lower plot - Epoch energy minus mean energy 77
4.50 Algorithm evaluation of the first trial 78
4.51 Expert evaluation of the 1 trial 78
4.52 Trial 2 EEG analysis. Upper plot - EEG data vector; Amplitude μV. Middle plot - REM identifier. Lower plot - Epoch energy minus mean energy 79

4.53 Total register time-step FFT. 79
4.54 Trial 1 EMG analysis. Upper plot - EMG data vector; Amplitude μV. Middle plot - REM identifier. Lower plot - Epoch energy minus mean energy 80
4.55 Trial 1 EOG analysis. Upper plot - EOG data vector; Amplitude μV. Middle plot - REM identifier. Lower plot - Epoch energy minus mean energy 80
4.56 Algorithm evaluation of the second trial 81
4.57 Expert evaluation of the 2 trial 81
4.58 Upper plot - Raw signal 25 seconds sample. Lower left plot - ICA result. Lower right plot - ICA result (2) 83
4.59 Left plot - Raw signal 25 seconds sample. Right plot - ICA result 84
4.60 Left plot - Raw signal 25 seconds sample. Right plot - ICA result 84
4.61 Left plot - Raw signal 1.8 second sample. Right plot - ICA result 85
4.62 Left plot - Raw signal 8 second sample. Right plot - ICA result 85

5.1 Standard sleep cycle. [67] 87

B.1 Signal example waveform. Top plot: Continuous representation. Bottom plot: Sampled version of the signal. [64] 96
B.2 Top plot: Bandlimited (to W Hz) signal spectrum. If the sampling interval T_s is chosen too large relative to the bandwidth W, aliasing will occur. Bottom plot: Sampling interval is chosen sufficiently small to avoid aliasing. Note that if the signal were not bandlimited, the component spectra would always overlap. [64] 97

C.1 A - Epoch's energy variability evaluation. B - Five second energy variability evaluation. C - Five second Δ variability evaluation. D - Five second θ variability evaluation. E - Five second α variability evaluation. 99
C.2 A - Epoch's energy variability evaluation. B - Five second energy variability evaluation. C - Five second Δ variability evaluation. D - Five second θ variability evaluation. E - Five second α variability evaluation. 99
C.3 A - Epoch's energy variability evaluation. B - Five second energy variability evaluation. C - Five second Δ variability evaluation. D - Five second θ variability evaluation. E - Five second α variability evaluation. 100
C.4 A - Epoch's energy variability evaluation. B - Five second energy variability evaluation. C - Five second Δ variability evaluation. D - Five second θ variability evaluation. E - Five second α variability evaluation. 100
C.5 A - Epoch's energy variability evaluation. B - Five second energy variability evaluation. C - Five second Δ variability evaluation. D - Five second θ variability evaluation. E - Five second α variability evaluation. 101
C.6 A - Epoch's energy variability evaluation. B - Five second energy variability evaluation. C - Five second Δ variability evaluation. D - Five second θ variability evaluation. E - Five second α variability evaluation. 101
C.7 Epoch's energy variability evaluation. 102
C.8 Epoch's energy variability evaluation. 102
C.9 Epoch's energy variability evaluation. 103
C.10 Epoch's energy variability evaluation. 103
C.11 Epoch's energy variability evaluation. 104

C.12 Epoch's energy variability evaluation. 104
C.13 Epoch's energy variability evaluation.ROC - Right Outer Cantus data. LOC - Left Outer Cantus data. 105
C.14 Epoch's energy variability evaluation.ROC - Right Outer Cantus data. LOC - Left Outer Cantus data. 105
C.15 Epoch's energy variability evaluation.ROC - Right Outer Cantus data. LOC - Left Outer Cantus data. 106
C.16 Epoch's energy variability evaluation.ROC - Right Outer Cantus data. LOC - Left Outer Cantus data. 106
C.17 Epoch's energy variability evaluation.ROC - Right Outer Cantus data. LOC - Left Outer Cantus data. 107
C.18 Epoch's energy variability evaluation.ROC - Right Outer Cantus data. LOC - Left Outer Cantus data. 107

E.1 EEG indicators. Top - Epoch Max/Energy. Middle left - 5sec Max/Energy. Middle right - 5sec Δ Energy/Total Energy. Bottom left - 5sec θ Energy/Total Energy. Bottom right - 5sec α Energy/Total Energy. 110
E.2 EEG indicators. Top - Epoch Max/Energy. Middle left - 5sec Max/Energy. Middle right - 5sec Δ Energy/Total Energy. Bottom left - 5sec θ Energy/Total Energy. Bottom right - 5sec α Energy/Total Energy. 110
E.3 EMG indicators. Top - Epoch Energy. Bottom - Max/Energy. 111
E.4 EMG indicators. Top - Epoch Energy. Bottom - Max/Energy. 111
E.5 EOG indicators. Top left - ROC epoch Energy. Top right - ROC Max/Energy. Bottom left - LOC epoch Energy. Bottom right - LOC Max/Energy. 112
E.6 EOG indicators. Top left - ROC epoch Energy. Top right - ROC Max/Energy. Bottom left - LOC epoch Energy. Bottom right - LOC Max/Energy. 112

Chapter 1

Introduction

One of the most common phrases concerning sleep is "A normal human being spends about a third of his live sleeping". It is also a commonplace to think that sleep is a sort of loss of time. Contradicting this idea, studies have shown that sleep is indeed one of the strongest forces guiding human - and animal - behaviour. In extreme situations it has been proven that forced sleep deprivation can even kill a living being [1].

Yet, it is obvious that one can not compare what it is known from sleep stages when comparing with other conditions. For instance, we can understand more easily a muscular contraction or even an organ function than "why is that complicated to avoid sleep and maintain a vigil state for more than 24 hours?" or "what is the exact function of each sleep stage? Why does the brain behaves so distinctly and actively during sleep?".

A better understanding of sleep could explain its functions, justifying what we are doing during that one third of our lives, as well as identifying pathologies which can be studied through sleep stages.

Wakefulness can be identified and monitored using several sensors, such as visual and hearing capabilities, muscular tonus; similarly sleep can also be identified and tracked by the use of EEG, EMG and EOG analysis.

A particular stage of sleep tends to gather the attention of several researchers. It attracts so much attention due to "strange" characteristics, such as, encephalic activity resembling wakefulness (paradoxical sleep), absence of muscular activity only disturbed by sporadic contractions, and the characteristic that gives the name do this sleep stage, rapid eye movements. Besides these manifestations it is of special importance to notice that this stage is associated with memory formation (especially regarding implicit procedural and emotional learning tasks) [2] as well as dreaming. All this information leads to the need of a correct REM stage identification so that future work can accurately take place. This is the goal of the present work.

This chapter will focus on sleep, its stages and the information that can be extracted throughout the different sources. This will allow a better understanding of the work guideline.

1.1 Background

Even though brain activity was discovered in 1875 by the hands of Richard Caton, and the first publication on EEG records took place in Russia in 1912 by the physiologist

Vladimirovich Pravdich-Neminsky, it is reasonable to consider that sleep studies truly arose only with Hans Berger invention when EEG was applied to the human being (1924). It was the first source of data to be related to sleep activity. Before this approach, other methods were used (some are still) focusing in variations of waking threshold, motility, breathing and other parameters. Nowadays these parameters can actually give some information, but in the beginning of the XX century they could only promote divergent opinions since no sleep stages were known, for sleep was considered a uniform condition, and in this sense it was a bit disturbing to see that the parameters were varying a lot throughout a night sleep.

The introduction of sleep stages came in mid XX century with Loomis et al. [3] with a scale from "A" to "E", in which "A" would correspond to early drowsiness and "E" would be deep sleep, later to be known as high-amplitude Δ waves sleep. In this classification the REM stage was not considered since it was mistaken with other stages, or even with arousal since the activity resembled an awoke subject. It was not until the discovery of rapid eye movements, by Aserinsky and Kleitman [4] that stage REM was identified as a sleep stage. Later on, justifying the cyclic evidences of sleep condition already noticed in breathing, cardiac cycle frequency and other parameters, Dement and Kleitman [5] introduced the cyclic patterns of sleep stages based on their large normative study. The four non-REM (NREM) stages and REM formed the basis of subsequent polygraphic sleep studies. These different sleep stages were firstly "created" due to different encephalic waves throughout sleep.

It is obvious that brain function does not resume to ON/OFF. It has several waves propagating through the conductive tissue, the brain. For this reason an electrode placed anywhere on the scalp will detect signals that could easily have been produced somewhere within the brain. This accumulation of signals complicates the electrode interpretation. Therefore, throughout time different approaches were tested.

Nowadays, besides the 21 electrode system (Fig.1.1), a single electrode evaluation is also used. This procedure is adequate due to high conductivity of brain tissue [34]. In this way redundant information may be avoided.

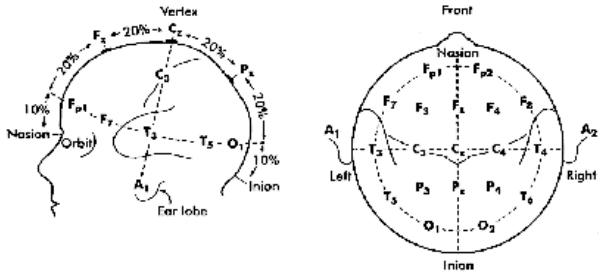

Figure 1.1: 10-20 system: Odd electrodes=left hemisphere, Even electrodes=right hemisphere; Fp=frontopolar, F=frontal, C=central, T=temporal, O=occipital, A=auricular. [6]

The brain activity detected by any of these electrodes is to be categorized by frequency in distinct groups: Δ, θ, α and β. These frequency bands aid in the identification of sleep phases since the predominance of one of them, or an event associated to a defined band would suggest a specific stage.

Using an EEG tool as a feature extractor, associated with other records - EMG and EOG - it becomes possible to generically study sleep by:

- Identifying sets of characteristics intrinsic to each sleep stage
- Evaluating each stage separately
- Evaluating the ratio of each stage
- Searching for sleep cycles by recognizing repetitive events
- Identifying normal vs. pathological sleep (Appendix A)

Once the tools became available and a good knowledge of sleep gathered, different analysis took place. Naturally, due to a large set of data to be analysed, different approaches and subjectivity associated to each researcher, some results were discrepantly classified by different polysomnographic expert analysts.

The need of a common platform for exchanging data and results was emphasized by the study of Monroe [7], in which he showed that the inter-rater agreement between different laboratories was low. This led to the establishment of the committee led by Rechtschaffen and Kales. The rules of the manual of Rechtschaffen and Kales (R&K) [8] are more or less a formalization of the Dement and Kleitman criteria. The main goals of the Committee were to standardize recording and scoring techniques in order to increase the comparability of results between laboratories (e.g. definition of a sleep time scale - epoch[1]). The manual provided the minimum requirements for meaningful comparison of polygraphic sleep studies of adult humans. The Committee also encouraged the use of other concepts, and revisions of the manual were suggested, with the addition of new information. However, instead of providing the necessary reference to novel developments the rules of the manual became in practice the only method of sleep analysis. As a consequence it became a gold standard and, unintentionally, a restriction to the development of subsequent sleep research [9].

As mentioned, the proposal to standardize recording techniques and scoring criteria was intended to increase the comparability of results reported by different investigators. Researchers who have applied the system correctly have increased the reliability of their sleep stage scoring. In the several decades since its publication, however, a number of serious points of unreliability in the 1968 standard scoring system have been identified. Particularly, researchers developing computer-based automatic sleep staging systems have encountered numerous vague and ambiguous areas in the current standard.

To increase both the within and between researcher groups agreement in sleep stage identification and to foster the development of computer algorithms for automatic analyses of sleep, in 1991 the necessity for additional definitions was recognized, reformulating the R&K rules to cover information that was identified from 1968 to 1991:

- Redefinition of epoch to a more broad concept. It was suggested that different sleep epoch discretization could lead to an improvement in sleep stage classification. In this sense researchers started evaluating sleep epochs from 5 seconds to the standard 30 seconds.

[1] according to R&K 30s were the time unit to be analysed and identified as a sleep stage

- Since sleep analysis does not focus only on healthy subjects, R&K rules were reformulated to cover situations such as pathological conditions [10].

It was also suggested that these rules should always be revised and updated with the moving force of technological breakthroughs and medical improvements.

Results deviation associated with previous mentioned barriers and the fact that sleep identification is an extremely time consuming task[2], have motivated an increased development of methodologies capable of detecting unequivocally, if possible, different sleep stages in the shortest time possible. This assumes significant proportions because certain sleep stages carry information beyond its sleep stage. For instance, REM sleep is one of the stages carrying more relevant information - e.g.: the number of rapid eye movements recorded can inform about a possible schizophrenic situation or depressive patients [11, 12, 13], [14]; studies of rapid eye movement occurrence in blind subjects [15]; narcolepsy detection; REM sleep behaviour disorder.

Motivated by the presented flaws and relevant research points, this work focus in the development of a device capable to detect several biosignals, manipulate the data and export through an interactive interface the output of REM stage identification.

1.2 Sleep

In a "macroscopic" physiological point of view one can identify sleep by system changes from the awake homeostasis:

Cardiovascular According to the sleep stage there can be a generalized vasodilatation promoting reductions in heart rate, cardiac output and blood pressure (commonly associated with NREM). But it can also occur in the opposite direction motivated by a generalized event variability (related to REM phasic events[3] intercalated by tonic REM[4] intervals).

Respiration Some neurons related to breathing stop firing in deep sleep. Overall, there is slight hypercapnia[5], a decrease in total ventilation, and a decreased sensitivity to inspired CO_2.

During NREM there is a slight hypoventilation[6] due to a relaxation of upper airway muscles, as well as a decrease in the firing of inspiratory neurons, which show a decreased sensitivity to stimuli. Accordingly pCO_2 levels rise while pO_2 levels fall. During this stage breathing is under chemical and mechanical feedback control.

During REM there is an overall higher and variable respiratory rate. It appears as though different processes maintain breathing during REM sleep, and it is not driven by vagal signals or peripheral or central chemoreceptors. It may be driven by higher cortical control, which may explain the variable rate. There is a lower tidal volume, and higher respiratory rate. As REM sleep is associated with a loss of muscle tone, there is an increase in the resistance of the upper airway.

[2]Sleep experts identify sleep stages by evaluating each 30 second epoch of a whole night sleep data
[3]periods with consistently high eye movement densities
[4]REM sleep periods lacking in REM occurences
[5]the presence of an abnormally high level of carbon dioxide in the circulating blood
[6]reduction in the amount of air entering the lungs

Nervous System Globally, neuronal wave patterns alter in frequency and amplitude, as well as the origin of depolarization, suggesting different activation areas. Additionally, postsynaptic inhibition of motor neurons takes place, affecting the muscular function - contraction and tonus.

More specifically, the discharge rate and brain metabolism are decreased during NREM sleep. During NREM sleep, there is an active inhibition of the reticular activating system[7]. Relevant neurons in this inhibition are located in the basal forebrain (anterior hypothalamus and adjacent forebrain areas); lesions of the basal forebrain result in insomnia, while electrical stimulation causes a subject to fall asleep. The thalamus, dorsal raphe, and nucleus tractus solitarius are also important in NREM sleep. There is also an increase in parasympathetic activity similar to relaxed wakefulness; sympathetic drives remain at about the same level as during relaxed wakefulness.

During REM sleep, many parts of brain (visual cortex, limbic lobe) show increased firing rate and metabolism. Brain transection studies have shown that the pons is necessary and sufficient to generate the basic phenomena of REM sleep. During tonic REM sleep, parasympathetic activity remains about the same as during NREM sleep, but sympathetic activity decreases, resulting in an overall predominance of parasympathetic activity. However, during phasic REM sleep, both sympathetic and parasympathetic activity increase; sympathetic activation is generally favoured.

Endocrinology Deep sleep stages are associated with increased secretion of Growth Hormone, especially in children approaching puberty. Other important hormones are differently regulated during sleep, e.g., prolactin[8] increases; cortisol[9] decreases.

Thermoregulation At sleep onset, the body temperature set point is lowered and body temperature falls. The body therefore activates heat loss mechanisms (sweating) to cool down the body to the new set point. Thermoregulatory cells in the central nervous system (CNS)[10] diminish its activity during NREM sleep, making us essentially poikilothermic creatures[11], only to stop firing entirely during REM sleep when thermoregulation ceases.

With the main sleep physiological manifestations identified, the methods to assess its relevant information can be selected. Conventionally, brain activity is monitored, as well as other sensors focusing on easily measurable correlated variables. As mentioned previously, for this work EEG, EMG and EOG were chosen. Others like ECG and pulse oximetry could probably also be used. Nevertheless, for the present study they were not

[7] name given to part of the brain (the reticular formation and its connections) believed to be the center of arousal and motivation by its involvement in the circadian rhythm. The activity of this system is crucial for maintaining the state of consciousness. It is situated at the core of the brain stem between the myelencephalon - medulla oblongata - and mesencephalon - midbrain

[8] a hormone secreted by the pituitary gland which affects growth of the mammary glands and secretion of breast milk

[9] The body's natural stress-fighting and anti-inflammatory hormone

[10] preoptic/anterior hypothalamus

[11] variable body temperature according to its surroundings; Animals kept at ambient temperatures in the thermoneutral zone - ambient temperature at which an animal does not have to actively regulate its' body temperature avoiding raising its metabolism - show maximal levels of REM sleep

implemented since their data is known to have a higher inter subject variability when compared with EEG, EMG and EOG registers.

As previously mentioned, the sleep cycle concerns more than sleep and awake. Within sleep two main stages are to be separated according to electrophysiological patterns - EEG, EOG and EMG - REM and NREM.

REM features are: EEG - high frequency, low amplitude more irregular waves, with sporadic sawtooth waves; EOG - rapid and coordinated movement of the eyes; EMG - extremely weak signal due to muscle tone inhibition.

As opposed, NREM is characterized by: EEG - high amplitude, low frequency waves; EOG - rolling, uncoordinated and slow movement of the eyes; EMG - passively decreased muscle tone.

NREM stage can be subsequently separated into 4 different stages (later presented), characterized by a progressive predominance of decreasing frequencies, increased sensory thresholds and punctual waveform events [16].

NREM always precedes REM in the adult, and is longer and/or deeper if the waking period preceding it has been long or contained vigorous exercise. This is valid for both day to day comparisons in an individual and for species to species comparisons of the average length of the period. In humans, the average is four to five REM bouts of 90-100 minutes each. The time span of the cycle varies in function of the animal and brain size, varying among species and individuals [17].

1.3 Detected Biosignals

In order to correctly detect and manipulate the desired data one must adequately recognize the signals, discarding artefacts and signal components dissociated to the required bio-potential. Consulted bibliography [18] lead us to the following standard values:

- EEG ought to be band-pass filtered for 0.3 - 100 Hz with amplitudes lower than 500μV.
- EMG does not exactly have unique referred values since different muscular contractions can be recorded. For the present evaluation, chin muscular contraction, values were considered to be below 1000μV. Since muscular contractions aren't evaluated according to frequency, the only remark is the use of a high-pass filter with cutoff frequency at 0.3Hz, discarding direct current (DC) component.
- EOG has to be treated in frequency and amplitude. Specifically, bandpass filtered for 0.5 - 100 Hz, discarding DC component, slow eye movements and high frequency noise. Amplitude criteria for artefact detection is also established at 500μV like the EEG.

1.3.1 EEG

As it is known from electrophysiology, neuronal cell membranes at rest maintain an electric potential difference between the axoplasm (i.e. the intracellular fluid) and the surrounding extracellular fluid. In result of this mechanism the intra-cellular fluid has a negative electric potential with respect to the extracellular fluid (in the order of -70 mV). In

biology this potential difference is called the membrane resting potential (strictly spoken this is incorrect, because it is a potential difference). A decrease of membrane potential (i.e. it becomes less negative) is called a depolarisation, and an increase in membrane potential is called a hyperpolarisation. It is important to note that by convention the electric potential of the extracellular fluid always serves as a reference. Neurons are electrically excitable: when the membrane is depolarised to a certain threshold value, an active mechanism is triggered, the Hodgkin cycle[12]. The result of this process causes a transient, spike-shaped fluctuation of the membrane potential, during which the polarity of the membrane potential temporarily reverses (the intracellular fluid becomes positive relative to the extracellular environment). The phenomenon is called an action potential. Action potentials have two important properties:

1. They are a all-or-none phenomenon, meaning that once triggered, nothing can stop the process anymore. The consequence of this is, that the shape and amplitude of an action potential of one particular type of neuron is always identical.

2. Once generated at some location in a neuron, the action potential propagate actively along the cell membrane. Obeying the all-or-none law, the shape and amplitude of the action potential does not change during its propagation.

Crucial to the description of bio-electric phenomena is the notion of a field potential. This is the electrical potential that can be measured at a certain distance from a source of electrical activity. A neuron undergoing membrane potential fluctuations can act as such a source. Such a fluctuation causes an electrical current to flow in the vicinity of the cell (there is spatial and temporal summation, as observed in Fig.1.2). These extracellular ionic currents form the actual origin of the EEG.

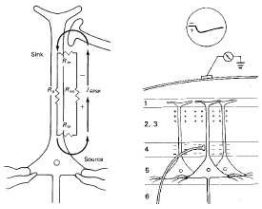

Figure 1.2: Neuronal interference: temporal and spatial summation. [31]

Signal characteristics: Time-domain and amplitude

The EEG amplitude characteristics (see Fig.1.3) vary the conditions under which they are measured as well as the electrode positions. EEG signals may have amplitudes of well over $\pm 100\ \mu$V (and even much higher during epileptic spikes) but often the amplitudes are limited to a much smaller range. EEG activity that does not exceed $\pm 20\ \mu$V is considered as "low-voltage" EEG [19] which incidentally may be encountered in normal healthy adults (but never in healthy children). Amplitudes not exceeding $\pm 10\ \mu$V are called "very low amplitude" and must be considered as abnormal. Finally, absence of cerebral activity of

[12] regenerative, circular sequence of events between depolarization and permeability to sodium occurring in excitable cells: depolarization increases permeability to sodium, thus increasing the entry of sodium (Na^+) into the cell, and the increased concentration of Na^+ further depolarizes the membrane.

over ± 2 μV is considered as "cerebral inactivity" which is a necessary - but not sufficient - condition to diagnose brain death. Modern EEG amplifiers usually have input amplitude ranges of ± 200 μV or higher. A practical consideration is that although the "true" EEG has a limited amplitude range, disturbances (artefacts) may very well induce levels of the input signals that easily lead the amplifiers to saturation, resulting in clipping[13] of the measured signal.

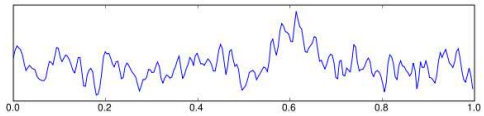

Figure 1.3: One second EEG signal. [30]

Due to the commonly considered noisy[14] character - mixed frequencies - of the EEG signal (see Fig.1.3) a different approach towards the signal analysis gives more relevant results.

Signal characteristics: Frequency

Power spectrum EEG signal analysis reveals that the signal is band-limited, coloured noise, i.e., only frequencies below some maximum exist in the spectrum and not all frequencies contribute evenly to the power spectrum. For monitoring purposes, it is generally assumed that frequencies of interest range from 0.5 to 30 Hz. However, in basic research, much higher frequencies are investigated, typically up to about 70 Hz. In addition extremely low-frequency phenomena with frequencies as low as 0.1 Hz often are investigated in neuro-cognitive research. Frequently the power spectrum contains one clear peak. The frequency at which this peak occurs is called the peak power, or dominant frequency. This is in agreement with the observation of the rhythmical EEG patterns we see in the time domain. Based upon the existence of a dominant frequency, a well known classification of EEG patterns, Δ, θ, α and β bands are recognized.

- Dominant Frequencies 0-4Hz; Δ Classification (Fig.1.4).

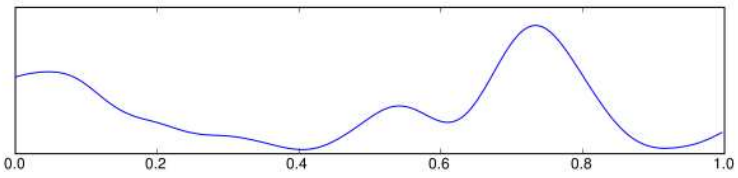

Figure 1.4: 1second Δ signal profile. [30]

Low frequency Δ waves are large, slow brain waves commonly associated with deep sleep. Physiologically these are present in deep sleep, brain injury situations and coma. Certain frequencies in the Δ range also trigger the release of Human Growth

[13] saturation due to the high levels of signal amplification
[14] as in random, stochastic, aperiodic signal

Hormone so beneficial for healing and regeneration. This is why deep restorative sleep is so essential to the healing process.

- Dominant Frequencies 4-8Hz; θ Classification (Fig.1.5)

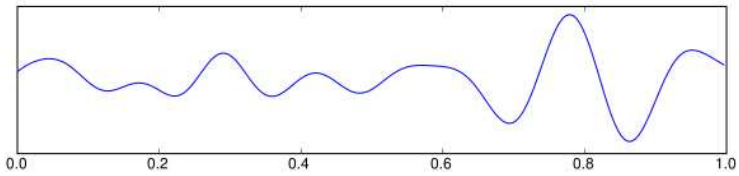

Figure 1.5: 1 second θ signal profile. [30]

This rhythm is associated with various sleep and wakefulness states. Besides sleep stages, θ rhythms are also observed during states of quiet focus, for example meditation [21] and short term memory tasks [22]. Studies have shown that θ waves involve many neurons firing synchronously in the hippocampus and through the cortex. In this sense it was suggested that θ activity is a monitor for hippocampus activity [23]. Other studies suggest θ oscillations have a correlation to various voluntary behaviours, such as, exploration and spatial navigation. Although θ activity has been quite studied its origins and functional significance still remain unclear.

- Dominant Frequencies 8-13Hz; α Classification (Fig.1.6)

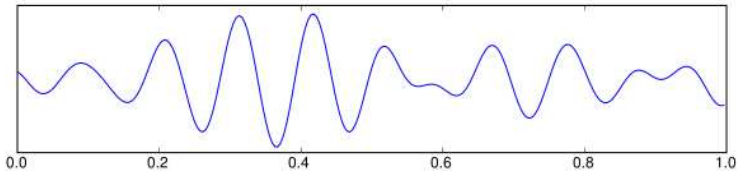

Figure 1.6: 1 second α signal profile. [30]

Also referred as Berger's wave, these waves are predominantly found during periods of relaxation with eyes closed but while still awake. Attenuated with open eyes as well as by drowsiness and sleep, α waves are thought to represent the activity of the visual cortex in an idle state.

- Dominant Frequencies 14-30Hz; β Classification (Fig.1.7)

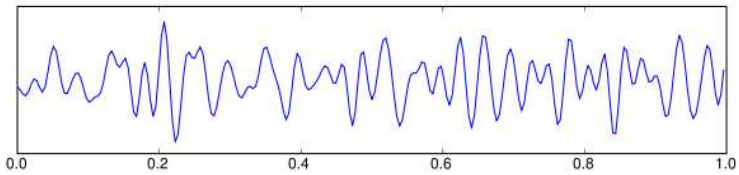

Figure 1.7: 1 second β signal profile. [30]

This frequency band can be internally divided into High β Waves ($\geq$19Hz) β Waves (15-18Hz) and Low β Waves (12-15Hz), although they are physiologically associated to the same events. Beta dominancy is associated with normal awake consciousness. Low amplitude beta together with multiple and varying frequencies is often associated with active, busy or anxious thinking and active concentration. Beta rhythm can be blocked by movement or intention to move (i.e., motor preparation) and tactile (i.e., somatosensory) stimulation.

Rhythmic beta with a dominant set of frequencies is associated with various pathologies and drug effects.

In literature, other rhythms such as μ and γ are often found. When γ waves (Fig.1.8) are identified the subject usually is developing a task that required perception and consciousness. Its frequency band is normally situated around 40 Hz with possible deviations to 26 Hz or 70 Hz (depending on the subject and its condition). Motivating the association with perception and conscience, researches have proven a correlation between the appearance of higher level cognitive activities and the transition of lower frequency γ waves into the 40 Hz range. Other evaluations have associated γ waves with awakening and active REM sleep.

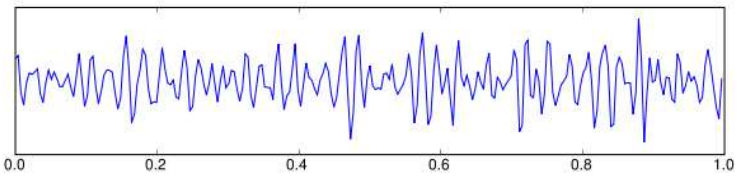

Figure 1.8: 1 second γ signal profile. [30]

Concerning μ waves, they are waves in the frequency range of 8-13 Hz and appear as bursts in the range of 9 - 11 Hz. Its activity decreases with movement or an intent to move, or when others are observed performing actions. It is frequently associated with the motor cortex. These, however, have a much smaller expression and therefore their study is more difficult and its data less informative. Some researchers do not distinguish γ waves as a distinct class but include them in β brain waves; the same happens with μ waves which are associated to the α band. Not exactly a frequency band, but some characteristic waveforms are also recognized and studied (see Fig.1.9)

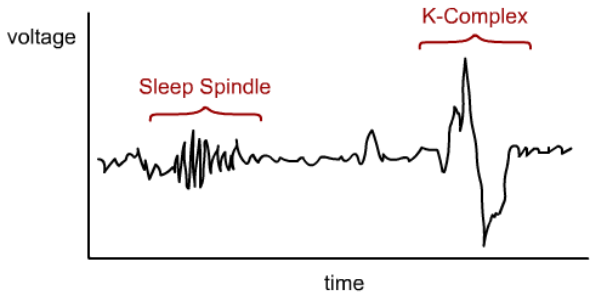

Figure 1.9: Representation of characteristic wave forms:sleep spindle and K-complex. [30]

Sleep spindles Brain activity bursts of 12-16 Hz waves occurring with a maximum duration of 3 seconds. These waveforms are thought to have a protective function of sleep since they inhibit the processing of unnecessary information, which would interrupt sleep. Due to its function they appear more frequently in light sleep in order to protect it.

K-complex Quick high-voltage polyphasic transient (more than 100μV) lasting longer than half a second. These complexes occur when auditory or intrinsic stimulation takes place. Together with sleep spindles they are thought to maintain a person's sleep state. On the other hand, recent findings [33] indicate that spontaneous K-complexes may be part of the non-REM stages, and their increased occurence would lead to the deepening of non-REM sleep.

Literature often mentions that the dominant frequency is roughly inversely proportional to the "level of alertness" of the subject. This observation comes from the fact that in a healthy, alert subject we predominantly see a dominant frequency in the β-range. When the subject is in a relaxed but awake state (particularly with the eyes closed), often α rhythms are observed, and some deeper sleep stages often are associated with dominant theta or even delta activity. Even though several studies were realized in order to prove the previously mentioned considerations, one should keep in mind that sleep criteria discretization is a somewhat utopic task. Such guidelines only describe generalized properties of the EEG and can not be considered golden rules. For instance, in normal sleep, it is common to observe beta-activity during REM (rapid eye movement) sleep, which is known to be the sleep stage during which subjects are most difficult to wake up. Bottom line: there are exceptions to all apparent relationships between EEG-related parameters.

Relation between frequency and amplitude characteristics

The most important global relationship between amplitude and frequency parameters is that EEG signals with a spectral content, which is predominantly in the higher frequency range, usually have smaller amplitudes than signals with dominant frequencies in the lower range. This is understandable since electrical activity of lower frequencies tend to sum up (temporal summation is easier in lower frequencies), augmenting its amplitude making it more visible in the EEG. However, here again one has to be careful not generalizing too easily since it is also arguable that higher frequency waves have a higher material penetration hence being easily detected by the electrodes. It is very well possible that high-frequency EEG patterns have large amplitudes. An extreme example of this is some types of epileptic activity (see Fig.1.10) which contains high frequency patterns with sometimes very high amplitudes. Clearly, the number of neuronal populations involved in EEG generation is of importance in the amplitude of signals.

As stated previously, the standard (and historical) procedure for an EEG analysis is the 10-20 system (1.1). This approach determines the potential differences between subsequent pairs of electrodes. It is based on 10% to 20% proportional distances between anatomic landmarks on the skull and the head (left and right preauricular points, nasion, inion). The measurements can be achieved by the use of an electrolytic gel between the electrodes and the scalp improving the electric conductivity at the contact places. Instead of placing the electrodes one at a time, one may also use an electrode cap.

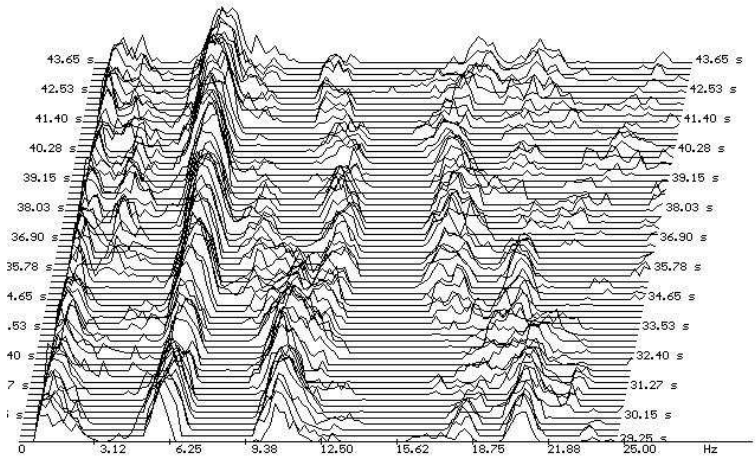

Figure 1.10: Frequency analysis of a epileptic attack - high frequencies are highly expressed. [29]

Besides this method (differential) also referenced electrode setups can be used. This referential technique determines differences in potential with respect to a single common electrode, allowing an amplitude comparison between the signals recorded at the different electrodes.

Lately, this second approach has become more used because several workgroups verified the occurrence of small regional differences between scalp areas critical for the scoring of sleep stages. In this sense, one derivation means easier setups, fewer artefacts to be detected[15] and consequently less "entropy" in the analysis. A differential setup was used in this work, as depicted in Fig.1.11.

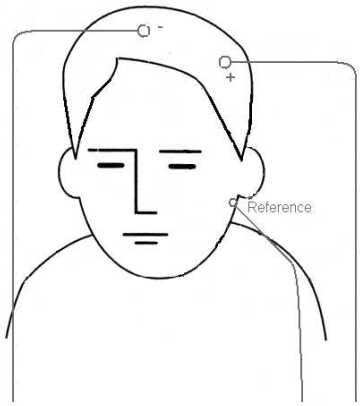

Figure 1.11: EEG Electrode placement. [26]

[15]detection of scalp signals; signals detected by the reference electrode

1.3.2 EMG

This technique serves the purpose of evaluating physiological properties of muscular tissue at rest and during activity. By detecting the electrical potential of muscular tissue one can say if it is contracted, relaxed or even without muscular tonus (see Fig.1.12).

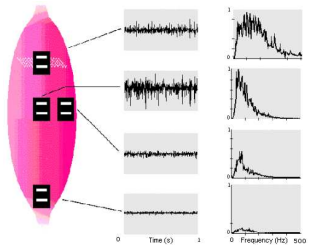

Figure 1.12: Generic muscular contraction detection setup. [28]

Depending on the muscular tissue to be evaluated the signals amplitude have a tremendous variability, so it is not strange that EMG signals can have $0 - 10mV$ peak-to-peak, or $0 - 1.5mV$, or $0 - 1.5mV$ Root Mean Square[16]. Focusing on the frequency domain, the signal is considered to be comprised in the 50 - 150 Hz band. This simply serves the purpose to inform what bandwidth is to be evaluated, avoiding unnecessary frequencies (noise); since EMG frequency analysis is not a common procedure. For the manipulation of the EMG data it is necessary to pay special attention to the fidelity of the signal. One must avoid contamination from electrical noise, which is extremely common in EMG setups. For this purpose maximizing the signal-to-noise ratio[17] must be performed with the minimal distortion of the signal.

In this work an electrode is placed in the submental chin muscle (see Fig.1.13) in order to detect the signal, evaluate its energy and determine whether it is with or without muscular tonus, since atonia[18] is a characteristic of REM sleep stage.

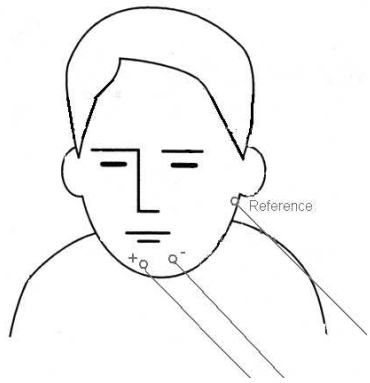

Figure 1.13: EMG Electrode placement. [26]

[16]defined as the square root of the expectation of - x^2
[17]power ratio between a signal and the background noise
[18]muscle tonus loss

1.3.3 EOG

It was not until 1954, with the publication by Aerinsky and Klietman that EOG became a cardinal sign for the classification of REM sleep stage. These Researchers showed that a polygraph device could measure electrical changes around the eyes, allowing the detection of sudden bursts of eye movements cyclically during night. These movements can be detected due to the Cornea Retinal Potential. The eye can be described as a fixed dipole with the positive pole at the corneaand the negative pole at the retina. Therefore electric potentials generated across the Cornea (+) and the Retina (-) (see Fig.1.14) of the eyes as a result of the movement of eyeballs, produce within the conductive skull environment a corneoretinal potential that can go up to 1 mV.

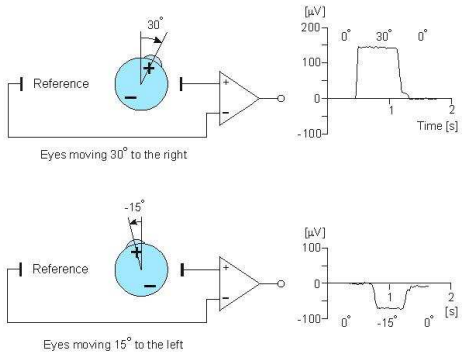

Figure 1.14: electro-oculogram signal generated by horizontal movement of the eyes. [27]

For a correct evaluation, electrode placement must be criteriously followed. In this work, each electrode is placed in the outside of each eye - left outer cantus (LOC) and right outer cantus (ROC) - one a little above while the other is below the eye line (Fig.1.15). It is important that the electrodes have the same reference so that left eye movement is completely out of phase when compared with the right eye movement, allowing the correct detection of horizontal and vertical eye movement, differentiating them from artefacts.

Figure 1.15: EOG electrode placement. [26]

The EOG information associated with the common practice EEG and EMG can "easily" identify REM sleep stages.

1.4 Sleep Stages

Since the early 20th century, human sleep has been described as a cycle, a succession of waking, non-REM stages and REM stage. Although the transition between the different stages and the exact function of each stage is still unknown, they are identified by specific manifestations.

In order to correctly detect and manipulate the desired data one must adequately recognize the signals, discarding artefacts and signal components dissociated to the required bio-potential.

Waking (Fig.1.16 and 1.17) is detected as a relaxed wakefulness.

This stage is a "slow down" condition in which the body prepares for sleep, transiting progressively from a state of tensile muscles with eyes moving erratically into a muscle and eye movement relaxation. This transition is also characterized by specific brain activity.

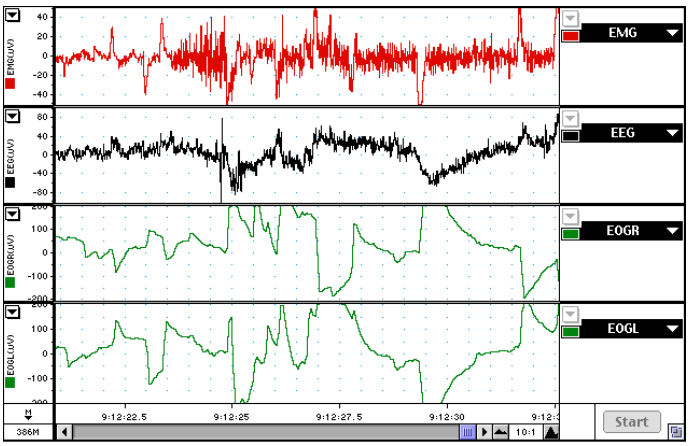

Figure 1.16: Awake subject demonstrating EMG activation and eye movements. [26]

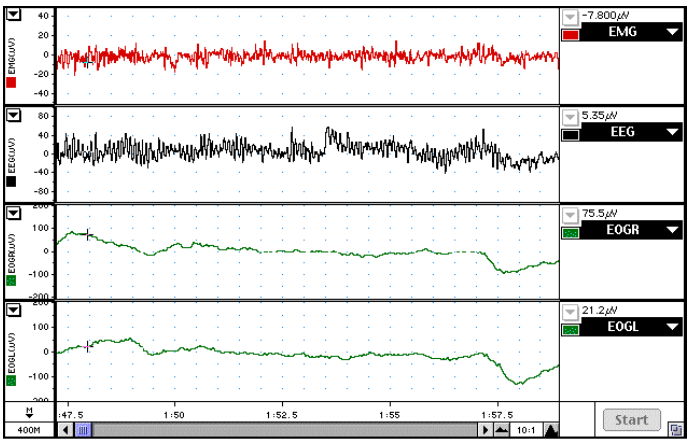

Figure 1.17: Subject with eyes closed and drowsy. Alpha frequency dominates the EEG record. [26]

More specifically, in this stage there are two different types of behaviors:

1) High α background showing occipital α rhythm with closed eyes; low amplitude mixed-frequency EEG with fast eye movements and blinking with open eyes.

2) Poor α producers with possible EEG signal maintenance whether eyes are closed or open.

Some studies evaluated whether α activity is always synonymous of wakefulness [25], stumbling upon two main α activity bands, one 8-12Hz and the other approximately 2Hz slower, which were associated with wakefulness and drowsiness/sleep, respectively.

Stage 1 - NREM1 (Fig.1.18) is usually the first stage in a sleep episode. It is commonly referred as light sleep. In this state a person's eyes are closed, but if aroused from it, he/she may feel as if he or she has not slept. It is defined by a low voltage mixed frequency EEG, with prominence in the 2 - 7 Hz band and absence of slow Δ waves. This stage is usually a small proportion of a night's sleep, occurring frequently only at sleep onset. So when it takes a large proportion of the night it usually indicates a sleep disturbance (or a misdefinition of the sleep stages).

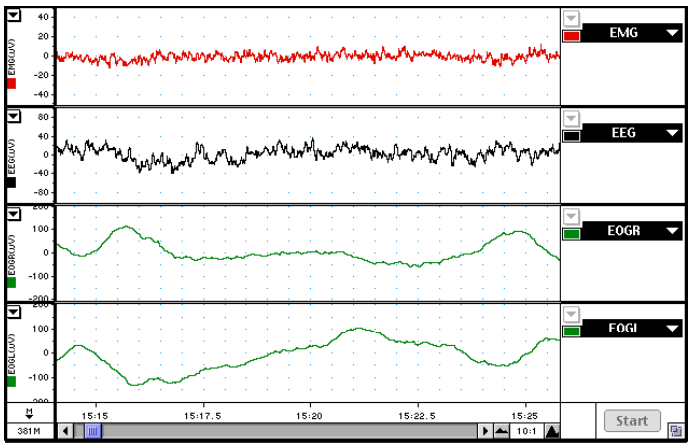

Figure 1.18: Stage 1 sleep. Alpha frequency EEG is no longer present. The EEG is now a lower frequency and amplitude than when awake. Slow rolling eye movements can be seen. [26]

Stage 2 - NREM2 (Fig.1.19) is another period of light sleep during which polysomnographic readings show intermittent peaks and valleys, or positive and negative waves. These waves indicate spontaneous periods of muscle tone mixed with periods of muscle relaxation. Muscle tone of this kind can be seen in other stages of sleep as a reaction to auditory stimuli. The heart rate slows and the body temperature decreases. At this point, the body prepares itself to enter deep sleep. Particularly its onset is characterized by the appearance of sleep spindles and K-complex in a low voltage EEG background activity. Onset of Stage 2 is defined by the first appearance of a 13-14 Hz sleep spindle or K-complex on a low voltage background EEG activity.

On the other hand, and once again introducing entropy into the sleep stages definition, other definitions consider stage 2 sleep a heterogeneous state, therefore defining them according to different criteria. It is assumed that delta activity episodes with amplitude not exceeding 75μV can also be scored as stage 2 sleep, even when sleep spindles and K-complexes are not prominent. This second definition is mainly motivated due to the weak definition of K-complex and sleep spindles.

The recognition of NREM 2 is highly dependent on the decision of what is considered a sufficiently recognizable sleep spindle and K-complex, with a background Δ activity <20%.

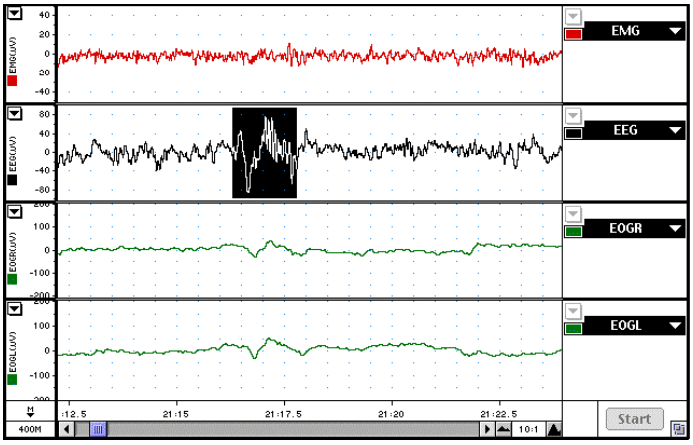

Figure 1.19: Stage 2 sleep. K-complexes and spindles now appear on the EEG record (highlighted). [26]

Stage 3&4 - NREM3&4 (Fig.1.20 and 1.21) also refered as deep sleep, it is standardly identified by its predominant Δ wave component. During these stages (especially Stage 4) the EMG records slow waves of high amplitude, indicating a pattern of deep sleep and rhythmic continuity. Observing these stages one may say that as sleep deepens, Δ wave activity increases (stage 2 <20%, stage 3 20-50%; stage 4 >50%).

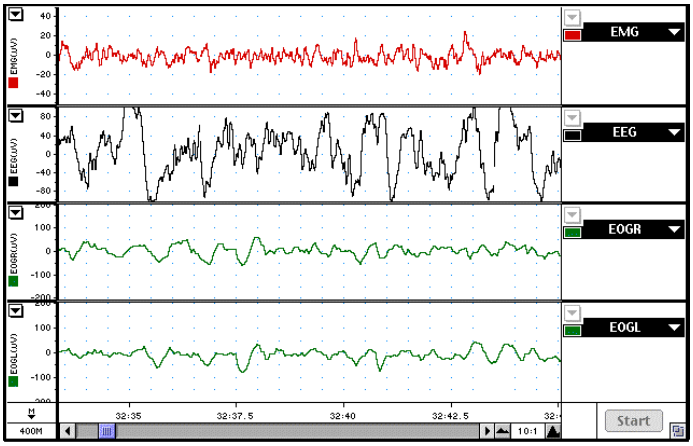

Figure 1.20: Stage 3 sleep. Delta waves (1-2 Hz) now represent at least 50% of the EEG trace. Parallel EOG traces represent EEG artefact. [26]

The previously mentioned stages are globally defined as non-REM sleep (NREM) and last from 90 to 120 minutes, each stage taking about 5 to 15 minutes. Sleep deepens progressively, returning to light sleep and ultimately enters REM stage. A normal sleep cycle - even though there is nothing standard or predefined in sleep - is WAKING, NREM1, NREM2, NREM3, NREM4, NREM3, NREM2, NREM1, REM.

The first cycle, which ends after the completion of the first REM stage, usually lasts up to 100 minutes. Each subsequent cycle REM periods last longer. At the same time

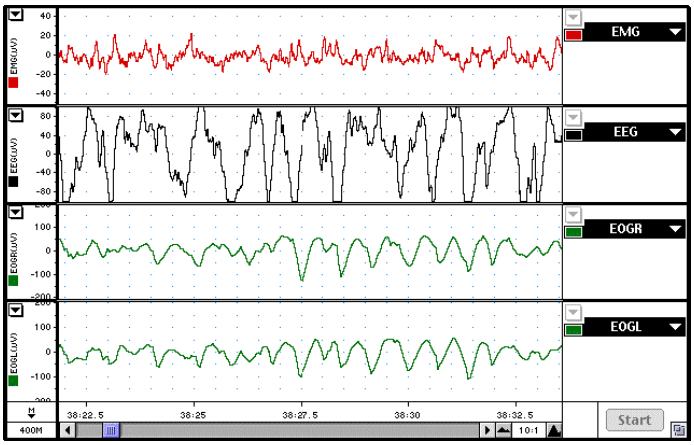

Figure 1.21: Stage 4 sleep. Delta waves (1-2 Hz) now represent at least 75% of the EEG trace. Parallel EOG traces represent EEG artefact. [26]

stage 3 and 4 shorten, leading to a reduced slow-wave sleep. At the end, a person may complete five cycles in a normal night's sleep, increasing REM stage and decreasing stage 3 and 4 each passing cycle.

REM stage (Fig.1.22) This stage is distinguishable from NREM sleep by more prominent changes in physiological states, including its characteristic rapid eye movements. It is usually called paradoxal sleep because of some manifestations: The heart rate and breathing speed up and become erratic, while the face, fingers, and legs may twitch. At the same time paralysis occur simultaneously in the major voluntary muscle groups, including the submental muscles, chin and neck muscles.

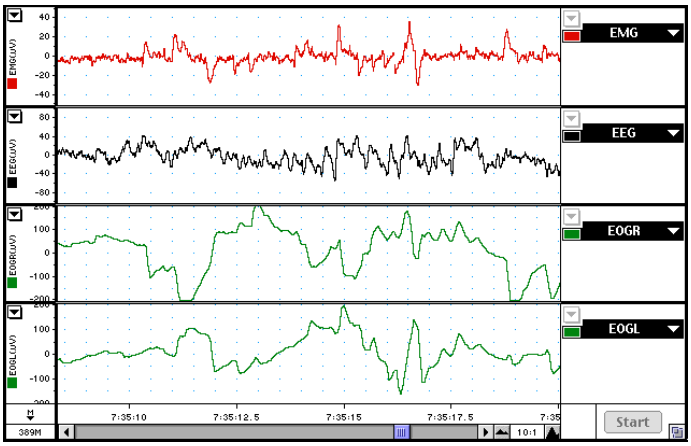

Figure 1.22: Rapid Eye Movement (REM) sleep. Signals similar to Stage 1 with rapid eye movements on the EOG channel and low amplitude EMG signal with sporadic muscle twitches. [26]

Detected brain activity may resemble the Stage 1 pattern. Sleep spindles and K-complexes verified during other sleep stages disappear and REM characteristic saw-tooth waves[19] may occur. By evaluating the α frequency band one can distinguish REM stage from wakefulness by noticing that the α component comprises less than

[19]superimposed rhythm generally manifest as 2- 3 Hz notched triangular waves that occur serially and have the appearance of teeth on a saw

50% of the evaluated epoch and there is no muscle tonus. Motivated by the mentioned intense cerebral activity, dreams occur frequently. A possible justification for the verified atonia is a defence mechanism that avoids the body from acting out the dreams that occur during this intensely cerebral stage. When this mechanism fails pathology occurs. The first period of REM typically last from 1 to 10 minutes, with each recurring REM stage lengthening, and the final one lasting more than half hour. As with Stage 2, the problem of scoring REM is that it is so heavily based on the presence of phasic events rather than continuous parameters.

Summarizing, different sleep stages can be catalogued according to different parameters (see Fig.1.23). These assumptions lead to the development of an algorithm for REM stage detection. This is the main goal of the present work.

Sleep Stage	EEG	EOG	EMG
Awake – eyes closed	α waves	Self control	Tonic activity relatively high; voluntary movement
Awake – eyes open	Low voltage; mixed frequencies	Self control	Tonic activity relatively high; voluntary movement
NREM1	Relatively low voltage; mixed frequencies; θ waves may be highly expressed	Slow eye movements	Tonic activity weaker than awake stage
NREM2	Low voltage; mixed frequencies; presence of sleep spindles and K-complexes	Slow eye movements on sleep onset	Weak tonic activity
NREM3	20% ≤ Δ waves ≤ 50% with variable amplitude	No activity	Tonic activity
NREM4	Δ waves > 50% with variable amplitude	No activity	Tonic activity
REM	**Low voltage; mixed frequencies; presence of θ and slow α waves; absence of Δ waves**	**Rapid eye movements**	**Atonia; muscular twitchs**

Figure 1.23: Summarized sleep stages rules. [32]

Chapter 2

Acquisition System

Someone less attentive could tend to forget that the real world around us is not digital[1] but an analog world and that consequently any signal processing system starts with the acquisition of analog signals[2].

Signals exist in many and various forms, ranging from drum signals to biopotentials. They represent a message, which does not necessarily depend on the nature of the signal. For instance, the mentioned drum signal can be converted by a microphone into an electrical signal for transmission to someplace else, where it will be converted into an optical signal to be recorded on a CD. For a biosignal the path is "slightly" different, yet the concept is similar: It detects a signal (transmission and storage), converts it and then processes it (data manipulation).

Bearing in mind these concepts a data acquisition system (DAQ) was defined [35] based on the following principles:

- High sampling frequency promoting a good signal resolution
- Adjustable amplification allowing a correct fitting of the acquired signals
- Differential input with high common mode rejection[3] (CMR) and input impedance
- Low energy consumption battery powered system (Li-Ion), guaranteeing good autonomy and no hazard for the user
- Portable device
- Electromagnetic compatibility[4]
- Highest possible flexibility. The use of a microcontroller allies optimal performance with the required flexibility for the desired purposes
- Universal Serial Bus (USB) communication with a Personal Computer (PC) for faster data transmission

[1] discrete signal in time and amplitude

[2] continuous signal in time and amplitude

[3] ability to reject a signal which, referenced to "ground" has the same amplitude and phase on both inputs [36]

[4] without causing electromagnetic interference (EMI) and without being affected by EMI from other sources

- Possibility of system update by altering the embedded system

- Low cost device

The present chapter will give general ideas on the DAQ, the motivation for its design and main characteristics.

2.1 Overview

2.2 Acquisition System Design

The previously mentioned signal variability reminds us of the differences between biopotentials and other measured potentials, as well as the intra-differences among biosignals: amplitude range varies in several dimensions; different sampling frequency requirements; relevant bandwidth. Associating this to the environmental bias presented in the following section, it is emphasized the need of a specific acquisition system device.

2.2.1 Environmental Conditioning

One should have in mind that some conditions and factors interfere directly with the signal acquisition. The electric signals are extremely small in amplitude and quite often they are to be acquired in electrically hostile environments. Besides, the human body is made up of much more than three or four biopotentials. In this sense it is necessary to take into account that:

- Measuring the desired biosignals is not dissociable from other biosignals such as skin surface biopotentials; artefacts associated to cardiac rhythm and blood conductivity; undesirable muscular contractions; etc.

- Different tissues have different bioimpedances, therefore different electrode placement may provide different results.

In this sense it is impossible to conceive a generic DAQ, for it is essential to correctly define the desired acquisition characteristics so that the designed system meets the required specifications.

Some interferences can be controlled with the use of filters, others simply have to be recognized and posteriorly discarded.

Therefore extra attention was paid to [35]:

- Electrode placement

- Possible low tissue conductivity[5]

- Movement artefacts

- EMI

[5] corrected by the use of conductive gel

2.2.2 Specifications

The design of the DAQ was based according to the previously stated requirements, resulting into a setup like the one presented in Fig.2.1.

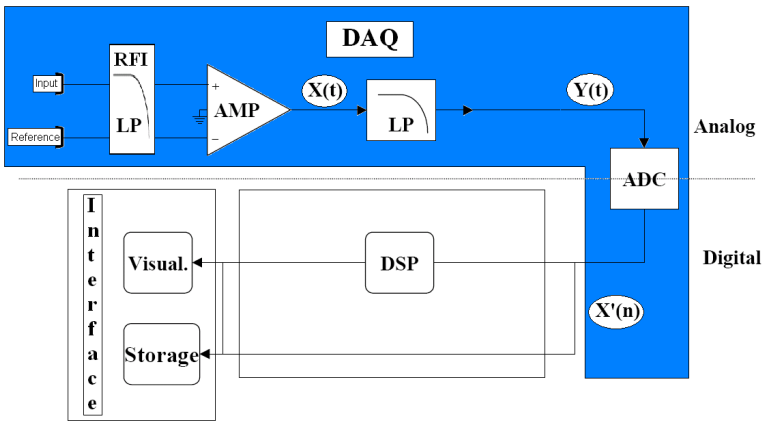

Figure 2.1: Structure of the designed biosignal digital analysis system. The upper branch of the scheme represents analog preprocessing of the signals and the lower branch digital processing steps.DAQ system is highlighted in blue. [31]

According to the suggested structure it is possible to recognize a number of relevant system components.

Transducers - This component converts energy from one form to another for measurement purposes.

Surface electrodes were used in order to detect biosignals as voltages.

Coupling Module - Improves signal quality by filter and amplification procedures.

Knowing that signals may be detected in inappropriate conditions, it becomes clear there is a need for signal processing. To meet these objectives filtering and amplification are used.

Filtering - Assuming "a priori" knowledge of the desired frequencies, filtering allows specific and relevant values to be selected, as well as undesirable frequencies to be discarded (e.g.: band rejection filter for the omnipresent power-line noise). For the purpose of rejecting precise artefacts and frequency bands, an anti-aliasing filterB is used as well as a Radio Frequency Interference filter (RFI) [6].

Amplification - Since an analogue-digital converter (ADC) is later used in the setup, it is necessary to adequate signal's amplitude to the ADC range. Besides, amplification is used to increase signal to noise ratio [7]

Acquisition Module - Is considered setup's core block for it is the one responsible for the data processing.

[6] Low pass filter for noise reduction purpose. [35]

[7] The use of a differential amplifier allows one to selectively amplify signal while maintaining noise as low as possible [63]

This module defines the procedures to be taken, scheduling to be respected and ultimately the communication with the PC. Making a long story short it receives the analog signals, processes them, converting to digital signals, and transmits the data to the PC where it will be manipulated and visualized.

For further Digital Signal Processing (DSP) analysis it is relevant to mention that this block is the one that defines 400 Hz as the sampling frequency, conciliating the system limitations with the desired information to be acquired.

Once the signal is acquired and converted it is transmitted to the Personal computer by a USB connection so that it can be manipulated and visualized through a specific application.

2.3 Interface

As presented in the diagram (Fig.2.2), the defined acquisition system can only play an important role in this project if there is a way to visualize the results and manipulate the acquired data.

Data processing, or more accurately, Digital Signal Processing (DSP), will be the focus of the next chapter. In what concerns visualization and organization of the acquired data, those topics will be analyzed in this section.

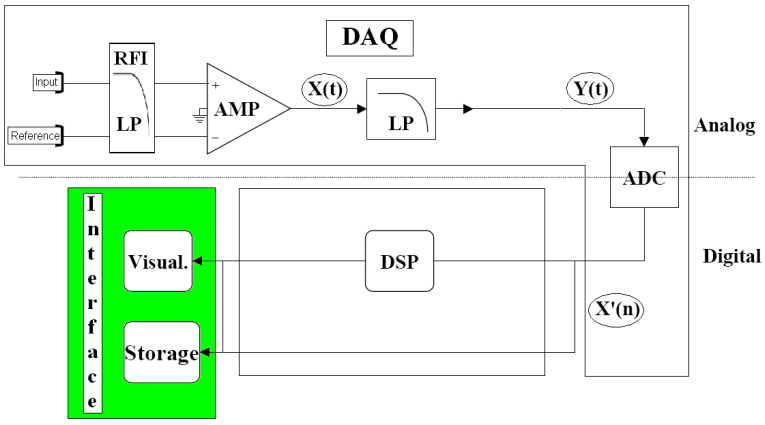

Figure 2.2: Structure of the designed biosignal digital analysis system. The upper branch of the scheme represents analog preprocessing of the signals and the lower branch digital processing steps.Interface system is highlighted in green. [31]

2.3.1 Features and Objectives

The purpose of an Interface is to allow one to reach and manipulate the acquired data. Taking this into account the desired graphical interface was created in a $MatLab^{TM}$ platform, allowing the user to manipulate and visualize data while it is being stored, enabling later evaluations/visualizations.

Since the environment in which this device is supposed to be used is extremely vast, user friendliness is a main goal, and therefore highly regarded in the design of the developed software.

For this purpose, the main characteristics of the designed Interface are [38]:

- Near real time acquisition and display of the EOG, EMG and EEG signals.
- Fast and stable communication with the acquisition device.
- Efficient management of data and record organization in files.
- Minimization of computing requirements.
- Easy access and navigation through extensive recorded signals.
- User friendly post-processor, in order to avoid operator errors and misinterpretations of the exploited data.
- Two available time scales for data visualization, a 30 seconds normal epoch and a more accurate 5 minutes display.
- Optional manual scoring by the use of sleep stage tags.
- Clear display of manual and automatic scoring results.

Data management considerations mainly focused in the amount of data that was recorded and transmitted to the PC. In this sense fast communication was essential (USB communication) so that this could not be the limitative factor for the data to be sampled and analysed.

Chapter 3

Digital Signal Processing

Having briefly explained the DAQ and Interface modules I will now focus on the remaining system component and the goal of this thesis, Digital Signal Processing: REM stage detecting algorithm. First, an overview of several similar (and different) approaches will be presented, followed by the required tools to understand the DSP algorithm. Finally algorithm methodology will be described.

3.1 Literature Review

As aforementioned among sleep researcher and clinicians, there is a need for a cost-effective and easy-to-use tool that can obtain objective, accurate and reliable sleep data in a free-living environment to assist in the screening, diagnosis and treatment of sleep disorders. Several approaches have addressed this need:

- V. Krajca et al. [42] approached sleep identification based on processing of time profiles computed by adaptive segmentation and subsequent classification of signal graphoelements. Adaptive segmentation algorithm criteria were based on frequency and amplitude differences. Consequent graphoelements were evaluated and labelled by experts according to pattern recognition.

- J. E. Heiss et al. [40] developed an Adaptive Neuro-Fuzzy Inference System[1] to classify sleep-waking states. Its methodology is based in the following inputs: five EEG channels; EOG; chin EMG; electrocardiogram (ECG) and limb movements. Transducer's data is evaluated on 20 second epochs assigning the analysed time span to one of five possible classes - wake, NREM1, NREM2, NREM3&4 or REM - according to well defined criteria - presence or absence of: slow delta; theta waves; Sleep spindles; REMs; muscular tone; disturbed cardiac frequency. A neuro-fuzzy classifier is applied on the detected patterns to perform sleep-waking state-stage classification.

- Yoshiharu Hiroshige [41] evaluated sleep stages only through slow eye movement (SEM) evaluation. SEM are a sensitive indicator of lowered consciousness or drowsi-

[1] A neuro-fuzzy system is a fuzzy system that uses a learning algorithm derived from or inspired by neural network theory to determine its parameters (fuzzy sets and fuzzy rules) by processing data samples [54]

ness. A linear regression analysis was applied in each moving window for approximation to the tangent line on the electro-oculogram curve. Results revealed that SEM were more frequent and their duration was shorter at stage wake than at sleep stages NREM1 and NREM2.

- Commercial Body Media's Sense Wear Armband device [39] uses a 2-axis accelerometer, heat flux sensor, a galvanic skin response sensor, skin temperature sensor and near-body ambient temperature sensor to acquire data. Manipulating the gathered information with the aid of an artificial neural network (ANN)[2] the device proved capable of detecting sleep onset, wake, total sleep time and differentiate sleep stages by using completely different approaches than those from traditional polysomnography (PSG). Besides, since it is a portable device it can also be used for other purposes such as daytime activity monitoring.

- P. Van Hese et al. presented a method for the detection of sleep stages only recurring to EEG analysis [43]. This method consists of four steps: 10 second segmentation; parameter extraction; cluster analysis[3]; classification. Parameter extraction evaluated three Hjörth time domain parameters[4], harmonic parameters and relative band energy. Last, classification of every point in a cluster is accomplished according to the manual scoring of the segments corresponding to the constructed codebook vector.

- P. A. Estevez et al. [44] presented another automated pattern recognition system for polysomnography data targeted to the sleep-waking state and stage identification. Five patterns were defined according to: slow-delta and theta wave predominance in the background EEG activity; presence of sleep spindles in the EEG; presence of REM in an EOG; and presence of muscle tone in an EMG. The performance of the automated system was measured indirectly by evaluating sleep staging, based on the experts accepted methodology. Several noise and artefact rejection methods were implemented, including filters, fuzzy quality indices, windows[5] of variable sizes and detectors of limb movements and wakefulness.

- Most accepted automatic sleep classifier, Somnolyzer [45] automaticaly classifies sleep stages based on one central EEG channel, two EOG channels and one chin EMG channel. It follows the decision rules for visual scoring as closely as possible and includes a structured quality control procedure by a human expert. It consists of a raw data quality check, a feature extraction algorithm (density and intensity of sleep/wake-related patterns such as sleep spindles, delta waves, SEM and REM), a feature matrix plausibility check, a classifier designed as an expert system, a rule-based smoothing procedure for the start and the end of stages REM, and finally a statistical comparison to age- and sex-matched normal healthy controls

[2]Computer model, loosely inspired by the neural network structure of the brain, consisting of interconnected processing units that send signals to one another and turn on or off depending on the sum of their incoming signals [55]

[3]method to determine the intrinsic grouping in a set of unlabeled data

[4]activity - mean power of the signal; mobility - estimate of the mean frequency; complexity - estimate of the bandwidth of the signal.

[5]zero-valued function outside a defined interval

(Siesta Spot Report^{TM}). The expert system considers different prior probabilities of stage changes depending on the preceding sleep stage, the occurrence of a movement arousal and the position of the epoch within the NREM/REM sleep cycles. Validation studies proved the high reliability and validity of the Somnolyzer and demonstrated its applicability in clinical routine and sleep research.

Clearly, standard PSG approaches are the most common and currently accepted standards for the diagnosis of some sleep disorders, yet it is not always affordable and accessible due to the size of the equipment, cost, and use in laboratory settings. Besides, as mentioned, several sleep evaluations do not require that much information, achieving their goals only by recurring to one or two parameters. In response, a variety of different approaches (more affordable and portable devices) have been developed for specific sleep conditions. Our setup is an example of such specific detection devices (Fig.1.11, 1.13, 1.15), for its objective is real time REM sleep stage automatic detection.

3.2 Tools

Firstly some data manipulation mechanisms must be presented since DSP is not a simple and obvious task.

3.2.1 FFT

For DSP analysis it is common to study signals spectral density. To do so one must first convert the original time domain signal into frequency domain by approximating a function as a sum of sine and cosine terms plus a constant term. This conversion can be achieved by a tool called Fourier transform. Considering our digital signal, Fast Fourier Transform (FFT) is the adequate tool to accomplish the task [56, 57, 58, 59, 60]. In order to explain FFT it is necessary to introduce Discrete Fourier Transform (DFT). We assume that a data segment of duration T_0 is sampled at a sampling frequency f_s or with a sampling interval T_s (relating each other by $f_s = \frac{1}{T_s}$). The consequent number of samples in a segment is N:

$$N = T_0 . f_s = \frac{T_0}{T_s} \tag{3.1}$$

I will further consider a sequence of samples with the notation $s[n]$, with n the sample index. This means that $s[n]$ is the sample measured at time $t = t_0 + n \cdot T_s$, with t_0 the starting time of the data segment, which by convention will be taken as time 0, so:

$$t = n . T_s = \frac{n}{f_s} \tag{3.2}$$

The basis for spectral analysis is the DFT of a data segment $s[n]$ of length N samples (i.e. $0 \leq n \leq N-1$) which is defined by equation3.3.

$$S[k] = \sum_{n=0}^{N-1} s[n] \exp\left(\frac{-j2\pi kn}{N}\right) \tag{3.3}$$

Here, $S[k]$ are the spectral coefficients which commonly are evaluated only for $0 \leq k \leq N-1$, and j is the imaginary number with property $j^2 = -1$. Together they form the Fourier spectrum of the signal under study. The interpretation of this transform can easily be seen when we look at the formula for a few consecutive values of k. The first spectral coefficient has $k = 0$ and consequently the argument of the exponential is 0. Since $\exp(0) = 1$, this results in simply the sum of all the sample values $s[n]$. Consequently, $S[0]$ is equal to N times the mean value, or Direct Current (DC) offset of $s[n]$. When $k = 1$, we get:

$$S[k] = \sum_{n=0}^{N-1} s[n] \exp\left(\frac{-j2\pi n}{N}\right) \tag{3.4}$$

In this summation, the argument of the exponential takes values from 0 to $-j2\pi(N-1)/N$ in steps of $-j2\pi/N$ (i.e. N steps) and consequently the real and imaginary parts of the exponential form exactly one cycle of a cosine and sine, respectively. What happens is that the original signal $x[n]$ is correlated with a cosine (for the real part) and a sine (for the imaginary part) with a frequency such that exactly one cycle fits within the entire signal period. The frequency of such a sinusoid that fits exactly one period in a segment is called the fundamental frequency. Note that the fundamental frequency is determined only by the choice of the segment length, and has nothing to do with the characteristics of the signal itself. It is now easily seen that for increasing k a similar correlation is made between the original time-domain signal and cosines or sines with frequencies such that exactly k cycles fit within the data segment. A sinusoid that meets this criterion is called the k^{th} harmonic of the fundamental frequency. The index k of a spectral coefficient uniquely determines the frequency associated with that spectral component, $S[k]$, or spectral line. Given the frequency spectrum $S[k]$ of a signal, it is possible to reconstruct the original time series with the inverse DFT (IDFT), equation3.5, where s[n] is evaluated for $0 \leq n \leq N-1$.

$$s[n] = \frac{1}{N} \sum_{k=0}^{N-1} S[k] \exp\left(\frac{j2\pi kn}{N}\right) \tag{3.5}$$

Above we noted that the index k in the spectral coefficients is associated with a harmonic frequency. This means that k is related to the frequency of the k^{th} harmonic. Usually we are interested in real world frequencies, expressed in Hertz (cycles per second). Since it is being presented a DSP approach and later on I will be using the DFT to investigate EEG data segments for presence of Δ, θ, α and β rhythms which are defined as frequency bands in real-world frequencies, it is necessary to transform normalized DFT parameters into true frequencies. Initially presented Eq.3.1 and Eq.3.2 relate real-world parameters (t, T_0 and f_s) and the sample number n, which in fact is the normalised time, and the number of samples in the segment, N. Combining these equations with the definition of the DFT in Eq.3.3 yields:

$$S[k] = \sum_{n=0}^{N-1} s[n] \exp\left(\frac{-j2\pi knT_s}{NT_s}\right) = \sum_{n=0}^{N-1} s[n] \exp\left(\frac{-j2\pi knT_s}{T_0}\right) \tag{3.6}$$

To convert an index k of a spectral coefficient to a "real-world" frequency f we will have to remodel the argument of the exponential in the form $-j2\pi ft$. Recalling that $n.T_s = t$ we thus can see from Eq.3.6 that

$$f = \frac{k}{T_0} \tag{3.7}$$

It was mentioned that the spectral parameters usually are evaluated for the specific values of $0 \leq k \leq N-1$. This is sustained by the evaluation of the DFT definition Eq.3.3. When calculating $S[k]$ for values of k outside this range, we would obtain a periodic sequence in k. In other words, $S[k] = S[k+N]$. Therefore there is no need to evaluate more than N values of $S[k]$ for $0 \leq k \leq N-1$. Using Eq.3.1 and Eq.3.7 this means that we evaluate real-world frequencies between 0 and $\frac{N-1}{T_0} = f_s - \frac{1}{T_0}$.

Bearing in mind Shannon's Theorem (B) stating that a continuous signal of limited bandwidth (i.e. containing only components up to a finite maximum frequency, f_{max}) may be completely represented by a set of equally spaced time-domain samples, provided the sampling frequency is at least $2.f_{max}$ samples per second. One considers whether it is relevant to evaluate frequencies up to f_s. Even though Eq.3.1 and Eq.3.4 are applicable for both complex and real valued signals, since the desired data to be evaluated is a real-valued signal, it will only be necessary to evaluate the first half of the spectral coefficients because the second half is the mirror image of the first $\frac{N}{2}$ coefficients. It is simple to demonstrate this by considering a data segment of 512 samples and 2 sinusoids that match the spectral coefficients with the index 200 and 150: $s[n] = 1.5 \cdot \cos(\frac{2\pi n}{512} \cdot 200) + 2 \cdot \sin(\frac{2\pi n}{512} \cdot 150)$. Evaluating $S[k]$, Fig.3.1.

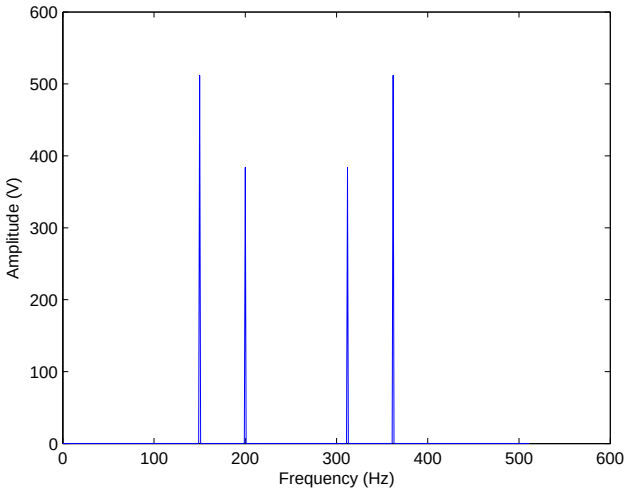

Figure 3.1: Spectral coefficients of the example signal containing only sinusoids.

Four different "spikes" (k=150, 200, 312 and 362) are verified. This confirms that the right half of the graph (k>256) is the mirror image of the left half: $S(k) = S(N-k)$. This property holds for any real-valued signal and is a consequence of the even and odd properties of trigonometric functions, cosine and sine respectively. Due to this phenomenon the center frequency $\frac{f_s}{2}$ is commonly called folding frequency. This symmetric property is verified for the magnitude of the spectral coefficients, for the phase an antisymmetrical relationship exists around the folding frequency, $S(k) = -S(N-k)$.

These statements yield the sufficiency of calculating the spectral coefficients for $0 \leq k \leq N/2$. Another premise that must be regarded is the fact that Fourier analysis assumes a periodic, or repetitive signal. Since the acquired signal is treated as 30 or 5s aperiodic signal epochs, each segment to be evaluated is assumed to be repetitive (see Fig.3.2). This can be seen by taking a closer look at the IDFT equation. If one calculates $s[n]$ for values outside the range $0 \leq n \leq N-1$ it will verify a periodic extension of the original segment.

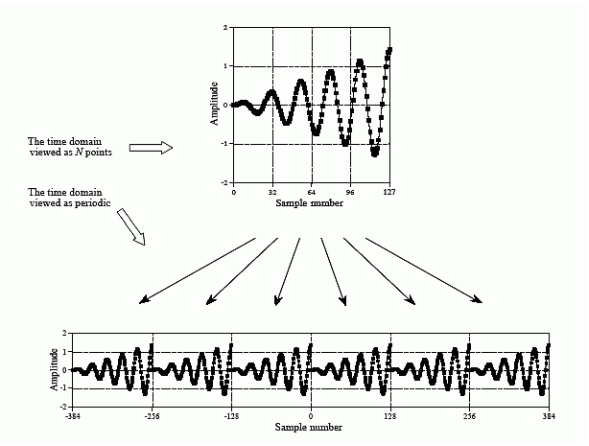

Figure 3.2: Periodicity of the DFT's time domain signal. In the upper figure the signal can be viewed as N samples, while the lower figure represents the signal as an infinitely long periodic signal. [46]

The consequences of this periodic extension in time implies that at the edge of each repetition discontinuities occur, caused by different amplitudes in the beginning and end point of each segment. This happens because a stochastic signal, like the ones measured in this work, contain frequencies that are not exact harmonics of the fundamental frequency. Those non-harmonics are associated with frequencies that do not fit exactly within an integer number of periods in the segment. Consequences arise from this condition. Using the previous example and applying some modifications so that the signal will contain one harmonic and one non-harmonic, $s[n] = 1.5 \cdot \cos(\frac{2\pi n}{512} \cdot 200.5) + 2 \cdot \sin(\frac{2\pi n}{512} \cdot 150)$, one can verify signal spectral modifications in Fig.3.3

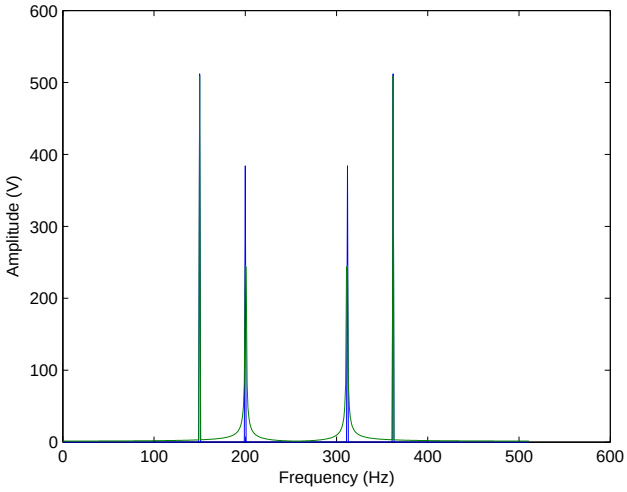

Figure 3.3: Spectral coefficients for two example signals. Blue signal consisting of two harmonic sinusoids; Green signal consisting of a harmonic and one non-harmonic sinusoid.

Beside the peaks at $k = 150$ and $k = 362$, corresponding to the sine-term, two spread components around $k = 200$ and $k = 312$ are also visible. This phenomenon is called spectral leakage and is caused by discontinuities in the extended signal of the data segment (see Fig.3.2).

A method to decrease this undesired phenomenon is windowing, a multiplication of the original signal with a window function so that the discontinuities at the segment edges are reduced or even completely removed. Even though this operation causes distortion of the computed spectrum it is in general less severe than the distortion caused by spectral leakage. In short, the DFT results in a discrete spectrum, containing values for only a finite number of frequencies. The step-size in the spectrum is uniquely determined by the duration of the segments, frequency step= $\frac{1}{T_0}$.

Let us now pay attention to the efficiency of this processing tool. In the practical application of the DFT the number of necessary operations is very important, since it determines the amount of time spent or the required processing capacity of the device. Assuming a N point DFT, and by looking at Eq.3.3, for each frequency entry $S[k]$, N multiplications and $N - 1$ additions occur. For each spectrum N^2 multiplications and $N(N-1)$ additions are accomplished. The direct calculation of an N-point DFT requires a number of operations (complex or not), of the order of magnitude of N^2. This amount of operations motivated several researchers to develop numerical methods that require fewer operations. These procedures intended to calculate a number of DFT's of shorter length ant then to combine the results appropriately. These methods are denoted as "Fast Fourier Transform". The most widely used, and applied in this work, are the FFT algorithms, where N is an integer power of 2, so that $N = 2^X$. When the number of samples is not $N = 2^X$, zero padding is done until $N = 2^X$ samples is reached. These algorithms allow one to reduce the number of operations required to the order of magnitude of $N \cdot \log_2 N = N \cdot M$.

Table3.1 gives a summary of the required operations for each case, and the last column shows how many times the speed of calculation can be increased by using an FFT instead of a direct calculation of the DFT.

	DFT	**FFT**	**DFT/FFT**
N	N^2	$N \cdot \log_2 N$	$N/\log_2 N$
2	4	2	2.00
4	16	8	2.00
8	64	24	2.67
16	256	64	4.00
32	1024	160	6.40
64	4096	384	10.67
128	16384	896	18.29
256	65536	2048	32.00
512	262144	4608	56.89
1024	1048576	10240	102.40
2048	4194304	22528	186.18

Table 3.1: Comparison between the number of operations in a DFT and a FFT

Plotting the previous table3.1, FFT advantages are even more clear (Fig.3.4).

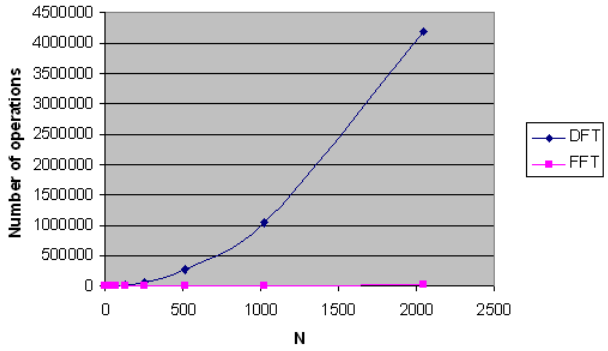

Figure 3.4: Comparison between the number of operations in a DFT and a FFT

To better comprehend FFT mechanism a N point DFT will be executed by calculating 2 $N/2$-point DFT's and combining the result. Assuming a discrete signal $s[n]$ of length N. Defining 2 signals, each one with a length of $N/2$ and which consist of the even and odd values of $s[n]$, $s_1[n] = s[2n]$ and $s_2[n] = s[2n+1]$ respectively.

Considering the literature accepted twiddle factor $\exp\left(\frac{-j2\pi}{N}\right) = W_N$, $s[n]$ can be expressed as:

$$S[k] = \sum_{n=0}^{N-1} s[n] \cdot W_N^{nk} = \sum_{n=0}^{(N/2)-1} s[2n] \cdot W_N^{2nk} + \sum_{n=0}^{(N/2)-1} s[2n+1] \cdot W_N^{(2n+1)k} \tag{3.8}$$

Using $W_N^{2kn} = W_{N/2}^{kn}$:

$$S[k] = \sum_{n=0}^{(N/2)-1} s_1[n] \cdot W_{N/2}^{nk} + W_N^k \cdot \sum_{n=0}^{(N/2)-1} s_1[n] \cdot W_{N/2}^{nk} \tag{3.9}$$

And consequently $S[k] = S_1[k] + W_N^k S_2[k]$, with $S_1[k]$ and $S_2[k]$ the $N/2$-point DFT of $s_1[n]$ and $s_2[n]$ respectively. Analysing the number of operations associated with these small DFTs, one verifies that it is of the order of magnitude of $(N/2)^2$, and therefore total $2(N/2)^2 = (N)^2/2$.

There is also the calculation of the $W_N^k S_2[k]$ and $S_1[k] + W_N^k S_2[k]$ for all the values of $S[k]$. For large values of N, the total number of operations nevertheless remains of the order of magnitude $N^2/2$. This indicates a 50% gain in comparison with a direct application of DFT to the whole signal.

If one considers each half signal to be even and therefore splitable in half so that this mechanism can be applied iteratively until 2 point DFT is reached, this algorithm implies a huge gain when compared with standard DFT.

The act of combining the "splitted" DFTs can be represented by the FFT butterfly (Fig.3.5).

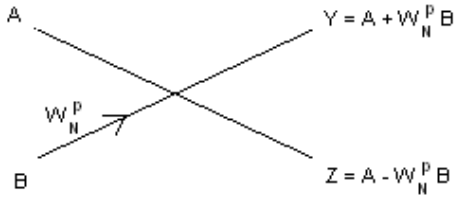

Figure 3.5: FFT butterfly. A and B - complex numbers ; W_N^p - Twiddle factor with p an integer between 0 and $N-1$

The FFT butterfly with $p = 0$ represents exactly the relation between the input samples $s[0] = A$ and $s[1] = B$ with the output samples $S[0] = Y$ and $S[1] = Z$ of a 2-point DFT. Therefore an 8-point FFT butterfly example can be represented as in Fig.3.6.

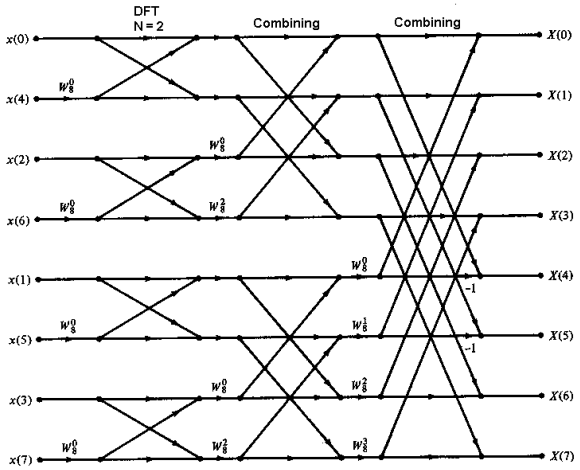

Figure 3.6: Detail of an 8-point FFT [47]

Evaluating this 8-point FFT it is verified that there are three successive steps, each containing four butterflies which each having one complex multiplication factor. In this way, for an arbitrary N-point FFT (where N is an integer power of 2), a number of $\log_2 N$ steps is determined, each containing $N/2$ butterflies. As initially presented, an FFT calculation following this pattern requires $(N/2) \cdot \log_2 N$ complex multiplications. Other spectral analysis are used in signal processing methodologies, however they require a larger timespan to process the data, and this is not appropriate for the present work since real time REM detection requires fast DSP tools. As previously mentioned, "Fast Fourier Transform (FFT) is the adequate tool to accomplish the task" of DSP.

3.2.2 Digital Filters

Signals passing through different mediums suffer different modifications, therefore it is not a complete nonsense to say that everything can be considered a filter. But one must have in mind that some mediums are conceived for that purpose while others are

not, therefore their interferences in the signal are quite different. In this sense, a more realistic definition for filter is a circuit (or an algorithm) that converts an input signal into an output signal whose spectrum is related in a controlled way to the spectrum of the input signal - suppression and/or attenuation of specific frequencies. There are two different types of filters.

Analog Filters are used before the signal is digitized. They have the disadvantage of tending to distort time relationships in the signal because of phase shifting [48].

Digital Filters are applied to the already digitized signal. These do not necessarily cause temporal distortion in the signal, although they have the disadvantage of being very expensive from a calculation point of view, especially when long filters are used and processing time is crucial.

Since I will be focusing on the DSP module, discrete filters are the ones to be applied, and hence they will be here presented. As mentioned, a digital filter is just a filter that operates on digital signals by performing numerical calculations on the sampled values. Hence, a computational routine is sufficient for the purpose.

The design of a discrete filter starts with a specification of the frequency behaviour required. These specifications usually take the form of a tolerance diagram as it is represented in Fig.3.7.

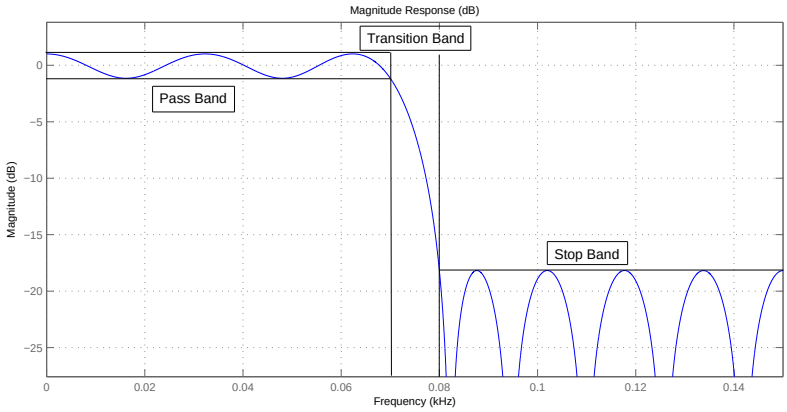

Figure 3.7: Example of a tolerance diagram for the amplitude characteristic of a low pass filter

In order to fulfil the objectives the signal must not leave the delimited areas in the pass and stop band. The amplitude deviation in the pass band is related to the maximum error allowed so that $ampl \geq x - \delta$ and $x - \delta \geq ampl \geq x - \delta$, and for the stop band a deviation is also considered.

Starting from the presented filter specifications implies that the design process contains the following stages:

- Deciding whether the desired frequency characteristics will be achieved using a Finite Impulse Response (FIR) or a Infinite Impulse Response (IIR) filter.

- Defining the filter order and calculate the coefficients of the system function of the filter.

FIR filter

The most essential feature of a FIR filter is by definition the finite length of the impulse length. For this reason the impulse response has a central part in the filter design process.

FIR filters can be designed as presented in the following example: Starting with the ideal continuous frequency response $H_d(\exp^{j\theta})$ that one pretends to mimic, a low pass filter for $\theta \leq 0.4\pi$ (Fig.3.8).

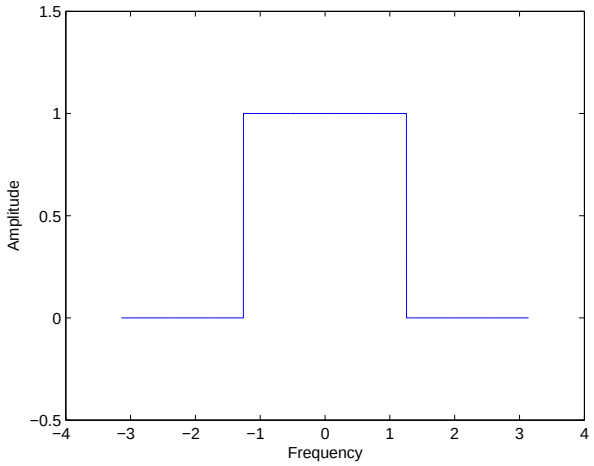

Figure 3.8: Example of a tolerance diagram for the amplitude characteristic $H_d(\exp j\theta)$ of a low pass filter

Making use of the Inverse Discrete Time Fourier Transform (Inverse DTFT[6]) an ideal impulse response $h_d[n]$ is found in Fig.3.9.

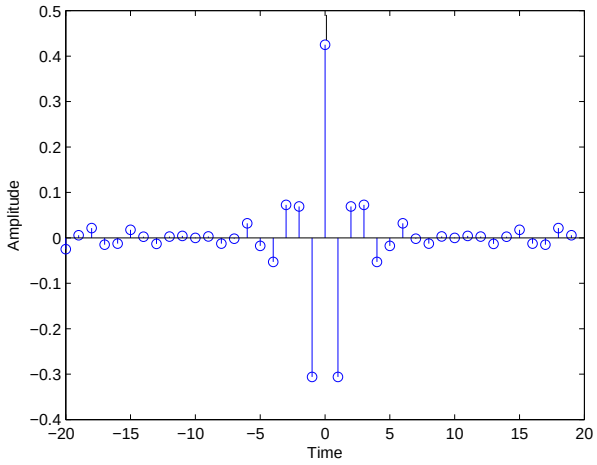

Figure 3.9: Ideal filter time domain signal $h_d[n]$

However, these coefficients can not be applied immediately as a filter due to: long (or even infinite) duration of the impulse response; non-causal[7] characteristic of $h_d[n]$,

[6]Fourier transform tool that creates a continuous and periodic spectrum from a discrete "time" function.

[7]causal systems use only previous samples from the input or output signal

opposed to the required real-time causal condition of the FIR filter. In order to adapt the previous impulse response one must: limit the signal's length (Fig.3.10).

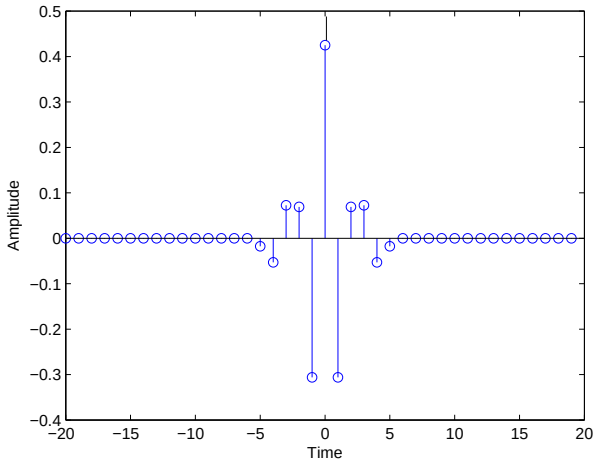

Figure 3.10: Truncated filter time domain signal $h_d[n]$

Followed by the introduction of sufficient number of delays, as represented in Fig.3.11. In this way a limited and causal impulse response is obtained, defining the filter coefficients.

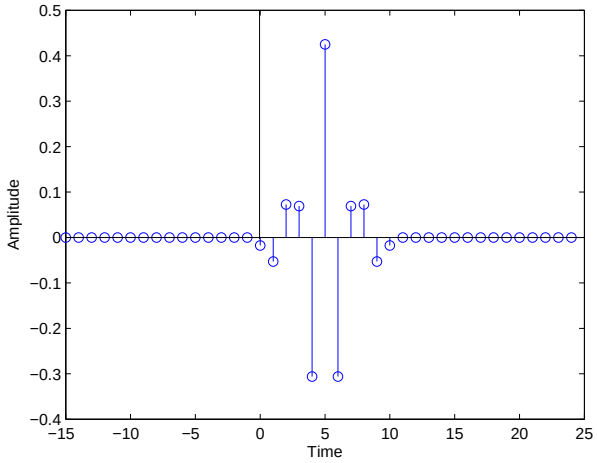

Figure 3.11: Shifted filter time domain signal $h_d[n]$

Although the described approximations lead to the desired filter they also introduce recognizable errors. Truncation implies frequency amplitude errors, while the introduced shifts lead to extra linear phase shift (for further reading on this subject consult [49]) while. These amplitude errors are expressed in different oscillatory variations created in both the pass and stop band, most prominently in the vicinity of the designed filter steep transitions.

If one bears in mind that a multiplication in time domain is a convolution in frequency domain and the truncation is a multiplication of the infinitely long signal in the time domain with a rectangular window of the desired length, then, truncation is understandable

as depicted in Fig.3.12.

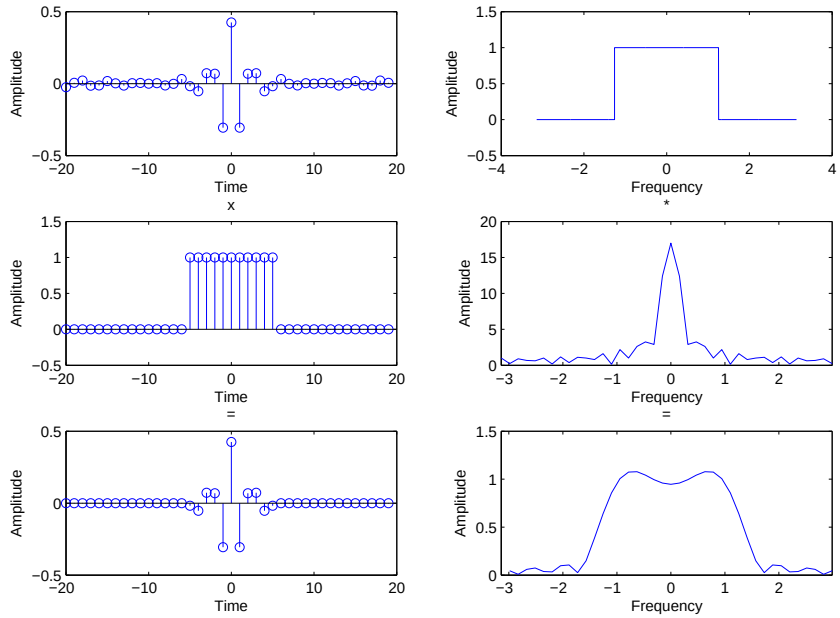

Figure 3.12: Time domain signal truncation. Left column: Time domain multiplication. Right column: Frequency domain convolution

Data manipulation in Fig.3.12 denotes the previously mentioned introduction of frequency amplitude errors. In order to minimize these interferences it is possible to apply different window functions, so that windows frequency characteristic ($W(\exp^{j\theta})$) have the narrower main lobe possible and low energy side lobes.

The described design method results in discrete filters which break away from the ideal filter characteristics mainly near the transition bands.

Away from the transition band such errors are in general much smaller. It is more logical, however, to distribute these approximation errors as evenly as possible over all the frequencies. In fact, this procedure provides the smallest maximum error, which occurs not once, as in the previous method, but several times. Such filters are called Equiripple [61]. The maximum error in the pass band can also be different from the maximum error in the stop band. Such filter was used in this work due to the previously mentioned advantage in comparison with other FIR filters.

The IIR filters were not considered since they provided undesirable characteristics for the purpose of this work: linear phase can only be approximated; the filter can be unstable; the initial state of the memory elements and any brief interfering signals can affect the output signal for an infinite length of time (IIR main characteristic).

In opposition, FIR filters: phase characteristic allows a exactly linear phase response; are always stable; initial state of the memory elements and any brief interfering signals (e.g. via the supply) can affect the output signal only for the length of the impulsive response.

Before defining the designed algorithm, another mathematical tool is here introduced. Independent component analysis (ICA) application was later tested for the removal of undesired events in specific signals.

3.2.3 ICA

This mathematical technique is a statistical and computational approach to identify hidden factors merged into a set of mixed signals. It allows one to separate independent sources linearly mixed in the acquired signals. As a multivariate data processing tool it processes the (assumed) linear mixtures of signals in order to identify each independent component, fraction of the mixed signal. From the starting point, from the acquired signals, a linear combination of the different sources is represented as Eq.3.10.

$$x_i = a_{i1}s_1 + a_{i2}s_2 + ... + a_{in}s_n \tag{3.10}$$

Matricial representation lead us to Eq.3.11:

$$x = A \cdot s, \tag{3.11}$$

With x the mixed signals, A a matrix with weight factor for each independent component and s the independent components. A representative situation of ICA analysis is depicted in Fig.3.13 and 3.14, in which the original components (assumed independent) are retrieved from the mixed signal.

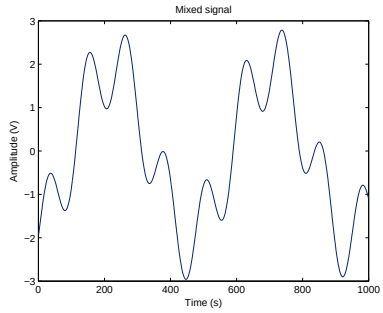

Figure 3.13: Mixed signal

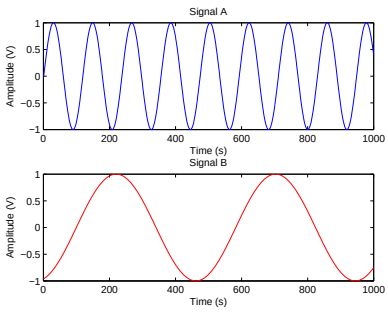

Figure 3.14: Independent components

The present problem is not linear since the values of matrix A and vector s are unknown. One can only observe the random vector x, estimating A and s. Therefore, some assumptions are made to promote its resolution: 1) s_i components are statistically independent; 2) s_i components have nongaussian distributions. Once matrix A is computed,

its inverse W is known and s_i are calculated. The used algorithm for ICA is FastICA algorithm [71], a computationally highly efficient method for performing the estimation of ICA. It uses a fixed-point iteration scheme that has been found in independent experiments to be 10-100 times faster than conventional gradient descent methods for ICA. This methodology uses as starting point the non-independent mixed signals, made up by the different independent components, and by manipulating the data towards nongaussianity of the signals it is possible to reach the independent components. Schematically, Fig.3.15.

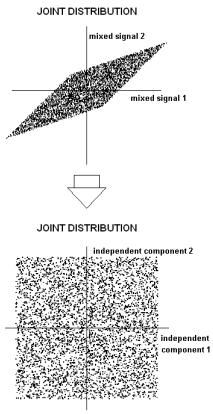

Figure 3.15: Manipulation towards Independent Components

This methodology has some drawbacks:

- One cannot determine the variances (energies) of the independent components. The reason is that, both s and A being unknown, any scalar multiplier in one of the sources s_i could always be cancelled by dividing the corresponding column a_i of A by the same scalar. As a consequence, we may quite as well fix the magnitudes of the independent components. As they are random variables, the most natural way to do this is to assume that each has unit variance. Then the matrix will be adapted in the ICA solution methods to take into account this restriction, complicating the energy analysis of the studied signals. Note that this conditions brings another complication, ambiguity of the sign: we could multiply the independent component by -1 without affecting the model. While this ambiguity is, fortunately, insignificant in most applications, for signals such as EOG registers it is unacceptable, since one expects out of phase registers of the two signals.

- One cannot determine the order of the independent components. The reason is that, again both s and A being unknown, we can freely change the order of the terms in the sum in Eq.3.11, and call any of the independent components the first one. Formally, a permutation matrix and its inverse can be substituted in the model. The newly defined matrix is just a new unknown mixing matrix, to be solved by the ICA algorithms. So the problem remains.

3.3 Algorithm

Having described the required tools for the DSP module, EEG, EMG and EOG signal processing methodology will now be presented (Fig.3.16). Firstly, three different algorithms were defined for the analysis of each signal. Later on, an "all-in-one" algorithm was designed with the goal of a real time REM evaluation.

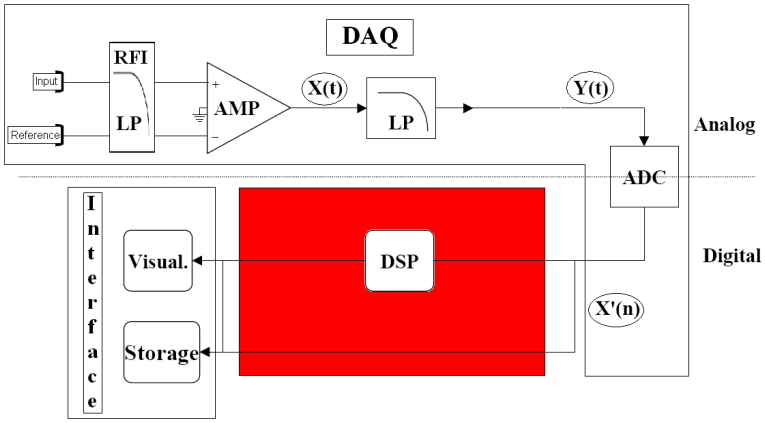

Figure 3.16: Structure of the designed biosignal digital analysis system. The upper branch of the scheme represents analog signal preprocessing and the lower branch digital processing steps.DSP system is highlighted in red. [31]

3.3.1 EEG Algorithm

As mentioned in chapter1, in what concerns the EEG, the goal of the work was to identify pattern detection schemes for REM sleep staging. Bearing this in mind, and Fig.1.23, a well designed algorithm could be conceived, represented in Fig.3.17.

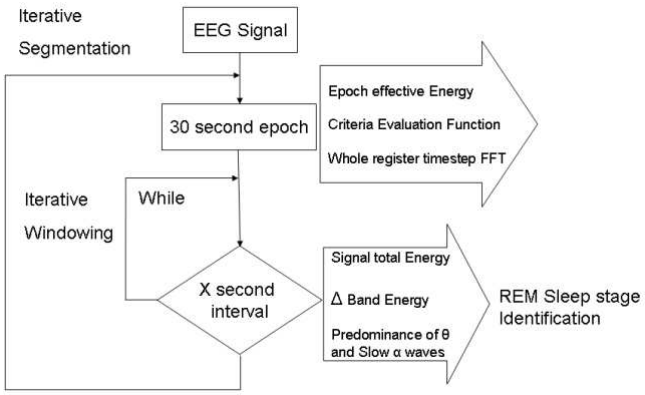

Figure 3.17: Suggested EEG Algorithm.

This approach uses as inputs: EEG data vector; acquisition time[8]; duration of the time fraction to be analyzed at each step; signal duration to analyze. In this study, each time-step was defined as five seconds intervals. With the inputs specified other important variables are defined: sampling frequency; frequency resolution; time and frequency domain axis specification; number of epochs to be evaluated. These are followed by the definition of vectors that will be used as outputs: REM epochs identification; epoch effective energy[9]; windowed total signal time-step FFT; ratio of epoch's maximum and effective value[10]. This last vector is used to evaluate possible high subject signal variability so that dynamic criteria definition is implemented if necessary. Fixed values were assumed for each criterion since EEG biological signals shown low variability (Appendix C). Criteria were established in order to detect EEG REM sleep stage characteristics. Threshold conditions were defined, based on test subjects signal evaluation, for: total energy value (35 μV RMS); Δ band energy value (25 μV RMS); low α band expression, with α activity being less than 50% of the total signal energy, or in poor α wave subjects a predominance of θ and slow α waves. This last characteristic distinguishes REM sleep stage from awake condition. Once the starting conditions and criteria have been defined, signal processing begins with segmentation step (Fig.3.18). This segmentation will always evaluate a 30 second signal period.

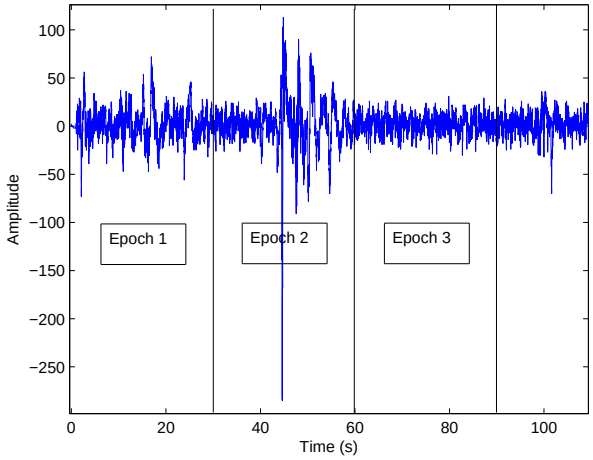

Figure 3.18: Example of an EEG signal segmentation.

In order to achieve a better resolution, and consequently a better identification of REM sleep stage periods, each epoch segment is analyzed according to the defined input fraction value. Five seconds was the applied window in the present work. A FFT tool is applied to each five second window in order to assess the desired characteristics.

[8]The acquisition time is used to calculate the sampling frequency, but the oposite could have been implemented.

[9]Epoch effective energy = Epoch energy minus Mean Energy

[10]Effective value or Root mean Square (RMS) is equal to the standard deviation of the signal considering the time a real variable with an uniform probability density function - $RMS = \sqrt{1/N \sum x^2}$ [65]

An example of such process is represented in Fig.3.19.

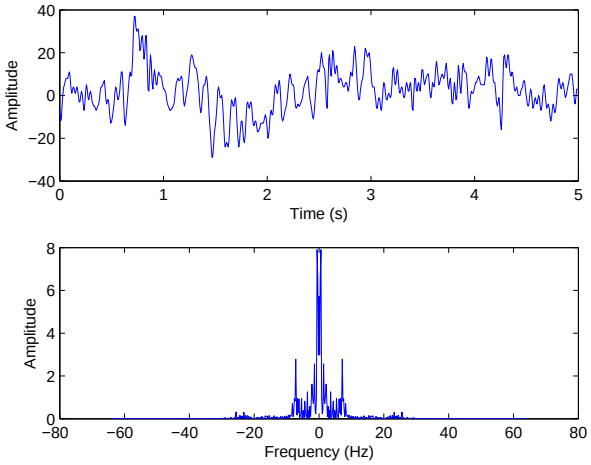

Figure 3.19: Example of signal analysis. The upper picture represents a 5 second EEG signal, while the lower picture represents the corresponding FFT transform.

The vizualized window is analyzed according to well defined features for REM sleep stage detection:

- Absense of Δ band activity
- Low α wave activity or predominance of θ and slow α waves
- Low amplitude signal

Once the total epoch has been analyzed, for each criterion, if $\frac{2}{3}$ of the epoch time span verifies the REM sleep stage condition, then that feature attributes a one third probability that the subject is in REM stage sleep. The one third value is atributed since there are 3 features with equidistributed weights for the EEG analysis.

As well as a REM episod detector, the algorithm exports a energy vector concerning each epoch and a whole register timestep FFT for criteria and frequency periodicity analysis, respectively.

3.3.2 EMG Algorithm

The EMG data acquisition system records data from the potential differences of electrodes on the chin, reflecting the muscle tone of a subject.

Knowing that atonia is a characteristic REM feature, the function of this algorithm is then to detect this occurrence, relating it to REM stage. Besides considering atonia, one must also bear in mind that possible sporadic muscular contractions may occur in the middle of a REM stage without disturbing or causing any stage transition.

Therefore periods of muscular atonia as well as periods with higher energy but with fast muscular contractions are detected as REM epochs.

Since no specific frequency band is attributed to muscular contractions, and no frequency analysis has proven to be relevant for the muscular DSP, only time domain analysis is performed.

A schematic of the designed algorithm is presented in Fig.3.20.

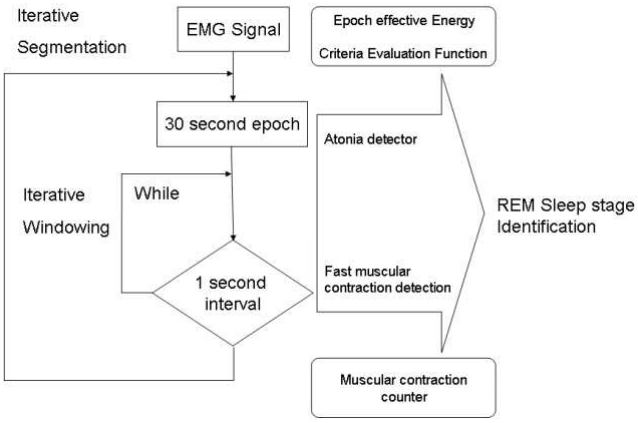

Figure 3.20: Suggested EMG Algorithm.

Similarly to the EEG approach, the EMG analysis also requires the following inputs: EMG data vector; acquisition time; epoch duration; signal duration to analyze. From these, other variables are defined: sampling frequency; time axis specification; number of epoch to be evaluated. After these calculations, besides the output vectors common to the EEG analysis (REM epochs identification; Epoch effective energy; ratio of epoch's maximum and effective value), counters for fast and slow muscular contractions were defined. Criteria definition is the next step of the procedure. Threshold values are defined constant since there is no significant signal variability (Appendix C). Therefore, atonia threshold values is defined for 5 μV RMS, while a 7μV amplitude signal variation is considered for the detection of fast muscular contractions in half second intervals.

Once the starting conditions and these criteria have been met signal processing begins with segmentation step. This step is similar to the EEG segmentation being timed in epochs and its energy calculated. If the RMS of the epoch is above the defined threshold it is possible that the evaluated interval is a NREM stage epoch (Fig.3.21), if not, one consider it to be a REM epoch (Fig.3.22).

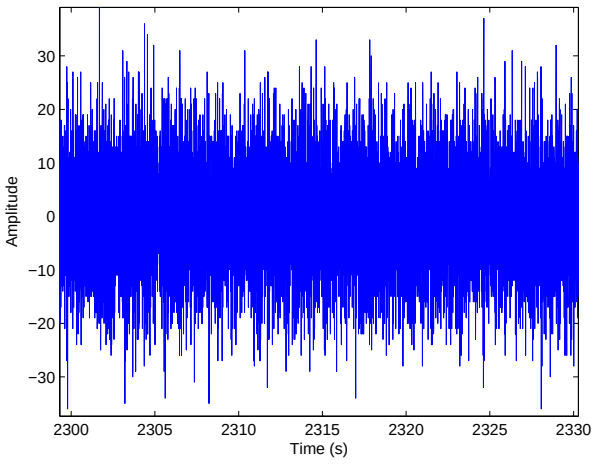

Figure 3.21: thirty second NREM epoch EMG register.

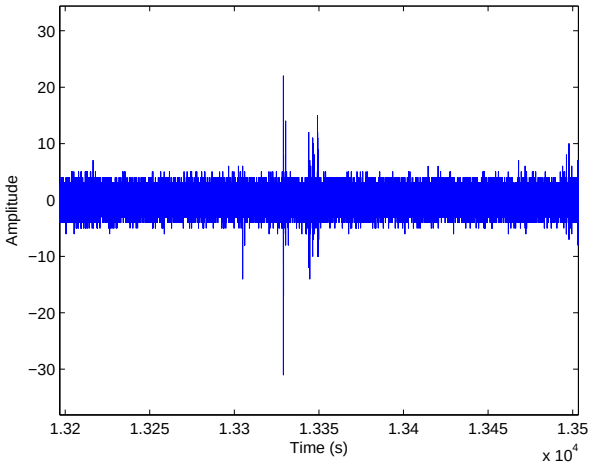

Figure 3.22: Thirty second REM epoch EMG register.

For the detection of fast muscular contractions one can not analyze the signal in a epoch time, instead windowing is applied in order to analyze more precisely each second of the epoch (see Fig.3.23).

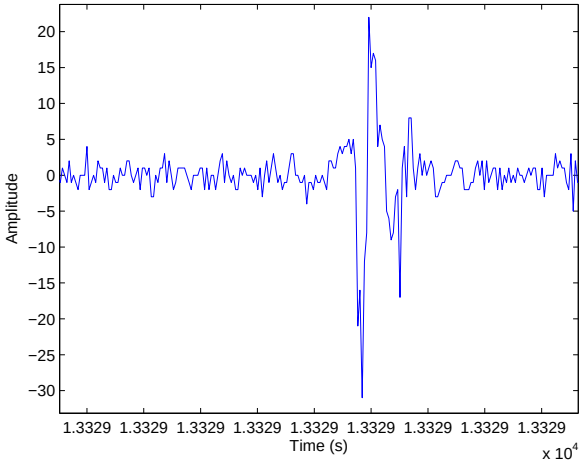

Figure 3.23: One second EMG data with fast muscular contraction.

This windowed signal is then split into half and both the resulting 0.5 second signals are evaluated in order to calculate its maximum variation ($EMG_{max} - EMG_{min}$). For a REM identification the maximum variation of one half second must be below the defined threshold while the other half must be above it. Since continuous fast muscular contractions may in fact be a slow twitch or even muscular tonus, the algorithm considers three muscular contractions in a row to be identified as a slow contraction and therefore discards the possibility of identifying the epoch as a REM period.

EMG analysis will consider an epoch to be REM if atonia is verified or, in cases where the RMS is higher, if this increase of energy is due to the presence of fast muscular twitches. Besides the REM stage detector, this algorithm also outputs an energy vector concerning each epoch and a muscular contraction counter for fast and slow twitches.

3.3.3 EOG Algorithm

The acquired EOG signal by measuring potential differences between the front and back of the ocular globe (see Fig.1.14) allow a correct monitoring of the eye movements. For this project, identification of REM sleep stage, the detection of synchronous and fast eye movements is essential. Rapid eye movements are detected as saccadic waves with phase-reversed synchrony in the left and right EOG channels. In this analysis since the feature to detect is a phasic event, one must not focus on frequency but only time domain. A schematic for the automatic detection of REM methodology is represented in Fig.3.24.

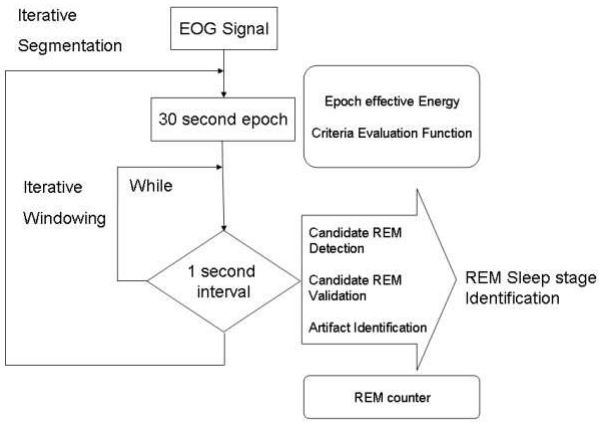

Figure 3.24: Suggested of EOG Algorithm.

The inputs for this methodology are: EOG of the ROC; EOG of the LOC; acquisition time; epoch duration; interval to analyze. With the mentioned inputs, sampling frequency, time axis specification and number of epochs to be evaluated are specified. Since EOG registers not only have REM but also Slow Eye Movement (SEM) signals, these two events must be separated in the initial data vectors. For this purpose a FIR digital bandpass filter is applied with cutoff frequencies at 1Hz and 5Hz see Fig.3.25. This filter effectively minimizes any SEM as well as high frequency noise.

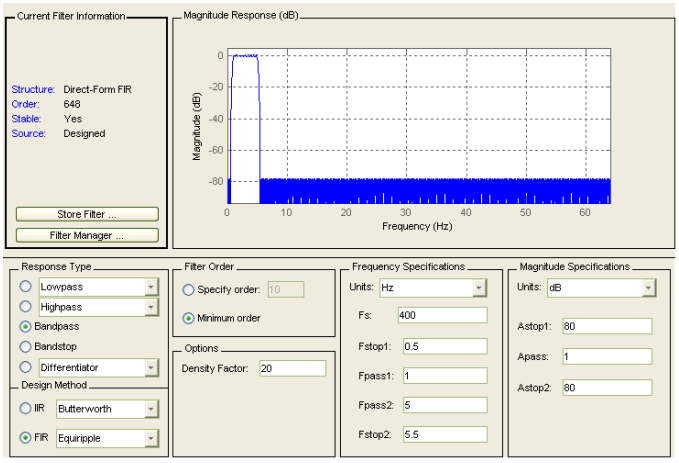

Figure 3.25: Tolerance diagram of the implemented digital filter.

After these calculations, output vectors common to the EEG and EMG analysis are created (REM epochs identification; Epoch effective energy; ratio of epoch's maximum and effective value) as well as a REM counter. The threshold values to be used as selective criteria are once again assumed constant since the ratio of epoch's maximum and effective value revealed little variability between different subjects(Appendix C). Therefore amplitude variations to be considered as REM manifestations were fixed in 50 μV in each side of the saccadic wave, or 30 μV and 70 μV (or vice versa) to consider different types of saccadic waves.

Having defined all the required variables and vectors, the algorithm starts signal analysis by detecting REM candidates. This is achieved by the Negative Instantaneous Product (NIP) of the two EOG data vectors, equation3.12.

$$NIP(n) = -LOC_{filt}(n) \cdot ROC_{filt}(n) \tag{3.12}$$

According to this method if ROC and LOC signals are completely out of phase (synchronous eye movement) a positive NIP value will occur. Instead, if eye movements are not synchronous or some other artefact is present resulting into in-phase signals, a negative value will be detected in the NIP (see Fig.3.26). This is a powerful discriminatory tool for REM detection. In Fig.3.26 two different situations are presented, a phase-reversed synchronous eye movement at 13037 s and artefacts or erratic movement at 13035 s.

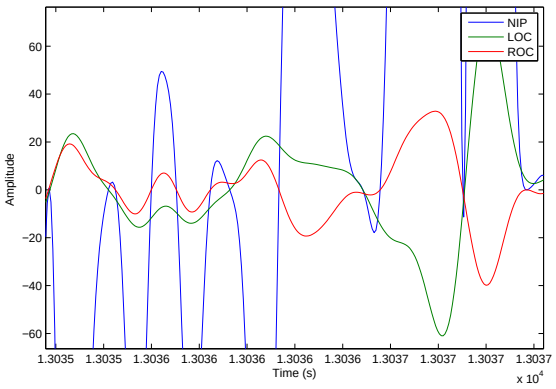

Figure 3.26: EOG data example. At 13037 seconds LOC and ROC registers are completely out of phase - Synchronous movement. At 13035 seconds data signals are in phase - Artefact or non-synchronous eye movement.

At this stage the data is segmented into 30 seconds epoch fragments as it is done in the EEG and EMG algorithm, for the purpose of a correct stage labelling. Afterwards, each epoch is analyzed with one second windows. The consequent one second interval is evaluated for possible REM by an easy and rapid procedure. The maximum NIP value (a possible REM) is focused, $NIP(x)$, and its vicinity evaluated 0.2seconds after and before, $NIP(x + 0.2s)$ and $NIP(x - 0.2s)$ respectively (see Fig.3.27). If the difference in amplitude of the ROC and LOC registers of these points is bigger than the initially defined criteria for saccadic amplitude variations (REM steep slopes), a REM event is considered to be detected.

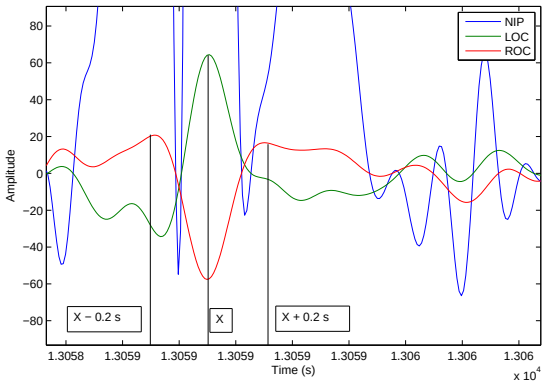

Figure 3.27: EOG data example. Instant of NIP maximum is focused and its vicinity evaluated 0.2 seconds before and after for REM detection

The SEM are rejected as well as some artefacts and non-synchronous eye movements by filtering and NIP. REMs are identified with the use of a steep slope identification criterion. Yet, other conditions have been introduced to facilitate REM detection:

- Input LOC or ROC signals above 500μV are considered artefacts and hence no REM stage can be considered
- No two REM events may be closer than 0.5 seconds
- A signal vicinity is evaluated in order to detect possible false positive surrounded by artefacts and signal behaviour resembling a NREM interval.

This last condition is clear in Fig.3.28 as one verifies that NIP behaviour has a sudden change at the 12000 second. Before that instant several artefacts are present inducing a NREM stage, oppositely, from that point forward an artefact free signal is detected. For such procedure the vicinity is defined as 20 seconds before and after the signal, artefact threshold fixed at -1000 μV^2, and the allowed number of artefacts is 1000.

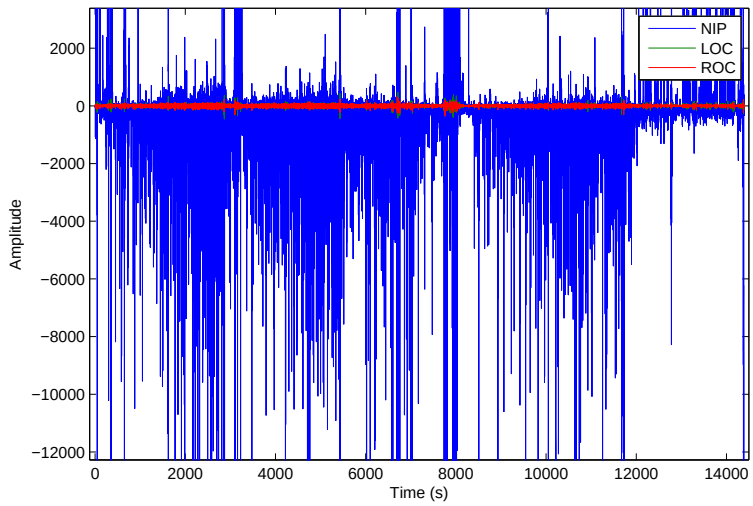

Figure 3.28: EOG data example. Two clear NIP patterns are recognized. Before reaching 12000 seconds several artefacts are detected inducing a NREM stage, from that point forward there is an artefact free interval.

This algorithm outputs the REM stage detector (based on the mentioned premises), an energy vector concerning each epoch and a REM counter.

3.4 Real Time Algorithm

Having defined the algorithms for the three different biological signals, one must gather the extracted information to identify REM sleep stage. To do so, the three processing tools are associated into a unique procedure, so that sinergetically REM sleep stages can be identified. Since the main purpose of this research is to develop a real time REM stage detector, some modifications must be implemented to the methodology for its correct functioning:

Redefinition of temporal analysis. In a real time approach only present and past signals are available, hence the EOG vicinity data to be evaluated can not comprise future signals like it was defined in the formerly described algorithm. In the real time REM detector the vicinity is the total epoch instead of 20 seconds before and after the evaluated instant.

Optimization to allow DSP while data is being transmitted. The digital EOG filter must be removed since its processing time is not compatible with the real time requirement. Alternatively the signal is treated with a moving average calculated within a 2.5 seconds window. With this method the DC component and the low frequency variations (typical of SEM) are minimized.

Chapter 4

Results

The methodologies in chapter 3 were tested and their results assessed for a training data set acquired by a different acquisition system. This data aggregates six different subjects[1], each with registers for EEG, EMG and EOG analysis, with sampling frequencies of 128, 256 and 128 respectively. Once analyzed, the results were subjected to the expert evaluation of Professora Teresa Paiva. Since the data vectors gathered a whole night record, the total analysis approach was used instead of the real time algorithm. Only afterwards could the designed DAQ system could be used by the real time DSP methodology.

4.1 Training Data

Using "subject 1" data vectors as inputs for the designed algorithms lead to the following results:

4.1.1 Subject 1

EEG

From the different EEG output vectors one can extract different conclusions.

- REM sleep stage detector (Fig.4.1 middle plot) showed well defined REM intervals, with the three criteria confirming the event.

- Epoch energy evaluation (Fig.4.1 lower plot) allowed to verify energy variability and thus conclude whether the defined criteria were correct. It was also possible to verify that the the signal did not have sudden changes in energy which could be associated with artefacts.

- The FFT analysis throughout the whole register (Fig.4.2) confirmed the existence of sleep cycles and its association to particular frequency bands. It is also clear that EEG signal is not a white signal, it has specific frequencies bands.

[1]Information kindly donated by Professora Teresa Paiva

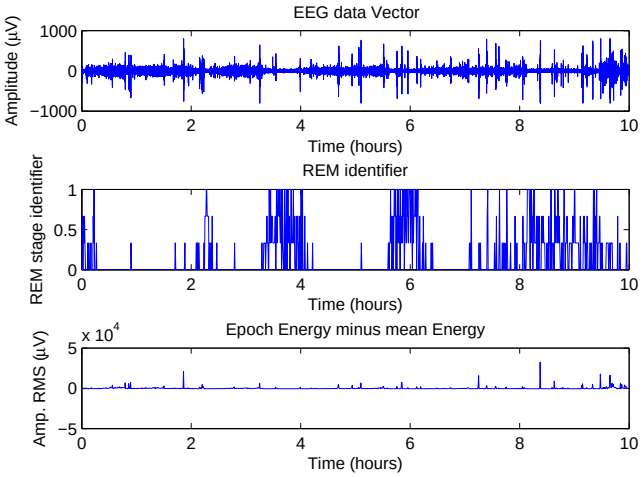

Figure 4.1: Subject 1 EEG analysis. Upper plot - EEG data vector; Amplitude μV. Middle plot - REM identifier. Lower plot - Epoch energy minus mean energy

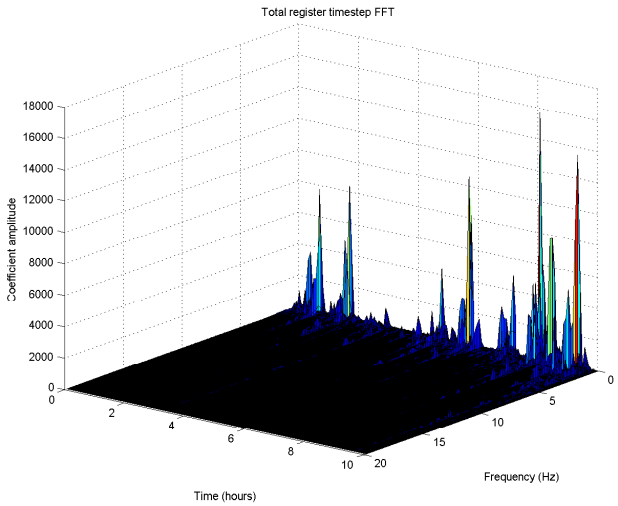

Figure 4.2: Total register time-step FFT.

EMG

With the first subject, and to assess the correct functioning of the algorithm, the possible situations for REM sleep stage were evaluated. For this purpose it was attributed different values for atonia and low energy epochs due to fast twitches, 1 and 2 respectively (Fig.4.3). Once the differentiation was confirmed and the correct identification of both situations verified, it was established a similar value for both states.

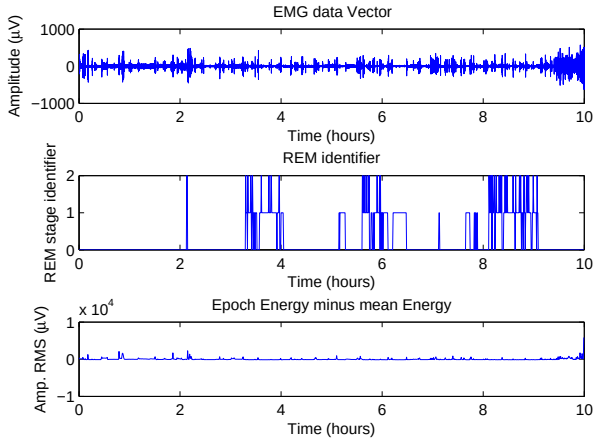

Figure 4.3: Subject 1 EMG analysis. Upper plot - EMG data vector; Amplitude μV. Middle plot - REM identifier. Lower plot - Epoch energy minus mean energy

Chin muscular evaluation demonstrated clear periods of muscular atonia (Fig.4.3 middle plot, value 1) intercalated with sporadic muscular contractions (Fig.4.3 middle plot with value 2). Epoch effective energy confirmed the absence of possible artefacts and allowed the evaluation of inter-subjects signal variability. The number of fast muscular contractions was registered as well as slow muscular contractions (not associated with REM stage), 448 and 7 respectively.

EOG

Prior to the REM stage detection it was plotted a methodology which quantified the number of REM events in each epoch, this allowed to verify if the algorithm had a high sensibility toward REM events. After having assessed the correct functioning of the algorithm, value 1 was established for any REM identification.

Results for the EOG evaluation are illustrated in Fig.4.4. Energy values were once again used to assess the existence of possible artefacts and the inter-subjects signal variability.

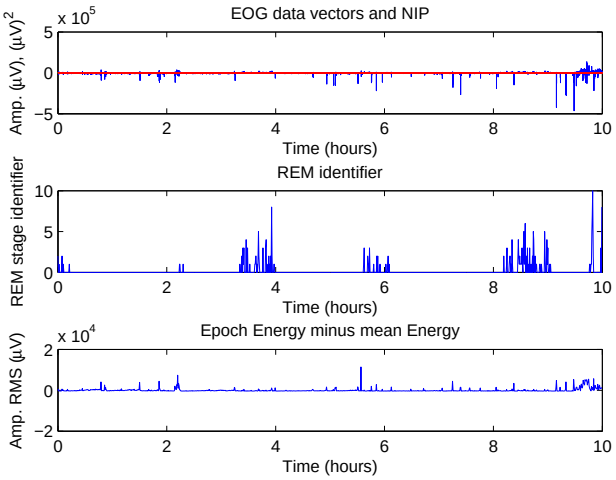

Figure 4.4: Subject 1 EOG analysis. Upper plot - EOG data vector; Amplitude μV. Middle plot - REM identifier. Lower plot - Epoch energy minus mean energy

The REM counter verified 231 events during the whole night sleep.

Global Evaluation

Associating the three different REM identifications a clearer picture is achieved, as it is depicted in Fig.4.5.

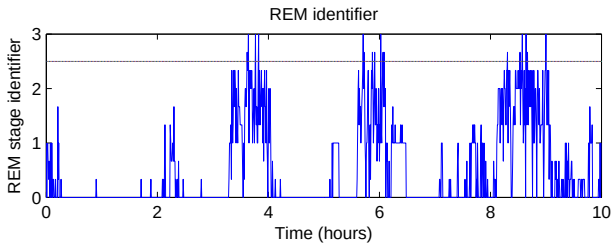

Figure 4.5: Algorithm evaluation of the presented subject

Confronting the algorithm evaluation, in which REM stage is considered when the result is above 2.5 (Fig.4.5), with the expert analysis (Fig.4.6) table 4.1 can be defined.

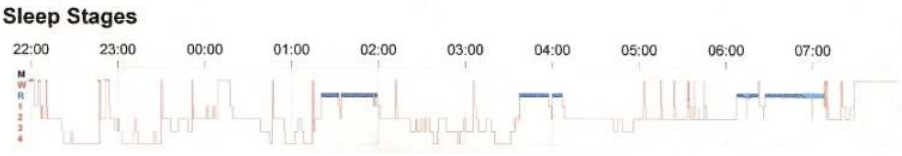

Figure 4.6: Expert evaluation of the presented subject

	Identified vs. Expert eval.		
Analysis	**Positive**	**False Positive**	**False Negative**
EEG	3	0	0
EMG	3	0	0
EOG	3	0	0

Table 4.1: Matching of identified REM periods with expert evaluation

A perfect match of the events is confirmed. Even though some REM periods were identified (separately) in the different analysis, they did not combine sinergetically, therefore one can not consider them to be REM sleep stage periods.

Similar analysis were accomplished for the 5 remaining subjects, with the REM stage threshold defined as 2.5.

4.1.2 Subject 2

Using "subject 2" data vectors as inputs for the designed algorithms lead to the following results:

EEG

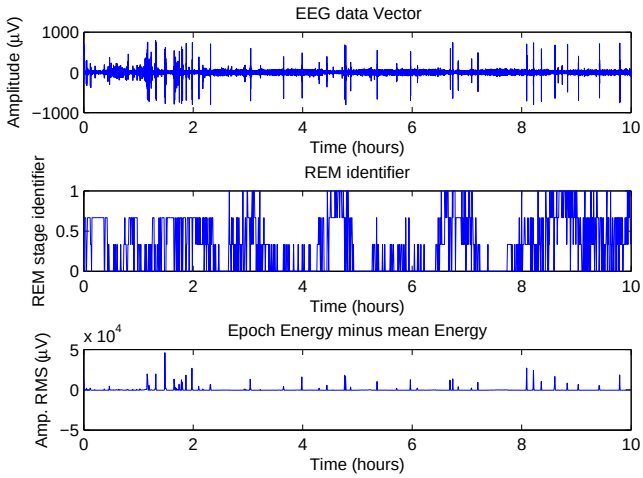

Figure 4.7: Subject 2 EEG analysis. Upper plot - EEG data vector; Amplitude μV. Middle plot - REM identifier. Lower plot - Epoch energy minus mean energy

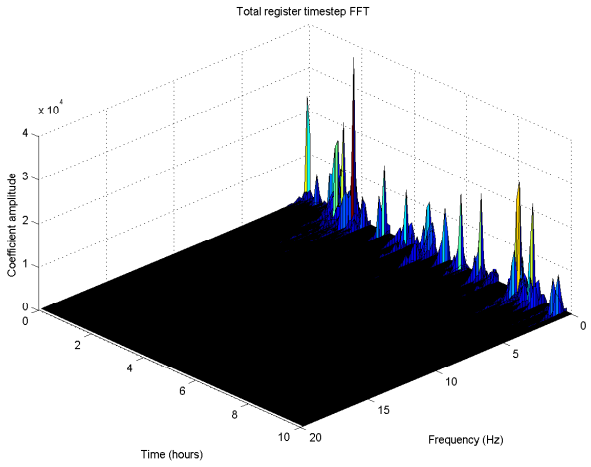

Figure 4.8: Total register time-step FFT.

EMG

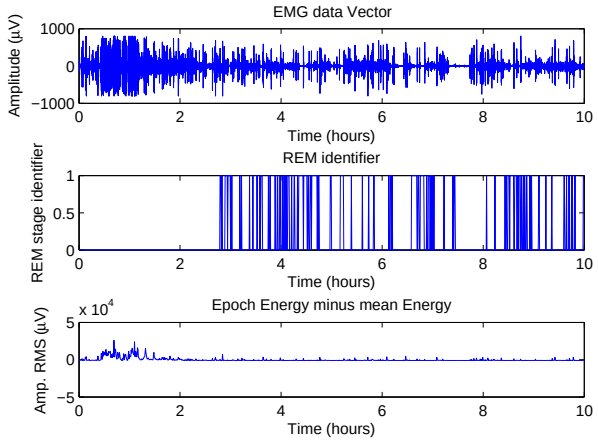

Figure 4.9: Subject 2 EMG analysis. Upper plot - EMG data vector; Amplitude μV. Middle plot - REM identifier. Lower plot - Epoch energy minus mean energy

The results for fast muscular contractions was 187 while no slow muscular contractions were registered.

EOG

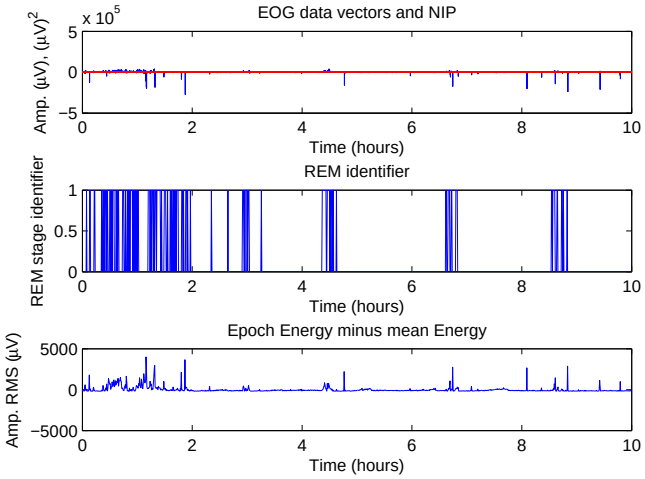

Figure 4.10: Subject 2 EOG analysis. Upper plot - EOG data vector; Amplitude μV. Middle plot - REM identifier. Lower plot - Epoch energy minus mean energy

For "subject 2" 394 REM were detected.

Global Evaluation

The association of the three different REM identifications is represented in Fig.4.11.

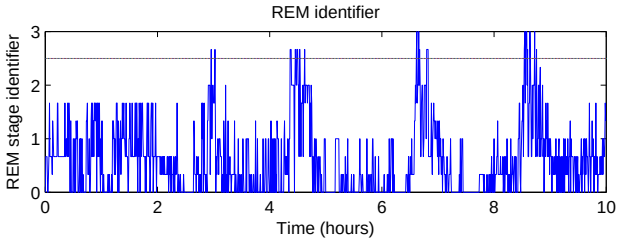

Figure 4.11: Algorithm evaluation of the presented subject

Confronting the algorithm evaluation with the expert analysis (Fig.4.12) table 4.2 can be defined.

Figure 4.12: Expert evaluation of the presented subject

	Identified vs. Expert eval.		
Analysis	**Positive**	**False Positive**	**False Negative**
EEG	3	0	0
EMG	3	1	0
EOG	3	1	0

Table 4.2: Matching of identified REM periods with expert evaluation

Since the expert evaluation only covered 8 hours out of 10, the two remaining hours were not considered for this evaluation.

EEG : No false positive or false negatives.

EMG : false positives - NREM sleep.

EOG : false positives - awake condition.

As it is visualized in Fig. 4.8, 4.9, 4.10 and 4.12, the separate analysis revealed some flaws of the process, as each of the analysis identified false positive REM events, associated to other specific stages. Nevertheless the association of the three vectors clearly identified the correct REM sleep stage periods, with REM stage identification value above 2.5.

4.1.3 Subject 3

Using "subject 3" data vectors as inputs for the designed algorithms lead to the following results:

EEG

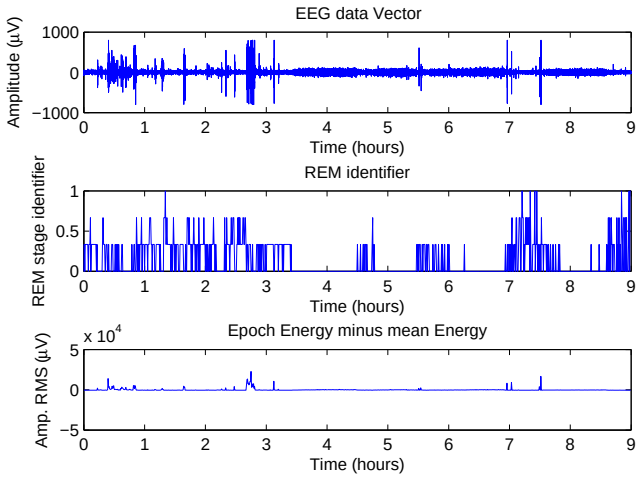

Figure 4.13: Subject 3 EEG analysis. Upper plot - EEG data vector; Amplitude μV. Middle plot - REM identifier. Lower plot - Epoch energy minus mean energy

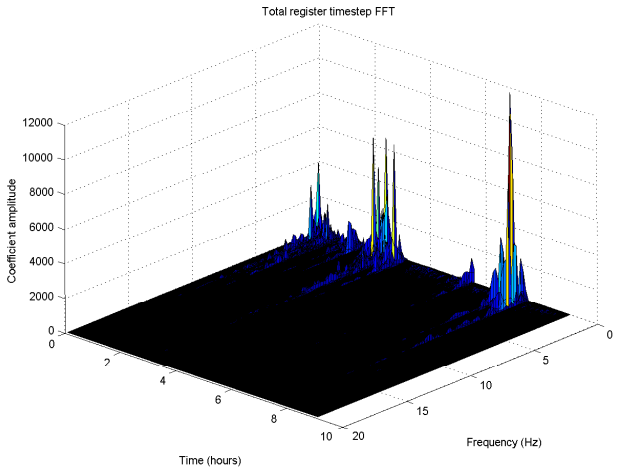

Figure 4.14: Total register time-step FFT.

EMG

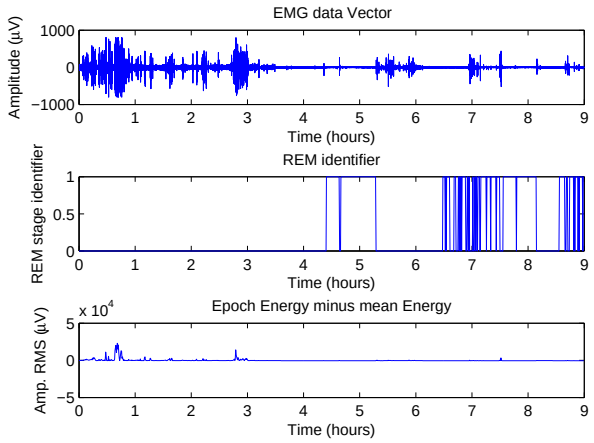

Figure 4.15: Subject 3 EMG analysis. Upper plot - EMG data vector; Amplitude μV. Middle plot - REM identifier. Lower plot - Epoch energy minus mean energy

The results for fast muscular contractions was 119 while 1 slow muscular contraction occured.

EOG

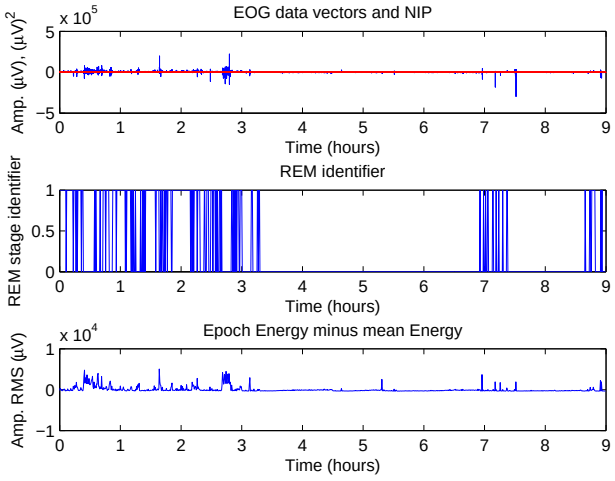

Figure 4.16: Subject 3 EOG analysis. Upper plot - EOG data vector; Amplitude μV. Middle plot - REM identifier. Lower plot - Epoch energy minus mean energy

For "subject 3" 781 REM were detected.

Global Evaluation

The association of the three different REM identifications is represented in Fig.4.17.

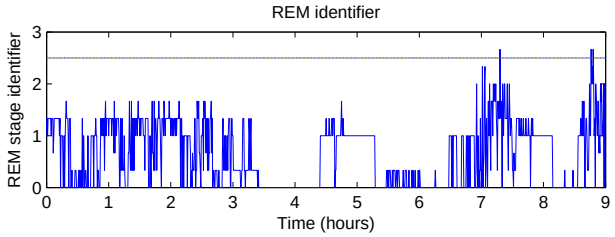

Figure 4.17: Algorithm evaluation of the presented subject

Confronting the algorithm evaluation with the expert analysis (Fig.4.18) table 4.3 can be defined.

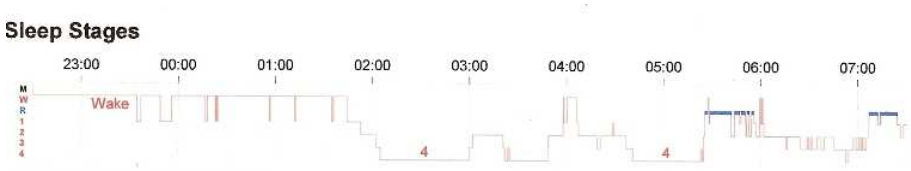

Figure 4.18: Expert evaluation of the presented subject

	Identified vs. Expert eval.		
Analysis	**Positive**	**False Positive**	**False Negative**
EEG	2	1	0
EMG	2	1	0
EOG	2	1	0

Table 4.3: Matching of identified REM periods with expert evaluation

EEG : false positives - awake condition.

EMG : false positives - NREM sleep.

EOG : false positives - awake condition.

The association of the three vectors correctly identified two intervals with high REM sleep stage probability, Fig.4.17, events confirmed with the expert evaluation, Fig.4.18.

4.1.4 Subject 4

Using "subject 4" data vectors as inputs for the designed algorithms lead to the following results:

EEG

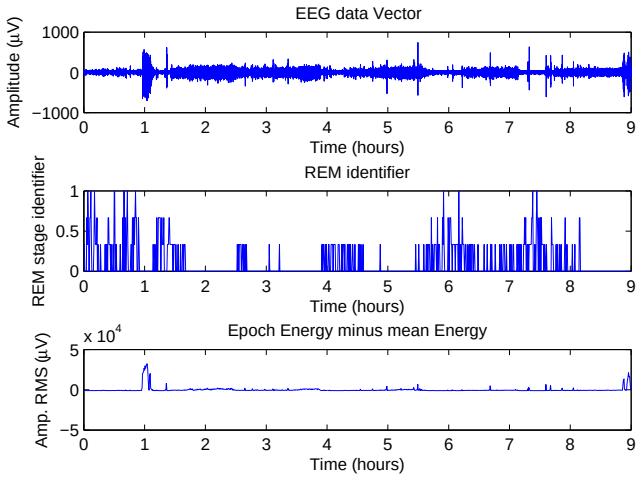

Figure 4.19: Subject 4 EEG analysis. Upper plot - EEG data vector; Amplitude μV. Middle plot - REM identifier. Lower plot - Epoch energy minus mean energy

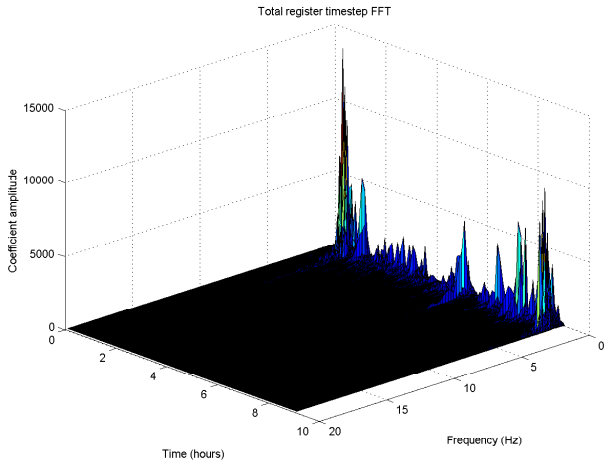

Figure 4.20: Total register time-step FFT.

EMG

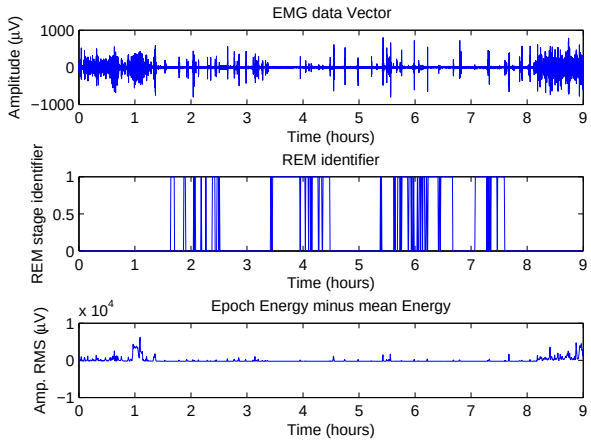

Figure 4.21: Subject 4 EMG analysis. Upper plot - EMG data vector; Amplitude μV. Middle plot - REM identifier. Lower plot - Epoch energy minus mean energy

The results for fast muscular contractions was 17 while no slow muscular contractions was registered.

EOG

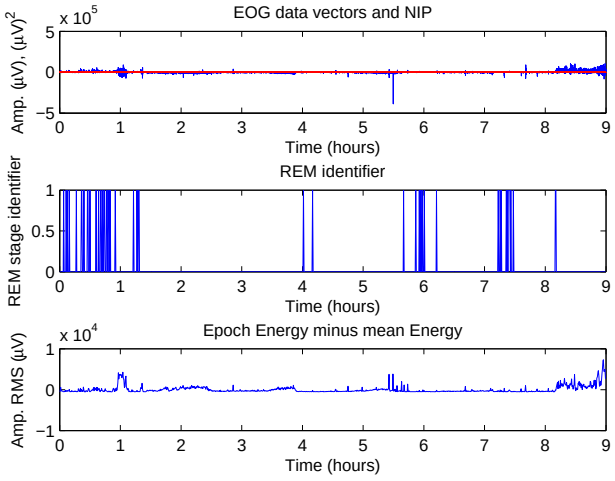

Figure 4.22: Subject 4 EOG analysis. Upper plot - EOG data vector; Amplitude μV. Middle plot - REM identifier. Lower plot - Epoch energy minus mean energy

For "subject 4" 87 REM were detected.

Global Evaluation

The association of the three different REM identifications is represented in Fig.4.23.

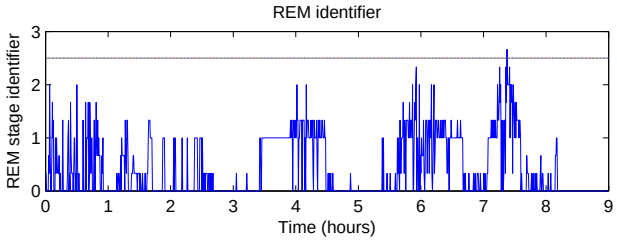

Figure 4.23: Algorithm evaluation of the presented subject

Confronting the algorithm evaluation with the expert analysis (Fig.4.24) table 4.4 can be defined.

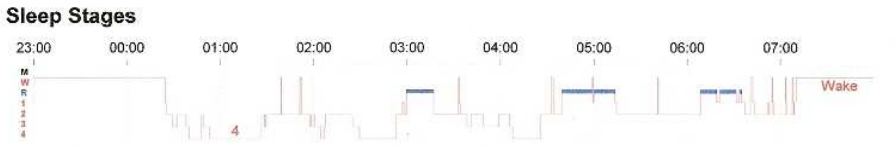

Figure 4.24: Expert evaluation of the presented subject

	Identified vs. Expert eval.		
Analysis	**Positive**	**False Positive**	**False Negative**
EEG	2	1	1
EMG	3	1	0
EOG	3	2	0

Table 4.4: Matching of identified REM periods with expert evaluation

EEG : false positives - awake condition.

EMG : false positives - NREM sleep condition.

EOG : false positives - awake condition.

Gathering the three vectors ended up identifying one REM stage period above the defined value of 2.5. Although if one analyzes Fig.4.23 independently of the defined 2.5 value for REM stage identification, it is clear that the intervals with higher REM stage probability match the remaining two REM stage intervals detected in the expert evaluation. This result suggested acquisition problems, or a misdefinition of criteria threshold values, indicating the need of an automatic criteria definition according to the evaluated test subject.

4.1.5 Subject 5

Using "subject 5" data vectors as inputs for the designed algorithms lead to the following results:

EEG

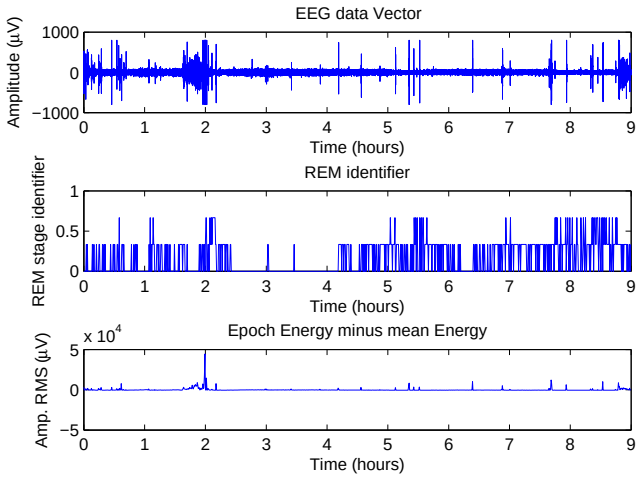

Figure 4.25: Subject 5 EEG analysis. Upper plot - EEG data vector; Amplitude μV. Middle plot - REM identifier. Lower plot - Epoch energy minus mean energy

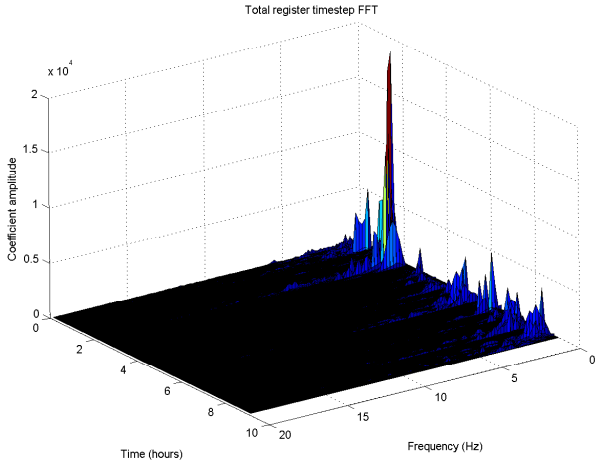

Figure 4.26: Total register time-step FFT.

EMG

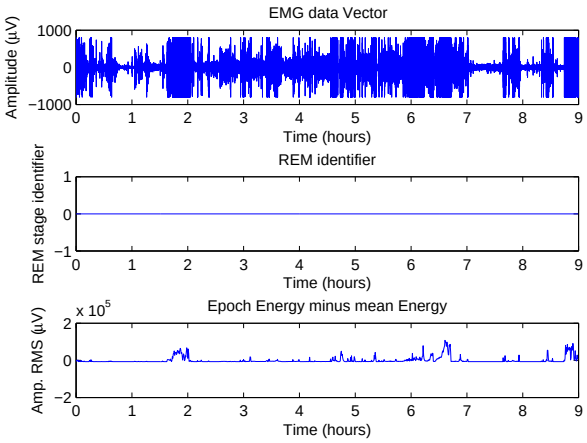

Figure 4.27: Subject 5 EMG analysis. Upper plot - EMG data vector; Amplitude μV. Middle plot - REM identifier. Lower plot - Epoch energy minus mean energy

No fast or slow muscular contractions were registered.

EOG

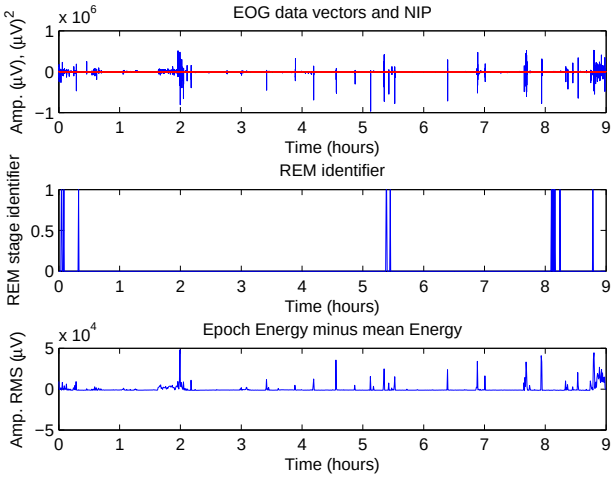

Figure 4.28: Subject 5 EOG analysis. Upper plot - EOG data vector; Amplitude μV. Middle plot - REM identifier. Lower plot - Epoch energy minus mean energy

For "subject 5" 17 REM were detected.

Global Evaluation

The association of the three different REM identifications is represented in Fig.4.29.

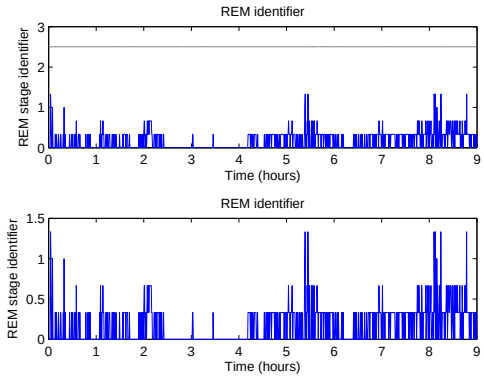

Figure 4.29: Upper plot - Algorithm evaluation of the presented subject. Lower plot - Zoomed algorithm evaluation of the presented subject

Confronting this result with the expert analysis (Fig.4.30) defines table 4.5.

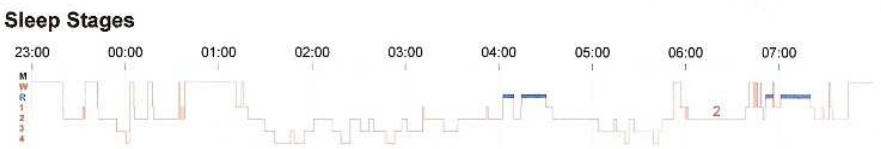

Figure 4.30: Expert evaluation of the presented subject

	Identified vs. Expert eval.		
Analysis	**Positive**	**False Positive**	**False Negative**
EEG	2	2	0
EMG	0	0	2
EOG	2	2	0

Table 4.5: Matching of identified REM periods with expert evaluation

EEG : false positives - awake condition.

EMG : The data was corrupted. This can be confirmed by analyzing Fig.4.27 upper plot, which reveals a constantly saturated signal.

EOG : false positives - awake condition.

The association of the three vectors could not identify the two REM intervals detected in the expert evaluation. This happened since the EMG data was corrupted, defining the maximum value for REM identification as 2 instead of 3. Associating this acquisition problem with a possible misdefinition of criteria, the identification of REM stage periods is not possible in an absolute perspective but only with a conditional analysis, by comparing the evaluation of each epoch with the result of the whole register (Fig.4.29 lower plot). In this sense, the two identified REM periods match the expert identification.

4.1.6 Subject 6

Using "subject 6" data vectors as inputs for the designed algorithms lead to the following results:

EEG

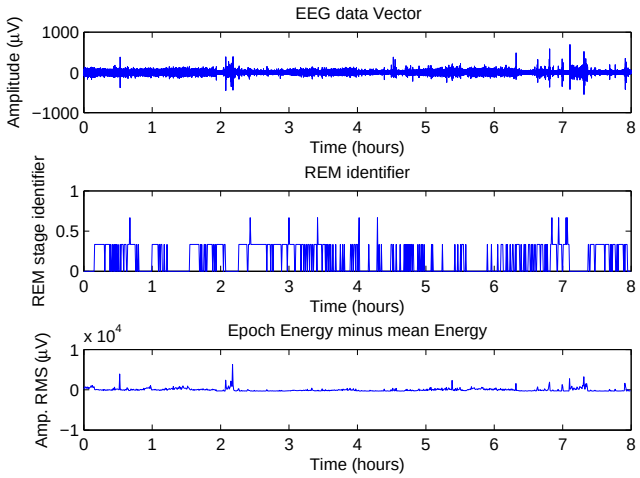

Figure 4.31: Subject 6 EEG analysis. Upper plot - EEG data vector; Amplitude μV. Middle plot - REM identifier. Lower plot - Epoch energy minus mean energy

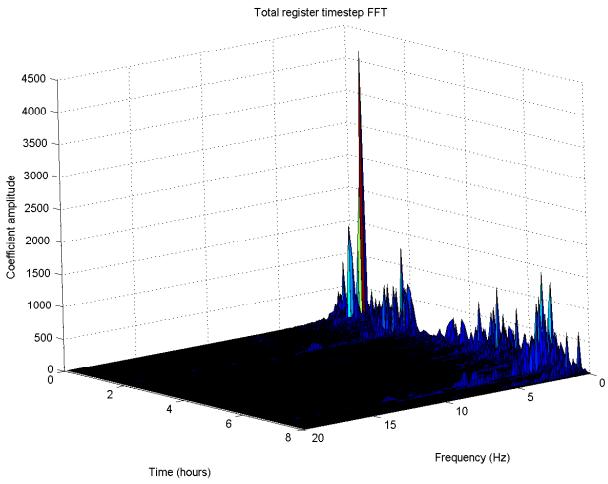

Figure 4.32: Total register time-step FFT.

EMG

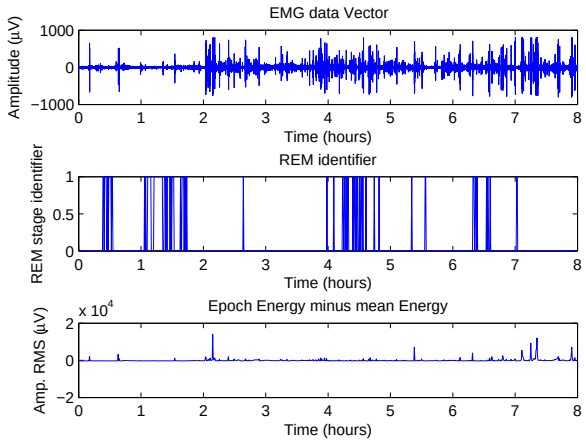

Figure 4.33: Subject 6 EMG analysis. Upper plot - EMG data vector; Amplitude μV. Middle plot - REM identifier. Lower plot - Epoch energy minus mean energy

The results for fast muscular contractions was 58 while no slow muscular contractions were registered.

EOG

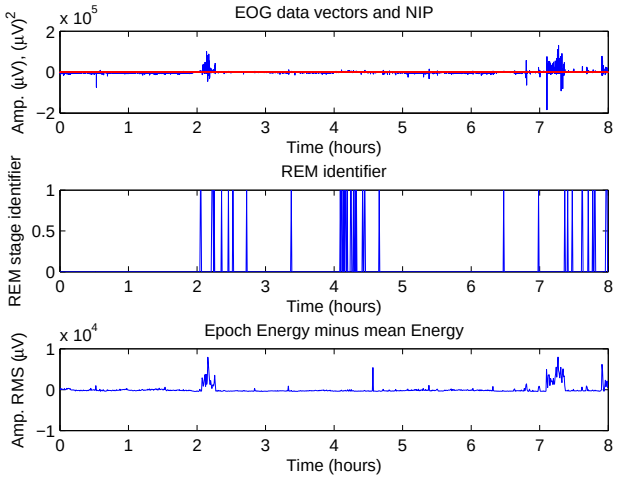

Figure 4.34: Subject 6 EOG analysis. Upper plot - EOG data vector; Amplitude μV. Middle plot - REM identifier. Lower plot - Epoch energy minus mean energy

For "subject 6" 65 REM were detected.

Global Evaluation

The association of the three different REM identifications is represented in Fig.4.35.

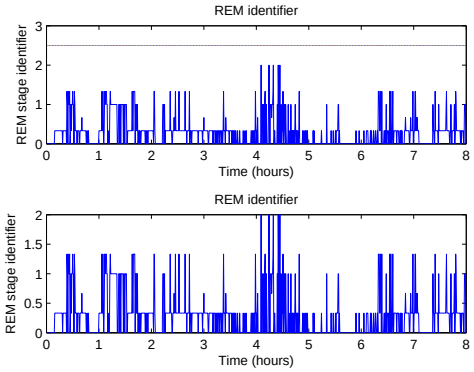

Figure 4.35: Upper plot - Algorithm evaluation of the presented subject. Lower plot - Zoomed algorithm evaluation of the presented subject

Confronting the algorithm evaluation with the expert analysis (Fig.4.36) table 4.6 can be defined.

Figure 4.36: Expert evaluation of the presented subject

	Identified vs. Expert eval.		
Analysis	**Positive**	**False Positive**	**False Negative**
EEG	1	3	1
EMG	2	2	0
EOG	2	2	0

Table 4.6: Matching of identified REM periods with expert evaluation

EEG : false positives - awake condition.

EMG : false positives - NREM sleep.

EOG : false positives - awake condition.

The association of the three vectors did not identify the two REM stage periods identified by the expert evaluation. Still, if one disregards the 2.5 REM stage threshold identification and evaluates the signal focusing on the periods with high REM stage probability (Fig.4.35 lower plot), it is verified that the algorithm correctly detected the REM stage intervals as well as a false positive awake period. This indicates that, similarly to subject 4 and 5, this trial could be caracterized by acquisition problems or possible misdefinition of criteria thresholds.

Some of the REM sleep stage detections did not confirm all the criteria, therefore the REM identifier vector was below the the desired maximum value, 3. This is comprehensible if one bears in mind that some data could not be considered part of the training set since the values were corrupted or inadequate (e.g. saturation); the training data set registers were acquired in a sleep evaluation laboratory, being feasible that some of the subjects could suffer from pathological sleep disturbances with their particular sleep register patterns; or even a misdefinition of criteria, due to the non adaptation of the thresholds motivated by the verified small inter-subject energy variability.

False positives of each analysis revealed a pattern: EEG were associated to awake condition; EMG were associated to deep sleep; EOG were associated to awake.

As previously mentioned, for a correct and precise identification, it is necessary to define criteria threshold values according to the evaluated test subject. In this sense there are two possible result interpretations: 1) By strictly considering a detected REM period when REM stage identification is above 2.5, the designed setup detected 9 positive detections with 6 false negative events. This statistic reveals a 60% REM detection percentage. 2) Although if one evaluates the REM detections bearing in mind acquisition problems and possible criteria threshold misdefinition, and therefore analyzes each epoch value comparing with the other epoch results of the same subject, a total of 14 positive detections, 2 false positives and 1 false negative were verified. In this sense the training data set revealed a satisfactory 82% of REM detection.

This global satisfactory agreement between the tested DSP methodology and the expert evaluation motivated the following trial of the designed setup.

4.2 DAQ trial

4.2.1 First evaluation

A first trial of the designed DAQ revealed some aspects one should take into account. A first approach using the real-time algorithm lead to unconclusive results since the signals did not have sufficient quality for the algorithm to automatically detect REM sleep stage. This can be confirmed as one observes signals appearance in Fig.4.37.

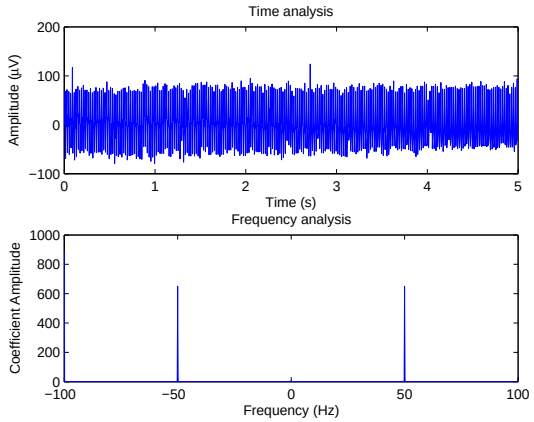

Figure 4.37: Designed DAQ signals preliminary analysis. Upper plot - 5 second signal. Lower plot - Frequency analysis of the acquired signal.

It was crucial to filter the signals so that a correct detection could be accomplished. For the present case, since the analysis was no longer real-time, different filters were studied and applied according to the processing needs of each independent signal. The specifications are here presented:

EEG : Low pass filter with cutoff at 45Hz.

EMG : Notch filter for 50Hz.

EOG : Band pass filter for 1 to 5 Hz.

Once the acquired signals were correctly preprocessed, it was possible to apply the previously defined algorithm for REM sleep stage detection only by making subtle changes. These adjustments were performed since the signals were acquired by the designed DAQ (Chapter 2) instead of the previously analysed training data set signals acquired by a commercial acquisition system used in standard sleep laboratories.

EEG :

1) Total energy value threshold from 35 to 20 μV RMS.

2) Δ band energy value from 25 to 5 μV RMS.

EMG :

1) Atonia threshold values from 5 to 35 μV RMS.

2) Amplitude signal variation considered for the detection of fast muscular contractions from 7 to 11 μV.

EOG :

1) Signal vicinity to be evaluated is changed from 20 seconds before and after to the analyzed epoch, allowing a real-time evaluation.

2) NIP artefact from -1000 to -250 μV^2, and number of artefacts allowed changed from 1000 to 1.

These adaptations allowed a correct application of the designed algorithm, leading to the following results.

EEG

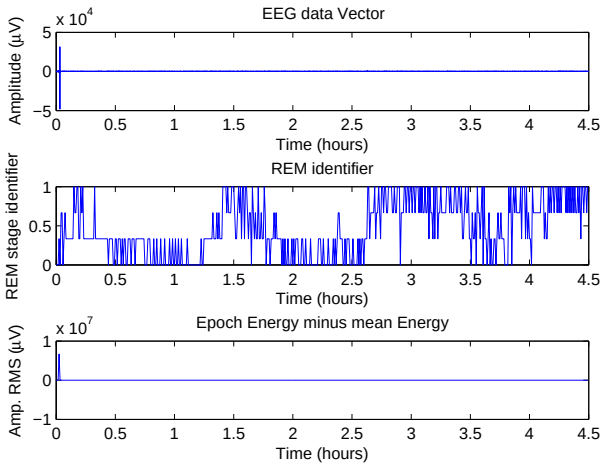

Figure 4.38: EEG analysis. Upper plot - EEG data vector; Amplitude μV. Middle plot - REM identifier. Lower plot - Epoch energy minus mean energy

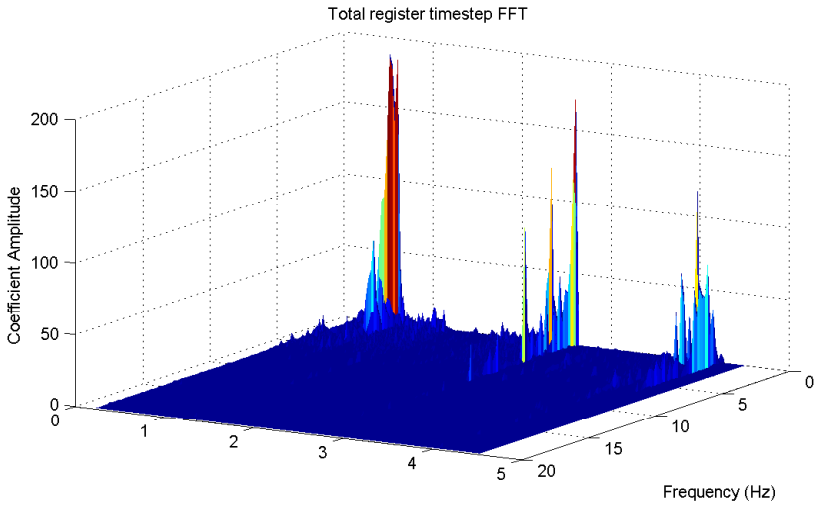

Figure 4.39: Total register time-step FFT.

As in the training data set, this EEG evaluation revealed clear periods of possible REM sleep stage as well as the expected cyclical patterns in the cerebral activity during sleep with characteristic frequency bands.

EMG

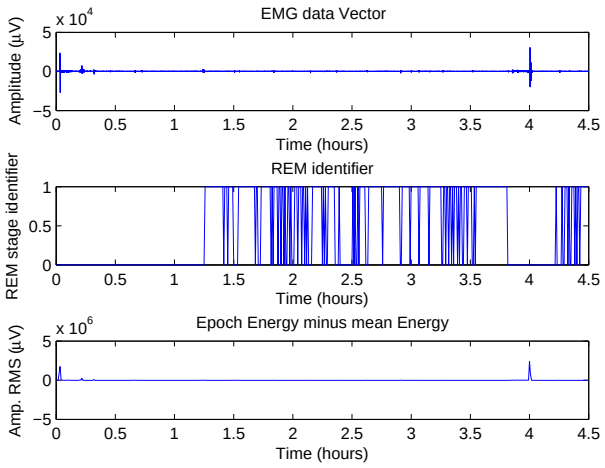

Figure 4.40: EMG analysis. Upper plot - EMG data vector; Amplitude μV. Middle plot - REM identifier. Lower plot - Epoch energy minus mean energy

The results for fast muscular contractions was 160 while 3 slow muscular contractions were registered.

EOG

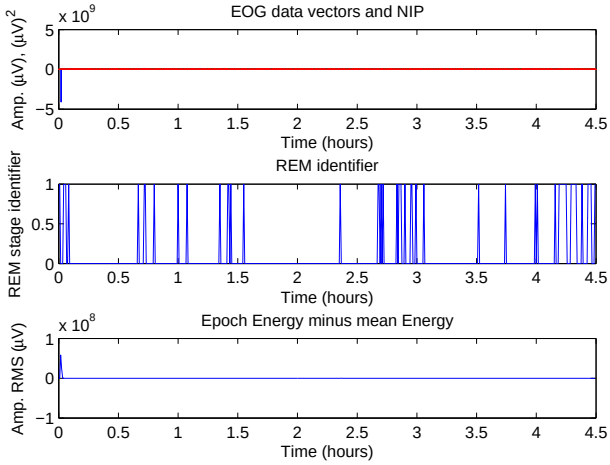

Figure 4.41: EOG analysis. Upper plot - EOG data vector; Amplitude μV. Middle plot - REM identifier. Lower plot - Epoch energy minus mean energy

For this trial 120 REM were detected.

Global Evaluation

The association of the three different REM stage detectors lead to three distinct possible REM stage periods, as it is represented in Fig.4.42.

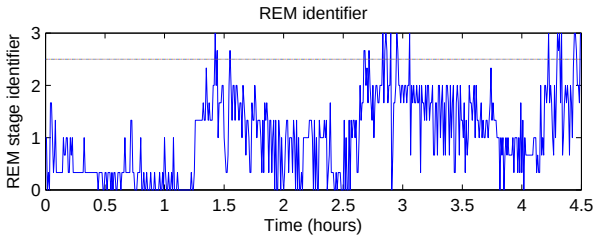

Figure 4.42: Algorithm evaluation of the presented trial

For this case no confrontation of the algorithm evaluation with an expert analysis was performed since modifications to the acquisition system were necessary to allow a real time evaluation in further studies. This first trial ended up being useful to detect system flaws. The identified insufficient signal quality, Fig.4.43 left column[2], motivated several modifications to the acquisition system towards signal quality improvement to allow the desired real time detection of REM sleep stage.

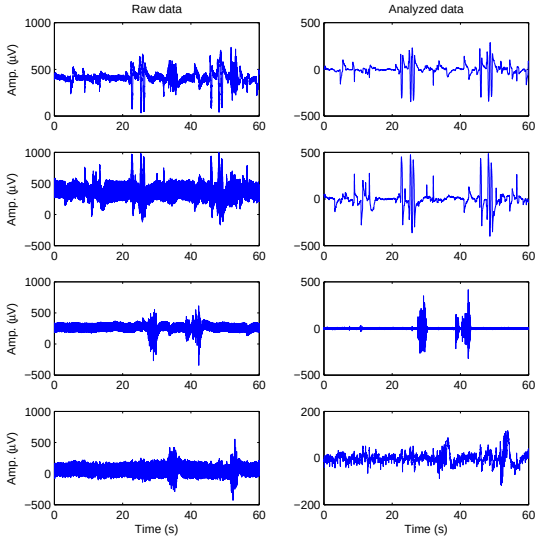

Figure 4.43: Raw signal vs. Desired signal quality. Left plots - Raw signal. Right plots - Desired signals.

First evaluation conclusions

Blinding : Protection of the DAQ system to EMI.

Cable : Instead of regular cables, coaxial cables were used reducing noise levels.

DSP : Development of parallel processes: Acquisition ; Preprocessing ; Display. With this methodology signal loss is avoided.

[2]in which the represented signals exhibit a fairly good aproximation of the signal quality

Concerning the last topic, parallel processes, modifications to the preprocessing setup took place so that signal quality changed from Fig.4.44 middle plot into Fig.4.44 lower plot[3].

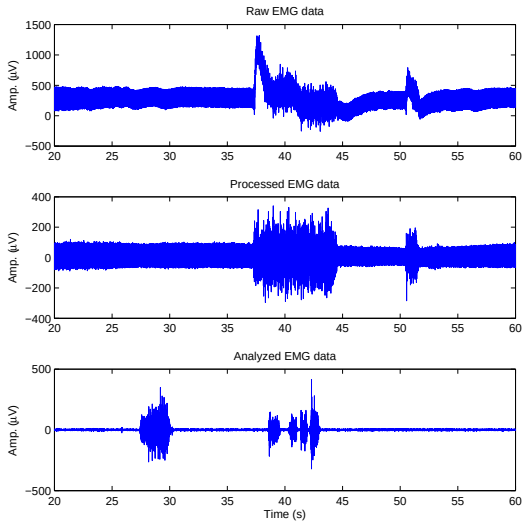

Figure 4.44: EMG analysis. Upper plot - EMG raw data. Middle plot - EMG processed data. Lower plot - EMG new processed data

The mentioned modifications were not applied instantly, they were being implemented and the results evaluated in terms of signal quality, as it is expressed in table 4.7.

	System configuration	
	Other Preprocessing steps	**Final Preprocessing**
Regular cables	4	0
Coaxial cables	4	**6**

Table 4.7: System configuration for different trials

The advantages brought with the preprocessing step modifications focused in noise reduction and acquisition of fairly pure signals, contrarily to some tested preprocessing steps that resulted in impure data. Bearing this in mind one should focus in the acquisitions in which coaxial cables were used as well as the final preprocessing step implemented.

From the 6 tryouts, only 4 were correctly acquired since the remaining two had the following acquisition complications: 1) dettachment of the electrodes, 2) low battery of the acquisition system, which incapacitated a good acquisition and therefore a correct identification of the REM sleep stage.

In order to validate REM sleep stage automatic detection an expert evaluation is essencial, for this purpose the acquired data had to be converted from ASCII format into European Data Format (EDF) (Appendix D) to be read and evaluated in commercial softwares[4] available in sleep laboratories. For the present project *Somnologica*^{TM} soft-

[3]Even though different signal intervals are here represented, differences in signal quality are easily identified

[4]*Alice Sleepware*^{TM}, *Nicolet*^{TM}, *DOMINO Somnomedics*^{TM}, *Somnologica*^{TM}, etc

ware was used to read the acquired data, Fig.4.45.

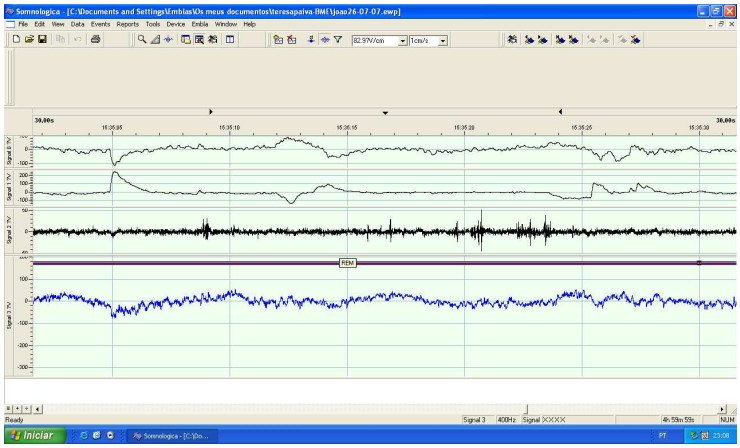

Figure 4.45: Somnologica software interface

The acquired and evaluated registers are presented in the next sections. Only 2 of the 4 trials are presented since the remaining were not confronted with the expert evaluation. For each presented trial different criteria threshold values were applied to correctly detect REM intervals. The need to modify these values, associated to the previously mentioned verified inter-subject criteria threshold variability, motivated the creation of a protocol for automatic threshold definition based on signals analysis (Appendix E).

4.2.2 Trial 1

Evaluating the acquired signals from trial 1 lead to the following results:

EEG

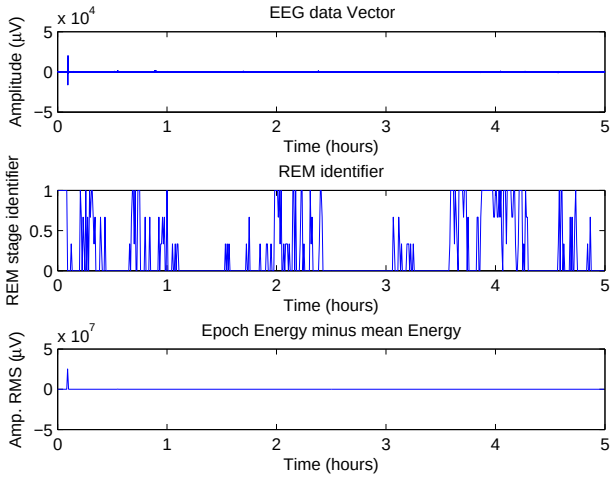

Figure 4.46: Trial 1 EEG analysis. Upper plot - EEG data vector; Amplitude μV. Middle plot - REM identifier. Lower plot - Epoch energy minus mean energy

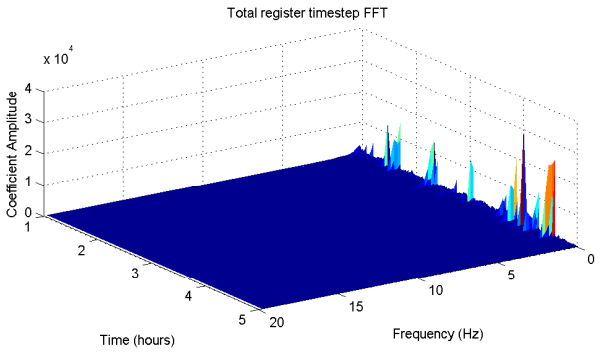

Figure 4.47: Total register time-step FFT.

The EEG results revealed possible intervals of REM sleep stage and the already previously identified cyclic pattern of EEG sleep activity.

EMG

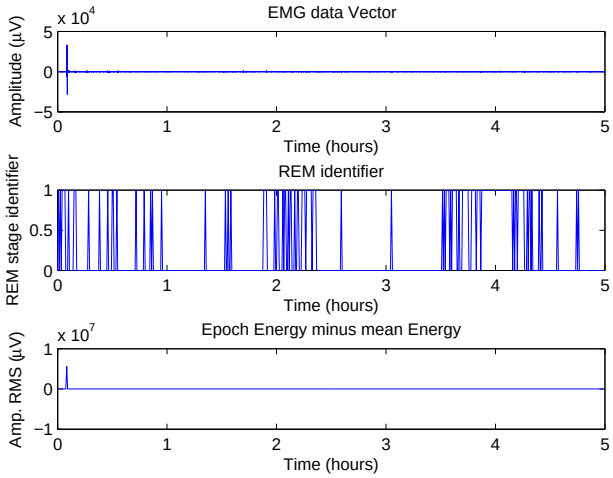

Figure 4.48: Trial 1 EMG analysis. Upper plot - EMG data vector; Amplitude μV. Middle plot - REM identifier. Lower plot - Epoch energy minus mean energy

No slow muscular contractions were detected while 25 fast muscular contractions were detected.

EOG

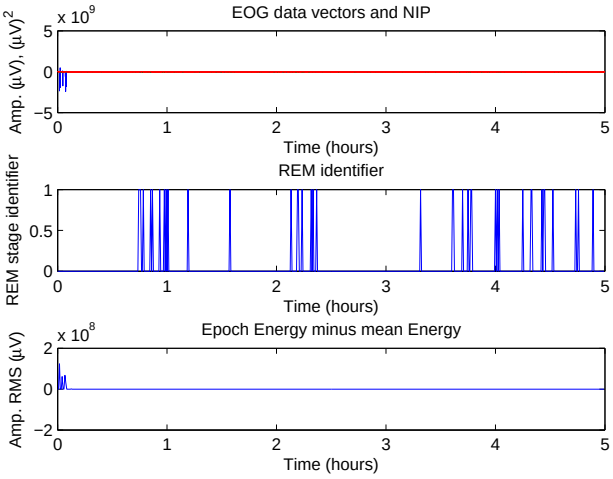

Figure 4.49: Trial 1 EOG analysis. Upper plot - EOG data vector; Amplitude μV. Middle plot - REM identifier. Lower plot - Epoch energy minus mean energy

The EOG analysis detected 77 REM.

Global Evaluation

The association of the three different REM identifications is represented in Fig.4.50.

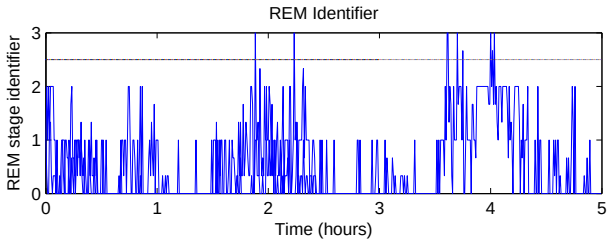

Figure 4.50: Algorithm evaluation of the first trial

Confronting the algorithm evaluation with the expert analysis, (Fig.4.51), table 4.8 can be defined.

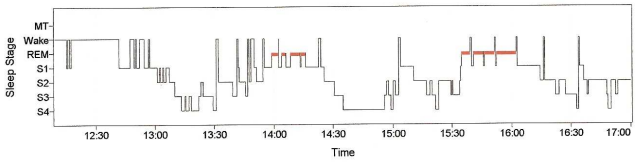

Figure 4.51: Expert evaluation of the 1 trial

	Identified vs. Expert eval.		
Analysis	**Positive**	**False Positive**	**False Negative**
EEG	2	2	0
EMG	2	2	0
EOG	2	2	0

Table 4.8: Matching of identified REM periods with expert evaluation

EEG : false positives - awake condition.

EMG : false positives - awake condition.

EOG : false positives - awake condition.

Similarly to the training data set, EEG analysis and EOG detected false positives in awake situations. The EMG analysis abnormally detected false positive in awake condition assumably due to a less strict criteria definition.

The association of the three vectors ended up identifying the correct REM sleep stage periods, with values above the 2.5 REM stage threshold.

4.2.3 Trial 2

Trial 2 data vectors evaluation lead to the following results:

EEG

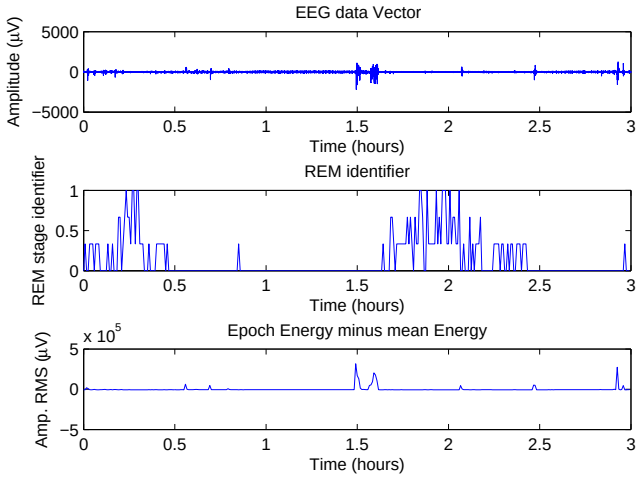

Figure 4.52: Trial 2 EEG analysis. Upper plot - EEG data vector; Amplitude μV. Middle plot - REM identifier. Lower plot - Epoch energy minus mean energy

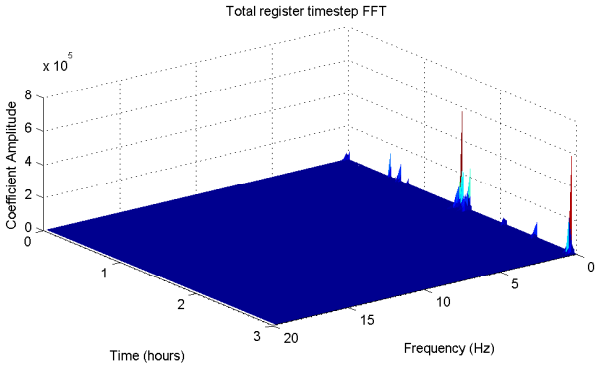

Figure 4.53: Total register time-step FFT.

The EEG results revealed 2 well defined possible intervals of REM sleep stage and the already previously identified cyclic pattern of EEG sleep activity.

EMG

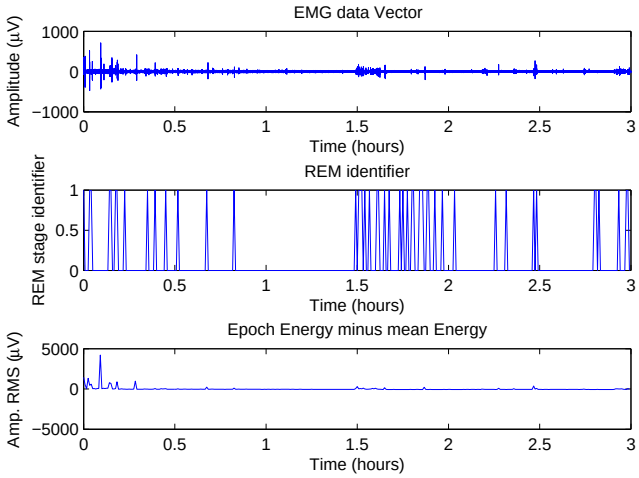

Figure 4.54: Trial 1 EMG analysis. Upper plot - EMG data vector; Amplitude μV. Middle plot - REM identifier. Lower plot - Epoch energy minus mean energy

The EMG analysis revealed 40 fast muscular contractions and no slow muscular contractions.

EOG

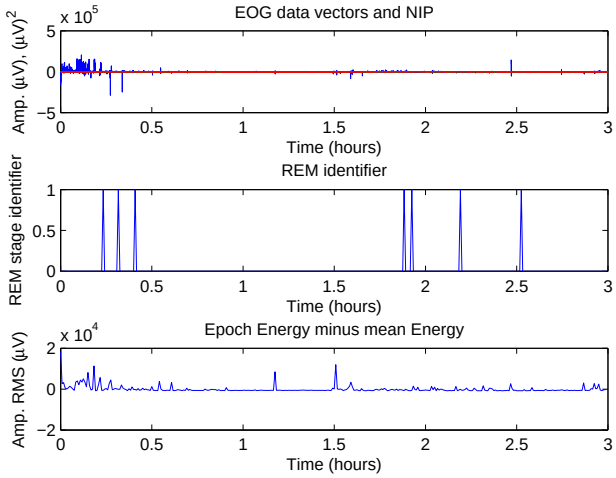

Figure 4.55: Trial 1 EOG analysis. Upper plot - EOG data vector; Amplitude μV. Middle plot - REM identifier. Lower plot - Epoch energy minus mean energy

The EOG analysis detected 7 REM. Possibly the criteria definition for REM detection was too strict, allowing the algorithm to detect only 7 events.

Global Evaluation

The association of the three analysis is represented in Fig.4.56.

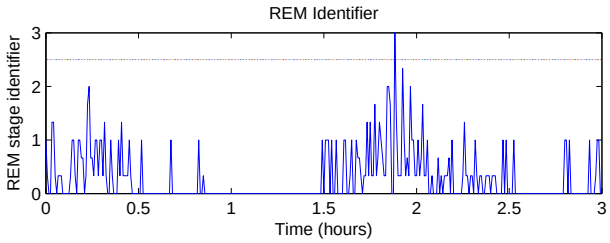

Figure 4.56: Algorithm evaluation of the second trial

Confronting the algorithm evaluation with the expert analysis, (Fig.4.57), table 4.9 can be defined.

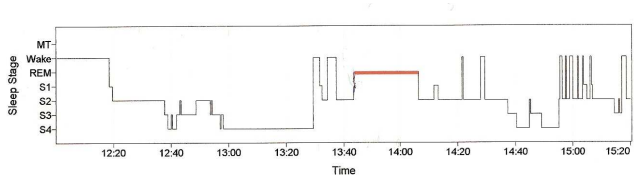

Figure 4.57: Expert evaluation of the 2 trial

	Identified vs. Expert eval.		
Analysis	**Positive**	**False Positive**	**False Negative**
EEG	1	1	0
EMG	1	3	0
EOG	1	1	0

Table 4.9: Matching of identified REM periods with expert evaluation

EEG : false positives - awake condition.

EMG : false positives - awake condition.

EOG : false positives - awake condition.

Similarly to the training data set and trial 1, EEG analysis and EOG detected false positive REM sleep in awake situations. Identically to trial 1, the EMG analysis abnormally detected false positive in awake condition assumably due to a less strict criteria definition.

The association of the three vectors ended up identifying the correct REM sleep stage periods with the REM stage identification above 2.5.

Trial conclusions

The presented evaluations revealed a satisfactory 100% REM detection. Although the algorithm achieved maximum correlation with the expert evaluation, the duration of each REM stage detected was extremely short, reflecting a high specificity, inadequate to the objective of this project. Considering this, and the verified inter-variability in the first 6 test subjects, it is essential to have an automatic definition of criteria to achieve an adequate REM detection. For this purpose an algorithm was defined, acquiring 2 minutes of signal, and with the aid of a protocol respected by the test subject, it defines the threshold values for each criterium (e.g. Δ energy in the EEG, atonia energy levels in EMG, amplitude variation considered in a REM event, etc.) according to the evaluation of different indicators (Appendix E). The two trials previously presented serve as the starting point for the definition of a database capable to define these thresholds. Summarizing into tables, table 4.10, table 4.11 and table 4.12 represent the mean value of each indicator.

EEG indicators					
Trial	**Δ/E**	**θ/E**	**α/E**	**Max/E**	**Energy**
1	0,6573	0,0998	0,058	0,1373	6513,9
1 (awake)	0,5499	0,0908	0,0848	0,1249	3039,3
2	0,5808	0,0736	0,0379	0,1696	44122
2 (awake)	0,4197	0,0887	0,088	1,4356	1053800

Table 4.10: EEG indicators

EMG indicators		
Trial	**Max/E**	**Energy**
1	0,8816	83,003
1 (awake)	0,4903	561,0341
2	1,6909	9421
2 (awake)	0,9217	233550

Table 4.11: EMG indicators

	Right EOG		**Left EOG**	
Trial	**Max/E**	**Energy**	**Max/E**	**Energy**
1	0,1768	859,6343	0,1413	1126,3
1 (awake)	0,0986	3953,8	0,0926	6152,6
2	0,1215	485720	0,1584	520160
2 (awake)	0,2158	12072000	0,2391	12959000

Table 4.12: EOG indicators

The analysis of the total register is here introduced, as well as the first 12 minutes of register, in which the subject is expected to be awake. By analyzing sleep onset intervals one expects the results to be similar to those acquired with the protocol to be applied for the automatic definition of criteria thresholds.

Besides the automatic definition of criteria thresholds, another modification should be implemented in the signal processing. Interference of ocular (and sometimes even muscular) signals in the EEG recording was verified, motivating the evaluation of different techniques to remove such artefacts. The aplication of an ICA tool is here presented.

ICA

This methodology is based on the assumption that if different signals are from different physical processes then those signals are statiscally independent. Therefore, using mathematical tools it is possible to "search" for the source signals (pure EEG, EMG and EOG) inside the mixed acquired signals.

With this approach one expects to extract artefacts common to every signal, such as movement artefacts, as well as separating the different signals so that no ocular or muscular artefacts are registered in the EEG signal.

Some tests with this tool lead to the following results and interpretations:

Fig.4.58 : The ICA tool, due to its iterative procedure in search of independent components can multiply the signals for -1 instead of multiplying the unmixing matrix. This leads to inverted signals as we can verify in Fig.4.58 in which one of the EOG signals have been multiplied by -1, resulting in in-phase ocular movements. It can also swap signal positions, complicating the analysis. Another problem that arises with the application of ICA tools is data normalization, disallowing the application of possible threshold values for energy and/or signal voltage.

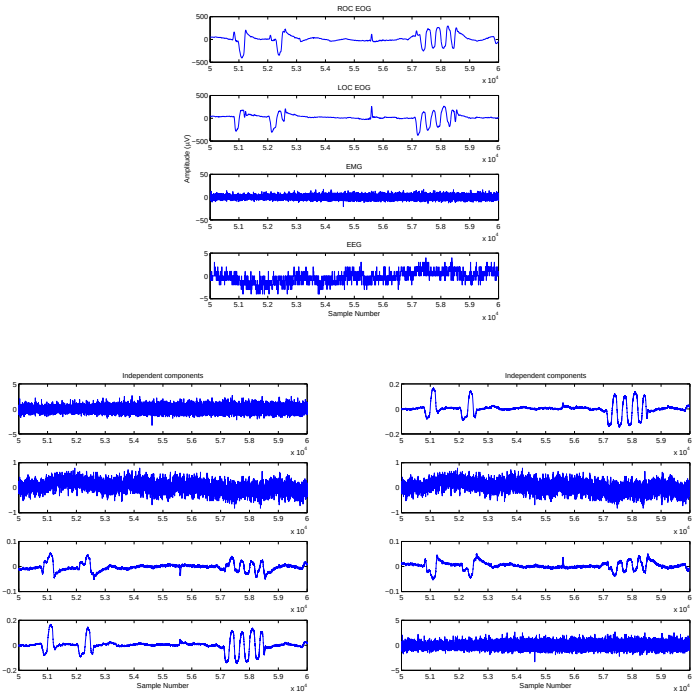

Figure 4.58: Upper plot - Raw signal 25 seconds sample. Lower left plot - ICA result. Lower right plot - ICA result (2)

Fig.4.59 :If an artefact is detected with an extremely high amplitude (ROC EOG artefact of -6000μV), it will propagate to the other signals by the application of the ICA toolbox.

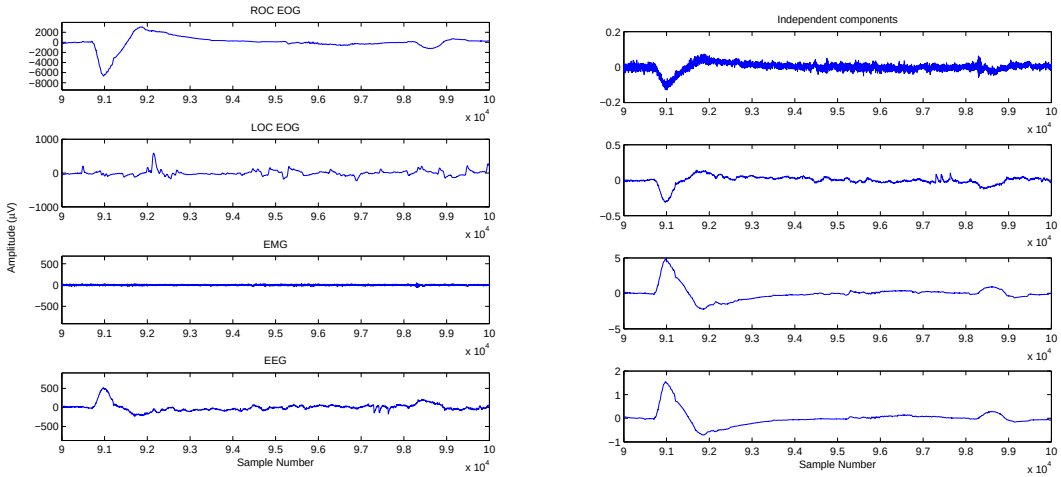

Figure 4.59: Left plot - Raw signal 25 seconds sample. Right plot - ICA result

Fig.4.60 :The application of the ICA toolbox did not remove efficiently the EOG artefact in the EEG register.

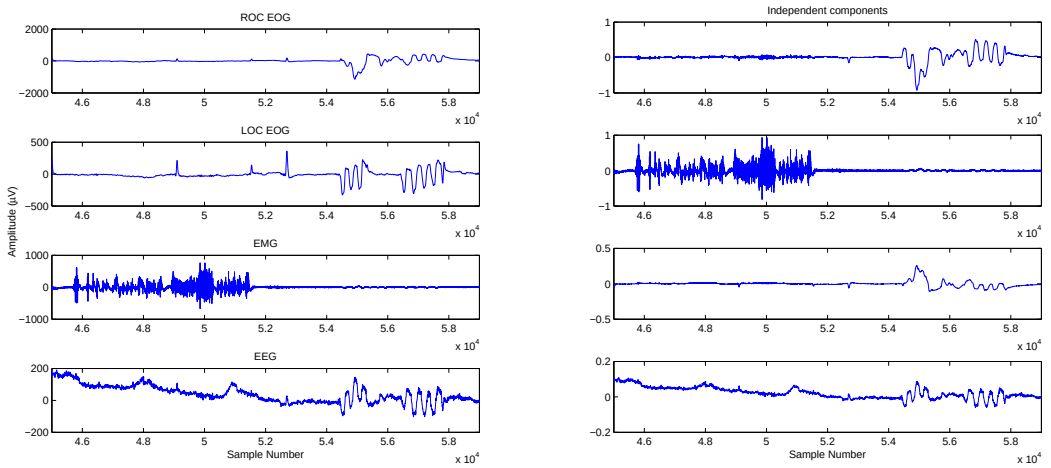

Figure 4.60: Left plot - Raw signal 25 seconds sample. Right plot - ICA result

Through these evaluations it became clear that ICA can not be applied to an entire data vector, expecting it to correctly separate signals and remove the ocular and muscular artifacts from the EEG register. This unsatisfactory results were assumed to be associated to the non stationarity of the used signals, due to its long time-span. Therefore, by applying ICA methodology to subsequent short intervals, followed by the gathering of

such signals, one assumes that this problem is reduced. Although the previously mentioned complications associated to normalization, inversion and signal order switch are still present.

Hence a methodology was designed to unfold these complications. In such method ICA is applied to small intervals of 100 points along the analyzed signal, afterwards the resultant ICA output vectors, normalized, possibly inverted and/or swapped in position, are correlated to the original vectors. In this way the signals will assume its original values and it is possible to verify if they have been inverted - correlation will be negative - or even swapped with other signal - if correlation is maximum with a different vector in the ICA output.

Since EEG is the signal more susceptible to artefact interference, due to its low amplitude, this method was applied in order to remove artefacts from such signal, therefore combinations of 2 signals were tested: EEG and ROC EOG; EEG and LOC EOG; EEG and EMG. The results of such method were first tested in a small interval with the following results, Fig.4.61:

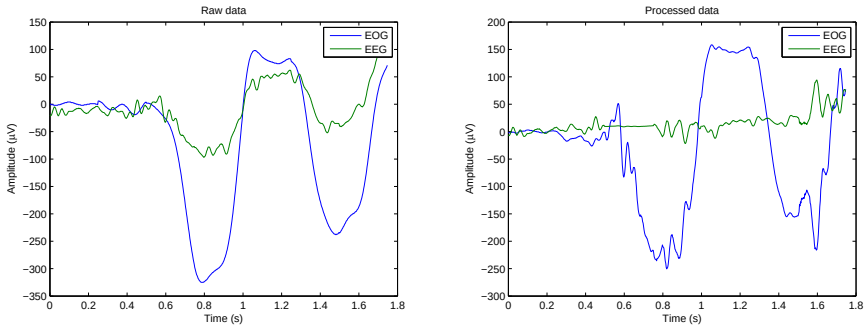

Figure 4.61: Left plot - Raw signal 1.8 second sample. Right plot - ICA result

This method was extended to larger intervals, as depicted in Fig.4.62

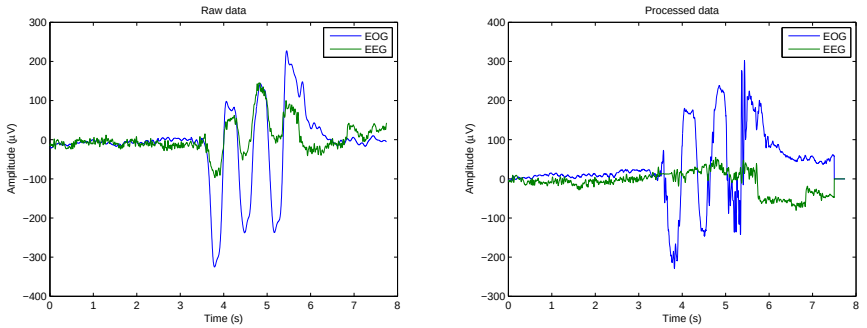

Figure 4.62: Left plot - Raw signal 8 second sample. Right plot - ICA result

From Fig.4.61 and Fig.4.62 it is verified that 1) ICA methodology is capable to extract ocular artefacts in the EEG data 2) EOG data should only be used in the ICA processing as input since its processing adulterates the data with EEG components.

Chapter 5

Conclusions

Sleep has always been a condition that triggered human curiosity and impelled several questions. These questions motivated approaches from genetics to physiological evaluations. Not surprisingly, sleep analysis is one of the major neuroscience research areas.

The segmentation of sleep according to well characterized intervals allowed researchers to identify and study sleep events relating them to particular stages. One of the stages known to be highly related to pathologies and other events such as dreams is REM sleep. The identification of such stage was the main goal of this study.

For the purpose of detecting REM sleep a designed DAQ [35] system was used to acquire data from EEG, EMG and EOG channels. The acquired data was manipulated through a DSP tool and the output visualized and analyzed by an interface [38].

This thesis focused on the development of the DSP tool for real time REM sleep stage identification. The designed algorithm by detecting characteristic patterns of EEG (absence of Δ waves; Low amplitude signal; low α wave expression), EMG (muscular atonia with possible fast muscular twitches) and EOG (REM events) differentiated REM sleep from other sleep stages.

Initially, the designed methodology was applied to a training set of 6 subject acquired by a different DAQ device. The results revealed a 60% agreement between the automatic detection and the expert evaluation, and 82% agreement if one bear in mind some considerations: the existence of corrupted data; inapropriate data due to possible pathological situations and possible misdefinition of criteria thresholds. In this later perspective, the REM stage detection is evaluated by comparing the result of the evaluated epoch with the result of the remaining epochs of the studied subject, independently of the 2.5 REM sleep stage threshold.

Besides the identification of REM sleep stage, and its agreement with the expert evaluation, the algorithm allowed other conclusions:

- EEG signals carry a great amount of information, nevertheless it is extremely complicated to objectively support conclusions from it due to its extremely low amplitude, potential summation of several depolarizations throughout brain tissue and interference of other electrical signals in the head.

- By evaluating total register time-step FFT one verifies that EEG coloured signal have a cyclic pattern of prevalence and decrease of slow waves. This is associated

with deep sleep stages (NREM3 and NREM4) and light sleep (or REM), respectively. These results supported the idea of a sleep cycle as it is depicted in Fig.5.1.

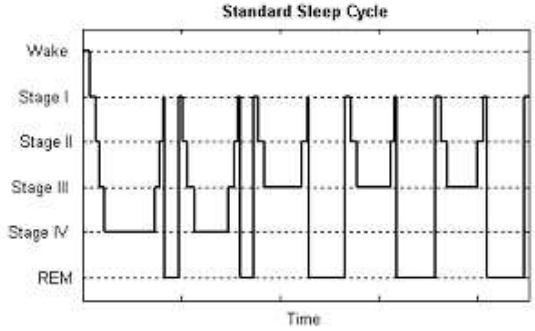

Figure 5.1: Standard sleep cycle. [67]

- Even though the REM counter was not used for any particular purpose of this work, it has been proven that REM events increase in humans following an intensive learning period [68] and in pathological situations such as esquizofrenia [11]. Therefore, future works focusing on this data could lead to important conclusions.

- Fast and slow muscular twitches were registered. Although in the present time these events do not have a specific relation with sleep studies, in the future probably it will be possible to assess some information from it.

This satisfactory aggreament lead to a trial with the designed DAQ [35] system. The results from such trial were not confirmed with an expert evaluation, still the recordings were used to detect flaws of the designed DAQ. Motivated by the recognized flaws and poor signal quality, modifications of the system took place: blinding of the DAQ; use of coaxial cables instead of normal cables; definition of parallel processes for acquisition, preprocessing and data display so that data was not lost. Besides these modifications, improvement of the preprocessing step was performed allowing further trials to take place with no complications.

These later trials data had to be converted to a specific file extension, EDF, so that they could be evaluated by an expert, contesting the automatic identification made by the DSP setup. It revealed 100% detection of REM intervals, but the detected intervals were of extremely short time span, which is not in accordance with the goal of this project. Instead, it is desired that the DSP setup be sensitive rather than specific since there will always exist a medical monitorization of the REM sleep stage detection. This, associated to the previously mentioned variability of criteria thresholds, lead to the development of a protocol to automatically define criteria thresholds. Besides this modification, in order to improve signal quality, ICA was tested to remove EOG and EMG artefacts in the EEG register, as well as separate signals from common artefacts such as movement artefacts. The results of ICA have proven to be useful when applied to short intervals, so that signal stationarity is conserved.

Notwithstanding some problems were identified throughout the project development, the designed algorithm fulfilled the goal of identifying REM sleep for completely acquired

data vectors, and also the possibility of its implementation in a real-time setup, since it proved to be capable of processing each epoch's signal while the data is acquired and visualized. This implementation will allow future studies of REM dreaming.

5.1 Discussion points and future work

Even though the methodology fulfilled the goal of the project, some discussion points are here described for further consideration and investigation.

- An improvement to the designed algorithm would be the detection of the various sleep stages. For such purpose other methodologies must be followed in order to evaluate EEG signal not only in frequency domain but also for its phasic events, K complexes and sleep spindles. A possible approach could be wavelet analysis [69] or correlation methods using previously known waveforms like K complexes. These approaches would be an improvement to the defined algorithm, although they could not be employed in a near real time scenario since their processing requirements are not compatible with the epoch time span.

- The interpretation of EEG signals is extremely context-sensitive. It can be compared to recognition of handwriting, one not only has to recognize individual patterns, but the interpretation depends on the specific conditions under which the signals are acquired. In this way, the designed near real time automated detection of REM sleep is an extremely complicated task and will only aid the physician by flagging possible REM events that must be confirmed in loco. Hence, as previously mentioned sensitivity is preferred rather than specificity, since the physician will always have to assume the decision of waking up the patient for REM dreaming evaluations.

- Since the final goal of this work was to detect near real time REM sleep stage, the designed algorithm was conceived bearing in mind non pathological conditions. Although, one must be aware that sleep rules are continuously being updated and therefore it is necessary to implement its conditions in the setup in order to consider every newly discovered relevant information. For instance, it is becoming common to consider abnormal sleep stage with EEG signal similar to REM stage, occurrence of REM events on the EOG and tonic activity intercalated with muscular contractions in the EMG.

- For the EEG analysis it was used a referenced setup. Future works should consider reviewing EEG electrode placement towards better EEG signals since no electrode placement evaluations were done in this work.

- For the present work the epoch was defined as a 30s interval. Bearing in mind that sleep is a continuous phenomenon, sleep should be engaged without time discretization. Since this is not possible, the chosen epoch length is clearly a compromise between accuracy and laboriousness. One should test different epoch definitions or even overlapping epoch segments for better results. An implication of long epochs is the increased frequency resolution for the EEG analysis, while the temporal resolution is decreased. By using overlapping segmentation it could be possible to

know how the transitions occur, hence promoting an easier identification of sleep stages. Another problem of sleep analysis discretization is that although they may include two, sometimes even three electrophysiologically different states, they will only identify one of the stages. This dubious definition of epoch could be controlled with probabilistic evaluations for sleep transitions. For this purpose, and knowing the typical sleep cycle, one could attribute a certain probability to each transition according to the present stage and Fig.5.1.

- Increased frequency resolution could be achieved by a different signal processing. Instead of the FFT tool a Chirp-Z transform [70] could be used. With this tool, specific time segments can be evaluated in a controlled frequency band. Focusing on the low frequency components, known to have higher expression, promotes an increased frequency resolution.

- Other signals could be used: oximetry, ECG, limb movement, body temperature. For the present study they were not implemented since their values could not be as easily controlled as the EMG, EOG and EEG. Artefacts commonly occur in limb movement registers due to natural body movement during sleep; ECG, body temperature and oximetry are not as biologically stable as EMG, EOG and EEG, therefore the threshold definition would have to assume a more dynamic behaviour.

- More tests must be realized to allow a liable definition of criteria values. With only two registers the threshold definition assume rough and abrupt transitions, as more tests are realized the intervals will become more specific and therefore the criteria more adapted to each situation.

- Even though ICA revealed good results, it must be further tested to evaluate whether it can bring satisfactory results in the time span available for real time identification, and evaluated using different sample intervals so that the stationarity problem is resolved with the best solution possible. It should also be tested to remove the strong signal of ECG frequently acquired in the designed setup.

Bibliography

[1] Martha S. Rosenthal, *Physiology and Neurochemistry of Sleep*. American Journal of Pharmaceutical Education Vol. 62, Summer 1998.

[2] Renate Wehrle, Michael Czisch, Christian Kaufmann, Thomas C.Wetter, Florian Holsboer. *Rapid eye movement-related brain activation in human sleep: a functional magnetic resonance imaging study*. LippincottWilliams & Wilkins Vol 16 No 8 31 May 2005.

[3] Loomis AL, Harvey EN, Hobart GA., *Cerebral states during sleep, as studied by human brain potentials*. J Exp Psychol 1937; 21: 127-144.

[4] Aserinsky E, Kleitman N., *Regularly occurring periods of eye motility and concomitant phenomena during sleep*. Science 1953; 118: 273-274.

[5] Dement WC, Kleitman N., *Cyclic variations in EEG during sleep and their relation to eye movements, body motility and dreaming*. Electroencephalogr clin Neurophysiol 1957; 9: 673-690

[6] http://www.mbfys.ru.nl/∼geertjan/mbt2003/chapter2/.hnode4tml

[7] Monroe LJ., *Inter-rater reliability and the role of experience in scoring EEG sleep*. Psychophysiol 1967; 5: 376-384

[8] Rechtschaffen, A., Kales, A. (eds)., *A manual of standardized terminology, techniques and scoring system for spleep stages of human sujects.*, U.S. Public Health Service, U.S. Government Printing Office, Washington D.C. 1968

[9] Himanen, S., Hasan, J., *A Limitations of Rachtschaffen and Kales*. Harcourt Publishers Ltd

[10] Mgr. Kristína . Šušmáková ,*Nonlinear Prediction of Sleep Electroencephalogram*, Institute of Measurement Science Slovak Academy of Sciences

[11] R. J. McPartland, B. L. Weiss, and D. J. Kupfer, *An objective measure of REM activity*, Physiolog. Psychol., vol. 2, pp. 441-443, 1974

[12] F. G. Foster, D. J. Kupfer, P. Coble, and R. J. McPartland, *Rapid eye movement sleep density. An objective indicator in severe medical-depressive syndromes*, Arch. Gen. Psych., vol. 33, pp. 1119-1123, 1976

[13] R. J. McPartland, D. J. Kupfer, P. Coble, D. H. Shaw, and D. G. Spiker, *An automated analysis of REM sleep in primary depression*, Biol. Psych., vol. 14, pp. 767-776, 1979

[14] CLARKE N. A. ; WILLIAMS A. J. ; KOPELMAN M. D., *Rapid eye movement sleep behaviour disorder, depression and cognitive impairment: Case study*

[15] Helder Bértolo & Teresa Paiva, *CONTEÚDO VISUAL EM SONHOS DE CEGOS*, Laboratório EEG/Sono - Centro de Estudos Egas Moniz - Faculdade de Medicina de Lisboa. PSICOLOGIA, SAÚDE & DOENCAS, 2001, 2 (1), 23-33

[16] Alejandro Backer, *To Sleep, Perchance to Dream*, Harvard Undergraduate Society for Neuroscience, 1994. http://www.hcs.harvard.edu/husn/BRAIN/vol1/sleep.html

[17] Hobson, J. A., *States of Brain and Mind*, 106-109, Birkhaeuser Boston, Boston, 1987

[18] http://www.gtec.at/products/g.BSamp/documents/g.BSamp.pdf

[19] R. Spehlmann, *Electroencephalography Primer*, 1981

[20] http://www.brainsync.com/brainlab_delta.asp

[21] Aftanas L., Golosheykin S., *Impact of regular meditation practice on EEG activity at rest and during evoked negative emotions*, Int J Neurosci. 2005 Jun;115(6):893-909.

[22] Vertes R.P., *Hippocampal theta rhythm: a tag for short-term memory.* Hippocampus 15(7):923-35. 2005

[23] Buszaki G., *Theta oscillations in the hippocampus.* Neuron 33(3):325-40. 2002

[24] http://planetmath.org/

[25] Kubicki St, Herrmann WM, Holler L. *Critical comments on the rules by Rechtschaffen and Kales concerning the visual evaluation of EEG sleep records.* In: Kubicki St, Herrmann WM (eds). Methods of Sleep Research. Stuttgart, New York: Gustav Fisher 1985: 19-35.

[26] Russell Conduit PhD, *Polysomnographic (PSG) Recording in Humans*, Department of Psychology, Monash University, AUSTRALIA

[27] http://butler.cc.tut.fi/∼malmivuo/bem/bembook/28/28.htm

[28] Carlo J. De Luca, *The Use of Surface Electromyography in Biomechanics*, DelSys Incorporated 1997

[29] M. Reuter, C. Zemke ,*Analysing Epileptic Events On-Line by Soft-Computing-Systems*, Department of Cumputer Science, Technical University of Clausthal, http://www2.in.tu-clausthal.de/∼reuter/eeg.htm

[30] http://www.wikipedia.org/

[31] Pierre J.M. Cluitmans, Ph.D. , *NEUROMONITORING*

[32] Malcon Anderson Tafner, *Sleep, Its Architecture And Monitoration*, http://cerebromente.org.br/n12/mente/sono_i.html

[33] Steriade M, Amzica F., *Slow sleep oscillation, rhythmic K-complexes, and their paroxysmal developments.* J Sleep Res 1998; 7 (Suppl. 1): 30-35

[34] Arden V. Nelson, *Differences in EEG properties resulting from analysis using nearest-neighbor Laplacian, referencial and bipolar recording methods.* Brain Physics Group Dept. of Biomedical Engineering and Dept. of Psychiatry and Neurology Tulane University New Orleans. LA 70 1 18

[35] Armando Granate Fernandes, *Sistema de aquisicao para a detecçao da fase REM do sono*

[36] http://www.benchmarkmedia.com/caig/html/caig04.html

[37] http://cnx.org/content/m12009/latest/

[38] Luís Gameiro Matos, *Acquisition System for Automatic Sleep Identification- The Interface*

[39] http://arup.com/arup/project.cfm?pageid=2516

[40] J. E. Heiss, C. M. Held, P. A. Estévez, C. A. Perez, C. A. Holzmann, J. P. Pérez, *CLASSIFICATION OF SLEEP STAGES IN INFANTS: A NEURO FUZZY APPROACH*, Department of Electrical Engineering, Universidad de Chile, Casilla 412-3, Santiago, Chile

[41] Yoshiharu Hiroshige, *Linear automatic detection of eye movements during the transition between wake and sleep*, Psychiatry and Clinical Neurosciences Volume 53 Issue 2 Page 179 - April 1999 doi:10.1046/j.1440-1819.1999.00528.x Volume 53 Issue 2

[42] V. Krajca, S. Petranek, K. Paul , M. Matousek, J. Mohylova, and L. Lhotska, *Automatic Detection of Sleep Stages in Neonatal EEG Using the Structural Time Profiles*, Proceedings of the 2005 IEEE Engineering in Medicine and Biology 27th Annual Conference Shanghai, China, September 1-4, 2005

[43] P. Van Hese, W. Philips, J. De Koninck, R. Van de Valle and I. Lemahieu, *Automatic Detection of sleep stages using EEG*, 2001 Proceedings of the 23 Annual EMBS Internacional Conference, October 25-28, Instanbul, Turkey

[44] P. A. Estevez, C.M. Held, C.A. Holzmann, C.A. Perez, J. P. Perez, J. Heiss, M. Garrido, P. Peirano, *Polysomnographic pattern recognition for automated classification of sleep-waking states in infants*

[45] Peter Anderer, Georg Gruber, Silvia Parapatics, Michael Woertz, Tatiana Miazhynskaia, Gerhard Klösch, Bernd Saletu, Josef Zeitlhofer, Manuel J. Barbanoj, Heidi Danker-Hopfe, Sari-Leena Himanen, Bob Kemp, Thomas Penzel, Michael Grözinger, Dieter Kunz, Peter Rappelsberger, Alois Schlögl, Georg Dorffner, *An E-Health Solution for Automatic Sleep Classifi cation according to Rechtschaffen and Kales: Validation Study of the Somnolyzer 24x7 Utilizing the Siesta Database*

[46] http://www.dspguide.com/ch10/3.htm

[47] http://www.cmlab.csie.ntu.edu.tw/cml/dsp/training/coding/transform/fft.html

[48] JULIUS O. SMITH III, *INTRODUCTION TO DIGITAL FILTERS WITH AUDIO APPLICATIONS*, August 2006 Edition, http://ccrma.stanford.edu/ jos/filters/filters.html

[49] http://ccrma.stanford.edu/∼jos/mdft/Linear_Phase_Terms.html

[50] Rabiner, L. R., Gold, B.. *Theory and application of digital signal processing*, 1975, Prentice-Hall Engelwood Cliffs. N.J.

[51] Oppenheim, A. V., Schafer, R. W., *Signals and Systems*, 1975, Prentice-Hall Engelwood Cliffs. N.J.

[52] Herrmann, O., Rabiner, L. R., Chan, D. S. K., *Practical design rules for optimum filter response low-pass digital filters*, 1973, Bell Syst. Tech. J..52: 769-99

[53] Rabiner, L. R., Kaiser, J. F., Herrmann, O., Dolan, M. T., *Some comparisons between FIR and IIR filters*, 1974, Bell Syst. Tech. J..53: 305-31

[54] http://fuzzy.cs.uni-magdeburg.de/nfdef.html

[55] http://www.geocities.com/templarser/complexglos.html

[56] http://mathworld.wolfram.com/FastFourierTransform.html

[57] http://grus.berkeley.edu/ jrg/ngst/fft/fourier.html

[58] http://me.oregonstate.edu/classes/me452/winter95/ButlerKeithMurphy/

[59] Steven W. Smith, Ph.D., *The Scientist and Engineer's Guide to Digital Signal Processing*, http://www.dspguide.com/pdfbook.htm

[60] Paul Bourke, *DFT (Discrete Fourier Transform) F F T (Fast Fourier Transform)*, 1993

[61] http://www.bores.com/courses/intro/filters/4_equi.htm

[62] http://www.wrongdiagnosis.com/s/sleep_disorders/stats-country.htm

[63] http://www.ecircuitcenter.com/Circuits/BJT_Diffamp1/BJT_Diffamp1.htm

[64] http://cnx.org/content/m0050/latest/

[65] Carneiro, Raul, *Instrumentação e Aquisição de Sinais Lecture notes,* 1^{st} *semester, 2005-2006*

[66] http://hyperphysics.phy-astr.gsu.edu/hbase/hframe.html

[67] Jessie Y. Shen *Sleep Stage Identification*

[68] Smith C. ; Lapp L., *Increases in number of REMS and REM density in humans following an intensive learning period*

[69] http://faculty.gvsu.edu/aboufade/web/dw.htm

[70] http://www.embedded.com/showArticle.jhtml?articleID=17301593

[71] Aapo Hyvärinen, *Fast and Robust Fixed-Point Algorithms for Independent Component Analysis*, Helsinki University of Technology Laboratory of Computer and Information Science P.O. Box 5400, FIN-02015 HUT, Finland, IEEE Trans. on Neural Networks, 10(3):626-634, 1999.

[72] James V. Stone, *Independent Component Analysis: A Tutorial Introduction*, MIT Press, 193?pp, ISBN 0-262-69315-1

[73] Bob Kemp, Alpo Varri, Agostinho C. Rosa, Kim D. Nielsen and John Grade, *A simple format for exchange of digitized polygraphic recordings*, Electroencephalography and Clinical Neurophysiology, 82 (1992): 391-393.

[74] Bob Kemp, Jesus Olivan, *European data format 'plus' (EDF+), an EDF alike standard format for the exchange of physiological data*, Clinical Neurophysiology, 114 (2003): 1755-1761.

Appendix A

Sleep Disorders

Usually, sleep disorders interfere with the quality, duration and onset of sleep. Causes like sleep deprivation, constantly changing sleep schedule, stress and environment all affect the progression of the sleep cycle, modifying sleep stages duration and rearranging its natural progression (e.g. Psychological conditions like depression shorten the duration of rapid eye movement). Motivated by the XXI century lifestyle it is reasonable to consider that sleep disorders are modern diseases with increasing prevalence. Such statement is supported by tableA.1. Using Unites States of America sleep disorders data, "US Census Bureau, Population Estimates, 2004", and extrapolating to several countries with life standards above the average, one verifies sleep disorders have a huge impact in modern society.

Country	Prevalence	Estimated Population
USA	43,184,617	293,655,405
Denmark	796,087	5,413,392
Sweden	1,321,529	8,986,400
United Kingdom	8,863,339	60,270,708
France	8,885,913	60,424,213
Netherlands	2,399,735	16,318,1992
Germany	12,121,265	82,424,609
Portugal	1,547,668	10,524,145
Spain	5,923,644	40,280,780
Italy	8,537,864	58,057,477

Table A.1: United States of America sleep disorders data and extrapolation to several other countries according to its population. [62]

Some of problematic sleep disorders are here described:

Sleep Apnea is characterized by periodic interruption of breathing and loud interrupted snoring. This condition affects more than 5% of adult males and can shorten lifespan more than common problematic issues such as smoking and drinking. This pathology is caused by the excessive relaxation of airway muscles during sleep. It can be treated by wearing a mask that pressurizes the airway, a procedure called Continuous Positive Airway Pressure (CPAP). In mild cases, weight loss and preventing patients from sleeping on their backs can help.

Insomnia is the perception or complaint of inadequate or poor-quality sleep because of one or more of the following: difficulty falling asleep; waking up frequently during the night with difficulty returning to sleep; waking up too early in the morning; or unrefreshing sleep. This situation is even more common than sleep apnea. Sleeping pills can be helpful for short-term insomnia, but may not benefit, and may even have significant adverse effects, on individuals with long-term insomnia. Insomnia is more common later in life, but the cause of this is unclear. One syndrome that is known to produce a profound insomnia is restless legs with periodic movements during sleep. "Restless legs" refers to an urge to move the legs that increases during quiescence. Periodic movement during sleep, a frequent accompaniment of restless legs, is a regular twitching, usually occurring every 5-90 seconds in the legs during NREM sleep and can also disturb sleep. Restless legs is present in as much as 10% of the adult population.

Parasomnias are particularly common in children. Night terrors, in which children scream during the night, sleep walking and bedwetting are some of the most common and are generally outgrown with age.

REM sleep behavior disorder is a pathology characterized by vigorous movements occurring during REM sleep as the dreamer acts out his or her dream.

Narcolepsy is a condition that causes patients to fall asleep uncontrollably throughout the day for periods lasting less than a minute to more than half an hour. These situations can occur even when a person is active and concentrated in a specific task. Besides, narcoleptic subjects tend to have a disturbed sleep cycle, with frequent sleep stage being skipped.

Appendix B

Signal Processing

Motivated by the way computers are organized, signal must be represented by a finite number of bytes. This restriction means that both the time axis and the amplitude axis must be quantized, one must deal with discrete signal. A methodology to correctly quantize the time axis without the introduction of errors was verified by Harold Nyquist, the Sampling Theorem. When analysing a sampled version of a generic analog signal $s(t)$, the $s(nT_s)$ (with T_s known as the sampling interval), one verifies that the values of the original signal at the sampling times are preserved, however some considerations must be respected so that the values between the samples can be reconstructed (Fig.B.1).

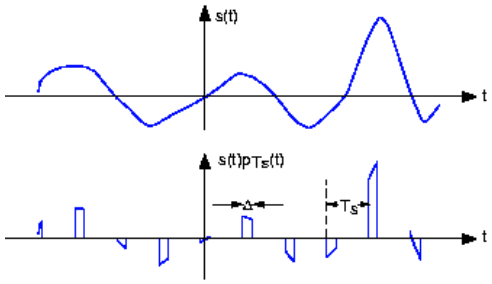

Figure B.1: Signal example waveform. Top plot: Continuous representation. Bottom plot: Sampled version of the signal. [64]

If the sampling procedure is properly done, it is possible to recover the original signal. To understand how signal values between the samples can be correctly defined, it is necessary to calculate the sampled signal's spectrum. Using the Fourier series representation of the periodic sampling signal:

$$x(t) = \sum_{k=-\inf}^{\inf} \left(c_k \cdot \exp\left(\frac{-j2\pi kt}{T_s} \right) \cdot s(t) \right) \tag{B.1}$$

Considering each term in the sum separately, we need to know the spectrum of the product of the complex exponential and the signal.

$$\int_{-\inf}^{\inf} s(t) \cdot \exp\left(\frac{-j2\pi kt}{T_s}\right) \cdot \exp\left(-j2\pi ft\right)dt = \int_{-\inf}^{\inf} s(t) \cdot \exp\left(-j2\pi\left(f - \frac{k}{T_s}\right)t\right)dt \tag{B.2}$$

$$\int_{-\inf}^{\inf} s(t) \cdot \exp\left(-j2\pi\left(f - \frac{k}{T_s}\right)t\right)dt = S\left(f - \frac{k}{T_s}\right) \exp\left(-j2\pi\left(f - \frac{k}{T_s}\right)t\right)dt \tag{B.3}$$

Thus, the spectrum of the sampled signal consists of weighted (by the coefficients ck) and delayed versions of the signal's spectrum (Fig.B.2).

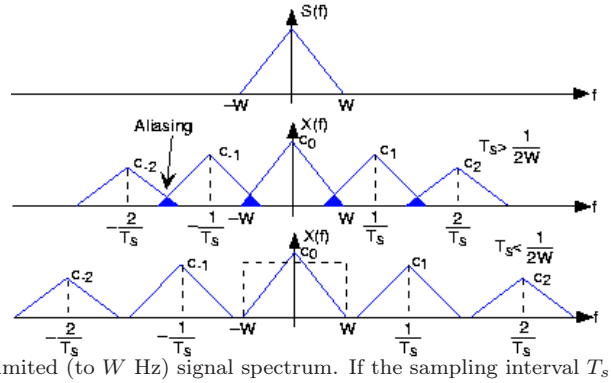

Figure B.2: Top plot: Bandlimited (to W Hz) signal spectrum. If the sampling interval T_s is chosen too large relative to the bandwidth W, aliasing will occur. Bottom plot: Sampling interval is chosen sufficiently small to avoid aliasing. Note that if the signal were not bandlimited, the component spectra would always overlap. [64]

$$X(t) = \sum_{k=-\inf}^{\inf} \left(c_k S\left(f - \frac{k}{T_s}\right)\right) \tag{B.4}$$

In general, the terms in this sum overlap each other in the frequency domain, rendering recovery of the original signal impossible. This phenomenon is known as aliasing.

If, however, two conditions are satisfied: The signal $s(t)$ is bandlimited to W Hz, and the sampling interval Ts is small enough so that the individual components in the sum do not overlap - $T_s < 1/2W$, aliasing will not occur. In this case, the original signal can be recovered by lowpass filtering x(t) with a filter having a cutoff frequency equal to W Hz. These two conditions ensure the ability to recover a bandlimited signal from its sampled version: the Sampling Theorem.

In order to avoid the problem of aliasing one must apply a low-pass filter to the signal, prior to the sampling stage, to remove any frequency components above the Nyquist frequency.

Appendix C

Data analysis

C.1 EEG criteria analysis

The EEG signals variability for 6 different subjects is presented in this section. For each subject five analysis were performed.

A is the ratio between signals maximum and effective value for each epoch.

B is the ratio between signals maximum and signals energy for each 5 second period.

C is the ratio between Δ band energy and total energy for each 5 second period.

D is the ratio between θ band energy and total energy for each 5 second period.

E is the ratio between α band energy and total energy for each 5 second period.

For B, C, D and E the ratios were calculated discarding energies associated to frequencies below 0.5Hz.

C.1.1 Subject 1

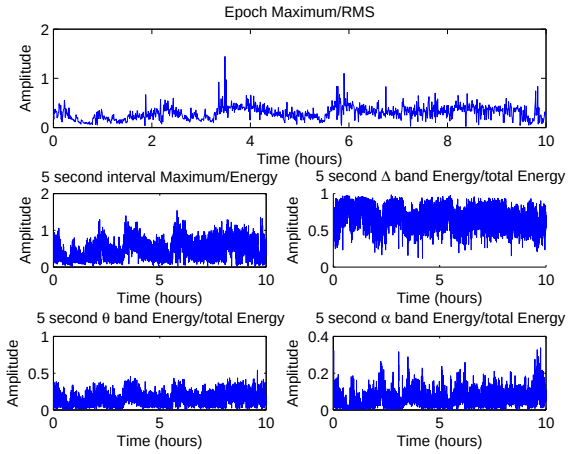

Figure C.1: A - Epoch's energy variability evaluation. B - Five second energy variability evaluation. C - Five second Δ variability evaluation. D - Five second θ variability evaluation. E - Five second α variability evaluation.

C.1.2 Subject 2

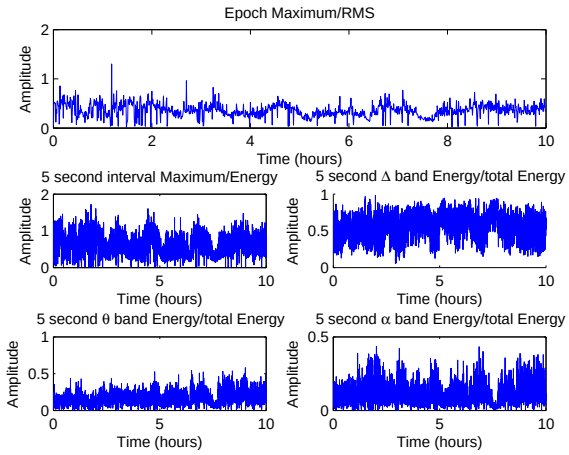

Figure C.2: A - Epoch's energy variability evaluation. B - Five second energy variability evaluation. C - Five second Δ variability evaluation. D - Five second θ variability evaluation. E - Five second α variability evaluation.

C.1.3 Subject 3

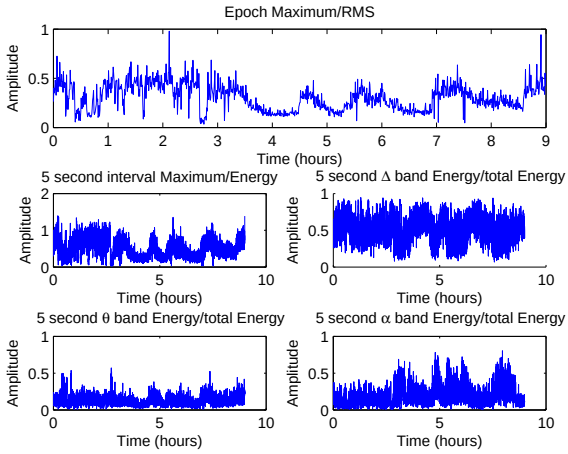

Figure C.3: A - Epoch's energy variability evaluation. B - Five second energy variability evaluation. C - Five second Δ variability evaluation. D - Five second θ variability evaluation. E - Five second α variability evaluation.

C.1.4 Subject 4

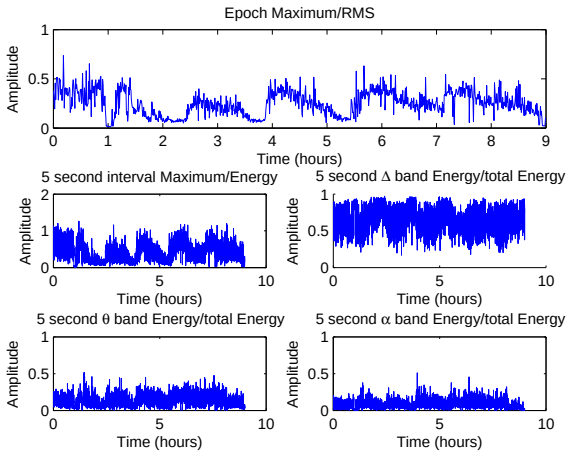

Figure C.4: A - Epoch's energy variability evaluation. B - Five second energy variability evaluation. C - Five second Δ variability evaluation. D - Five second θ variability evaluation. E - Five second α variability evaluation.

C.1.5 Subject 5

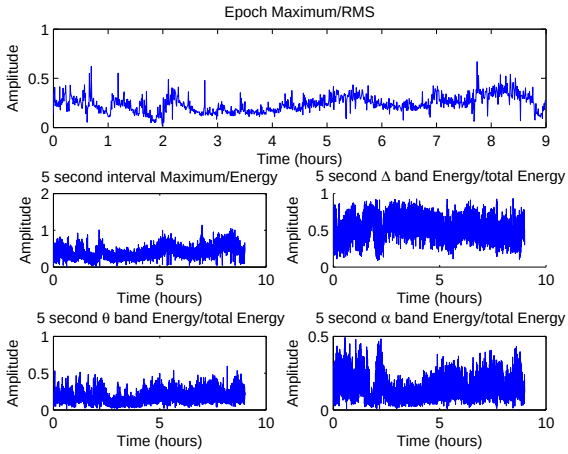

Figure C.5: A - Epoch's energy variability evaluation. B - Five second energy variability evaluation. C - Five second Δ variability evaluation. D - Five second θ variability evaluation. E - Five second α variability evaluation.

C.1.6 Subject 6

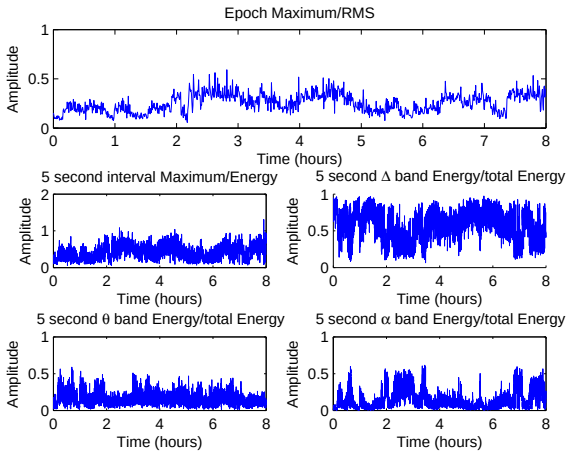

Figure C.6: A - Epoch's energy variability evaluation. B - Five second energy variability evaluation. C - Five second Δ variability evaluation. D - Five second θ variability evaluation. E - Five second α variability evaluation.

All five analysis revealed little variation among subjects hence no dynamic criteria definition was established. It is also possible to verify that Δ band (Plot C) is more represented than other sleep waves, θ (Plot D) and α (Plot E).

C.2 EMG criteria analysis

The EMG signals variability output for 6 different subjects is presented in this section. It was evaluated the ratio between signals maximum and effective value for each epoch.

C.2.1 Subject 1

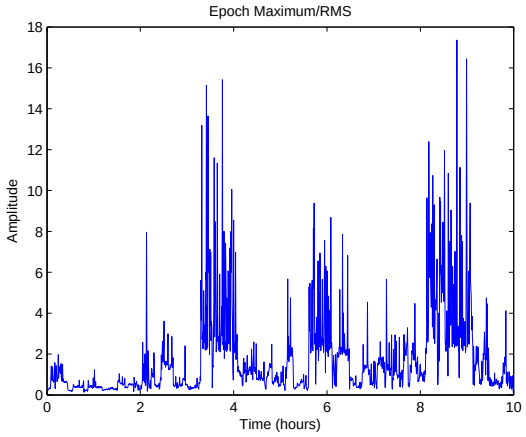

Figure C.7: Epoch's energy variability evaluation.

C.2.2 Subject 2

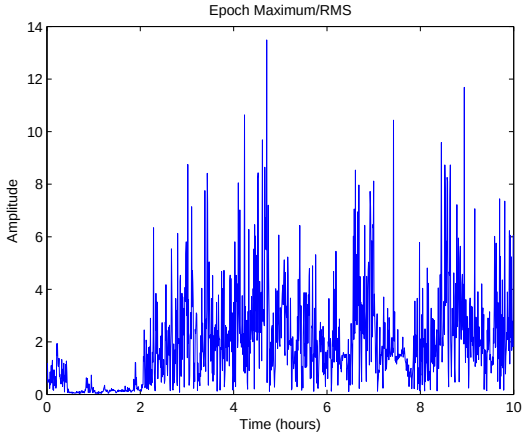

Figure C.8: Epoch's energy variability evaluation.

C.2.3 Subject 3

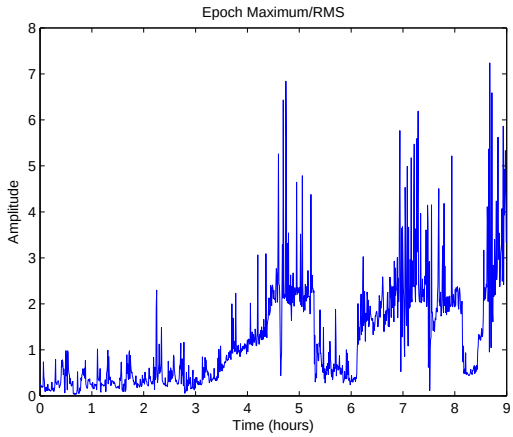

Figure C.9: Epoch's energy variability evaluation.

C.2.4 Subject 4

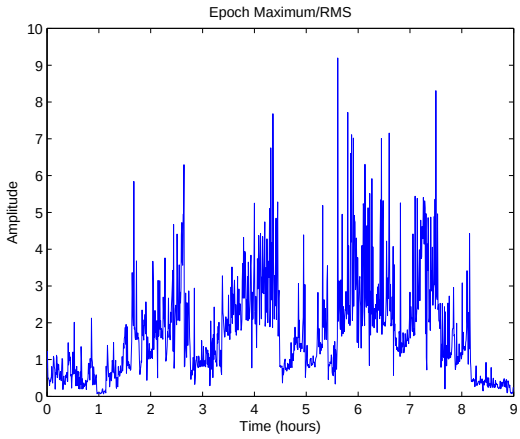

Figure C.10: Epoch's energy variability evaluation.

C.2.5 Subject 5

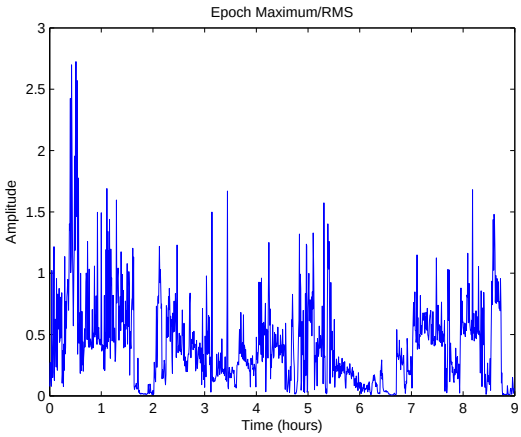

Figure C.11: Epoch's energy variability evaluation.

C.2.6 Subject 6

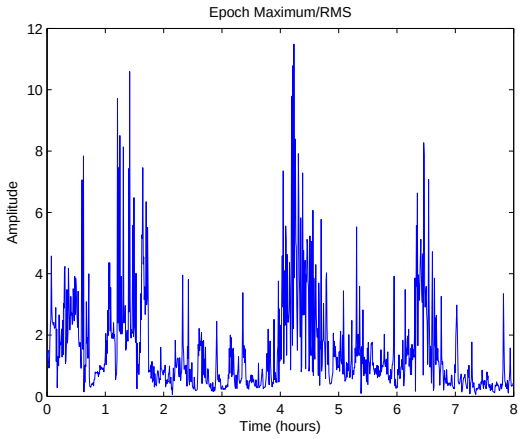

Figure C.12: Epoch's energy variability evaluation.

From the presented data one can verify that EMG variability is low between different subjects, therefore no dinamic criteria mechanism is necessary.

C.3 EOG criteria analysis

The EOG signals variability output for 6 different subjects is presented in this section. It was evaluated the ratio between signals maximum and effective value for each epoch.

C.3.1 Subject 1

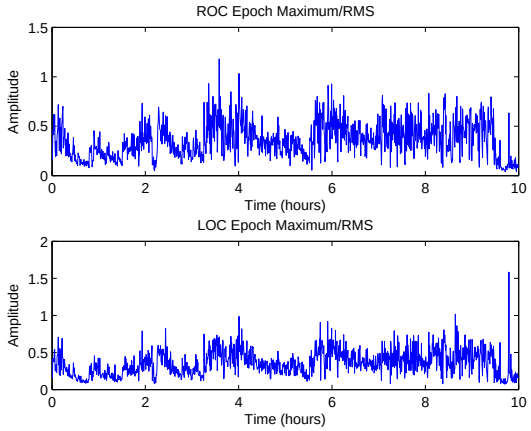

Figure C.13: Epoch's energy variability evaluation.ROC - Right Outer Cantus data. LOC - Left Outer Cantus data.

C.3.2 Subject 2

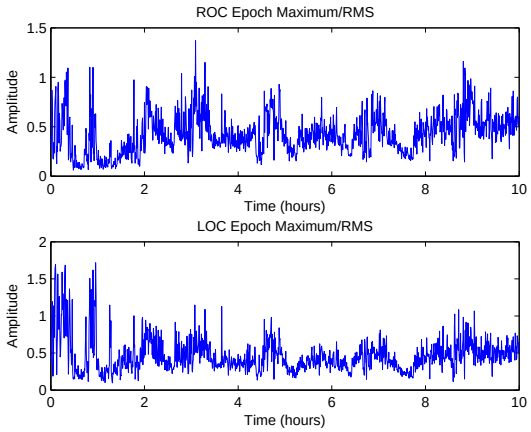

Figure C.14: Epoch's energy variability evaluation.ROC - Right Outer Cantus data. LOC - Left Outer Cantus data.

C.3.3 Subject 3

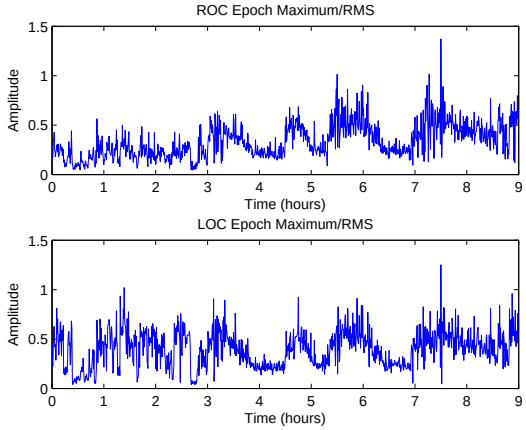

Figure C.15: Epoch's energy variability evaluation.ROC - Right Outer Cantus data. LOC - Left Outer Cantus data.

C.3.4 Subject 4

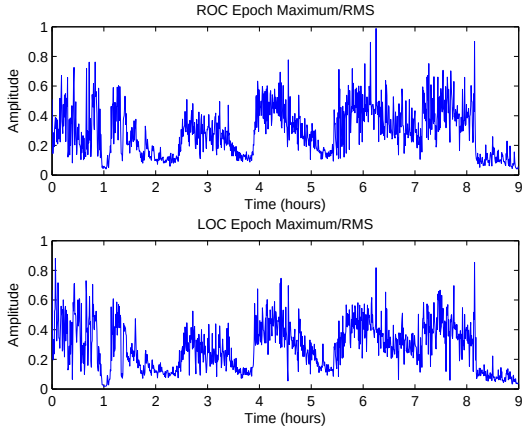

Figure C.16: Epoch's energy variability evaluation.ROC - Right Outer Cantus data. LOC - Left Outer Cantus data.

C.3.5 Subject 5

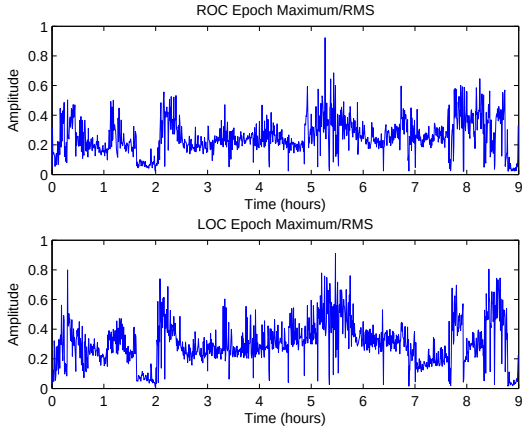

Figure C.17: Epoch's energy variability evaluation.ROC - Right Outer Cantus data. LOC - Left Outer Cantus data.

C.3.6 Subject 6

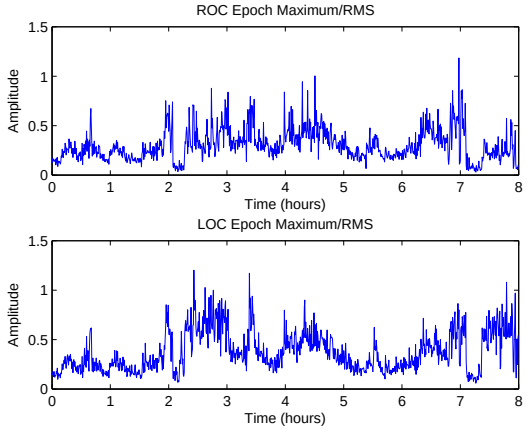

Figure C.18: Epoch's energy variability evaluation.ROC - Right Outer Cantus data. LOC - Left Outer Cantus data.

Similarly to the other analysis (EEG and EMG), one can verify that EOG variability is low between different subjects, therefore no dinamic criteria mechanism is necessary.

Appendix D

European Data Format

This data format was developed in 1990 due to the need of different researchers to analyse each others registers. It consists of a header record followed by data records. Within the header record subject and acquisition information is specified, followed by signals data records. Representing the header and data:

HEADER RECORD
8 ascii : version of this data format (0)
80 ascii : local patient identification
80 ascii : local recording identification
8 ascii : startdate of recording (dd.mm.yy)
8 ascii : starttime of recording (hh.mm.ss)
8 ascii : number of bytes in header record
44 ascii : reserved
8 ascii : number of data records
8 ascii : duration of a data record, in seconds
4 ascii : number of signals (ns) in data record
ns * 16 ascii : ns * label (e.g. EEG Fpz-Cz or Body temp)
ns * 80 ascii : ns * transducer type (e.g. AgAgCl electrode)
ns * 8 ascii : ns * physical dimension (e.g. uV or degreeC)
ns * 8 ascii : ns * physical minimum (e.g. -500 or 34)
ns * 8 ascii : ns * physical maximum (e.g. 500 or 40)
ns * 8 ascii : ns * digital minimum (e.g. -2048)
ns * 8 ascii : ns * digital maximum (e.g. 2047)
ns * 80 ascii : ns * prefiltering (e.g. HP:0.1Hz LP:75Hz)
ns * 8 ascii : ns * number of samples in each data record
ns * 32 ascii : ns * reserved
DATA RECORD
nr of samples[1] * integer : first signal in the data record
.. nr of samples[ns] * integer : last signal

Appendix E

Criteria analysis

In this section different criteria indicators are represented for the distinct signals of the two reported trials.

E.1 EEG indicators

For the EEG it was evaluated: Max/Energy; Δ Energy/Total energy; θ Energy/Total energy; α Energy/Total energy. These indicators are here represented:

E.1.1 Trial 1

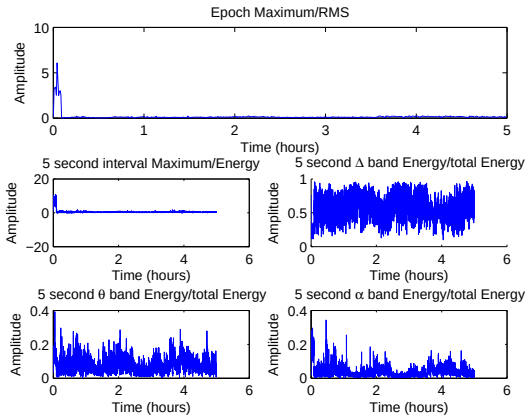

Figure E.1: EEG indicators. Top - Epoch Max/Energy. Middle left - 5sec Max/Energy. Middle right - 5sec Δ Energy/Total Energy. Bottom left - 5sec θ Energy/Total Energy. Bottom right - 5sec α Energy/Total Energy.

E.1.2 Trial 2

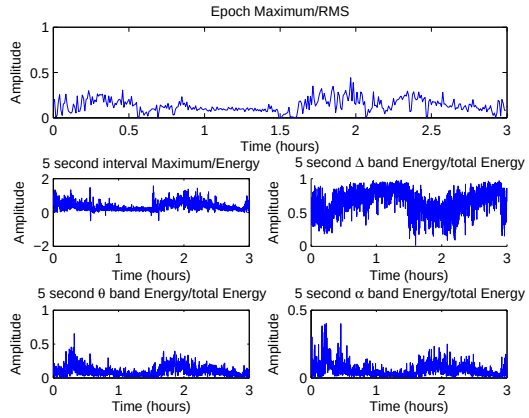

Figure E.2: EEG indicators. Top - Epoch Max/Energy. Middle left - 5sec Max/Energy. Middle right - 5sec Δ Energy/Total Energy. Bottom left - 5sec θ Energy/Total Energy. Bottom right - 5sec α Energy/Total Energy.

E.2 EMG indicators

For the EMG it was evaluated: Energy; Max/Energy. These indicators are here represented:

E.2.1 Trial 1

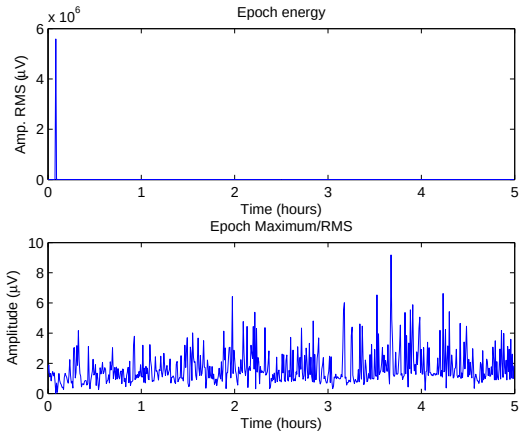

Figure E.3: EMG indicators. Top - Epoch Energy. Bottom - Max/Energy.

E.2.2 Trial 2

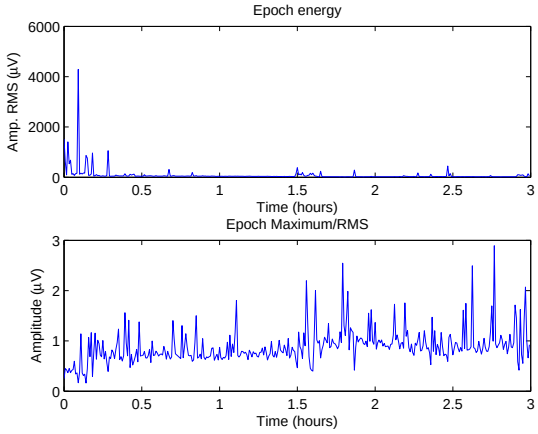

Figure E.4: EMG indicators. Top - Epoch Energy. Bottom - Max/Energy.

E.3 EOG indicators

For the EOG it was evaluated: Energy and Max/Energy for each oculogram register. These indicators are here represented:

E.3.1 Trial 1

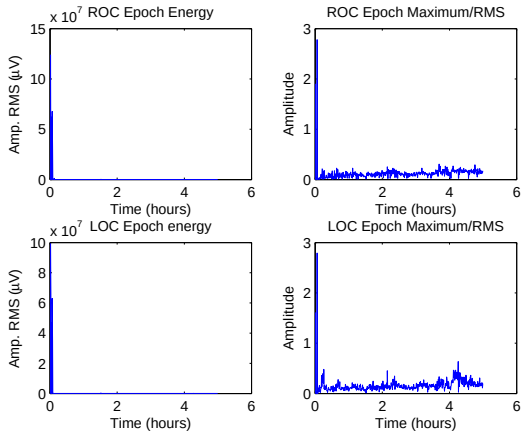

Figure E.5: EOG indicators. Top left - ROC epoch Energy. Top right - ROC Max/Energy. Bottom left - LOC epoch Energy. Bottom right - LOC Max/Energy.

E.3.2 Trial 2

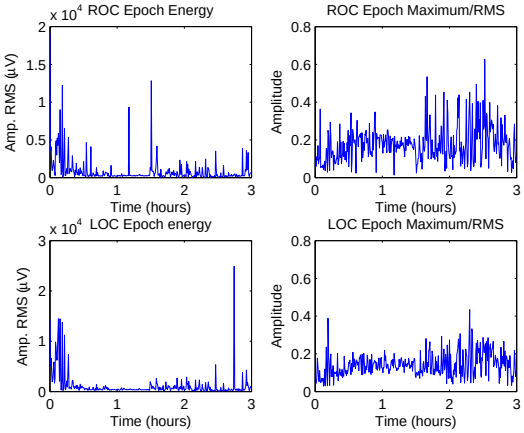

Figure E.6: EOG indicators. Top left - ROC epoch Energy. Top right - ROC Max/Energy. Bottom left - LOC epoch Energy. Bottom right - LOC Max/Energy.